

The Development of BET BD1 Selective Chemical Probes

Erin Bradley MSci

Medicines Design, GlaxoSmithKline

Department of Pure & Applied Chemistry, University of
Strathclyde

Thesis submitted to the University of Strathclyde in fulfilment
of the requirements for the degree of Master of Philosophy

Acknowledgements

I would firstly like to thank my supervisors, Dr. Rosa Cookson, Dr. Marc Reid, and Professor William Kerr, for their supervision and guidance during these past 15 months. Thank you to Rosa for the day-to-day support in the lab, and always being there to answer any questions that I have. I have really appreciated that you have taken time to meet with me every week to discuss my project, especially when you are so busy! I also cannot thank you enough for the assistance you have provided when writing this report, I really appreciate the detail to which you have provided me with feedback. You have always been so approachable and supportive, and I could not have asked for a better supervisor.

Thank you to Marc and Billy for providing constructive feedback on my written work, and always being available when needed for discussions about my project. I would also like to thank you both for inviting me to join in with group meetings when I visited Strathclyde.

I would also like to extend my thanks to Lucia Fusani for the time you have spent working on the computational aspects of this project, including the modelling and calculations you have conducted which have been key to this project.

I would like to thank the members of the Epigenetics DPU for welcoming me into the department when I first joined. Additionally, I would like to thank members of the Fibrosis DPU for also welcoming me into their department when I joined last April.

I must extend my thanks to Nicholas Measom, Hannah Lithgow, and Emma Grant for their continued support, advice, and encouragement. I would not have got here with you!

Finally, I would like to thank Professor Harry Kelly and Professor William Kerr for accepting me onto the collaborative PhD programme, and giving me such an amazing opportunity to perform well-supported research. I am very grateful for all the support I have received.

Declaration of Copyright

This thesis is the result of the author's original research. It has been composed by the author and has not been previously submitted for examination which has led to the award of a degree.

The copyright of this thesis belongs to GSK in accordance with the author's contract of engagement with GSK under the terms of the United Kingdom Copyright Acts. Due acknowledgement must always be made of the use of any material contained in, or derived from, this thesis.

Signed:

Date:

Table of Contents

Acknowledgements	2
Abbreviations	5
Abstract	8
1.0 Introduction	9
1.1 Epigenetics	9
1.2 Bromodomains	13
1.3 Bromodomain inhibitors	15
1.3.1 BD1/BD2 selective BET inhibitors	20
1.4 Chemical probes	28
2.0 Proposed Work	31
3.0 Results and Discussion	34
3.1 Spotfire visualisation of the benzimidazole series	34
3.2 Functionalising the R5 vector	40
3.3 Investigation of an amino acid point change between BD1 and BD2	45
3.3.1 Synthesis of amine functionalised benzimidazoles	47
3.3.2 Investigating the hypothesis of BD1 selectivity in the amine functionalised benzimidazole series	61
3.3.2.1 Computational efforts and X-ray crystallography used towards the understanding of BD1 selectivity	67
3.4 Dual functionalisation of the benzimidazole core	72
3.5 Investigating an alternative core structure	75
4.0 Conclusions	80
5.0 Future Work	82
6.0 Experimental	85
7.0 References	154
8.0 Appendix	157

Abbreviations

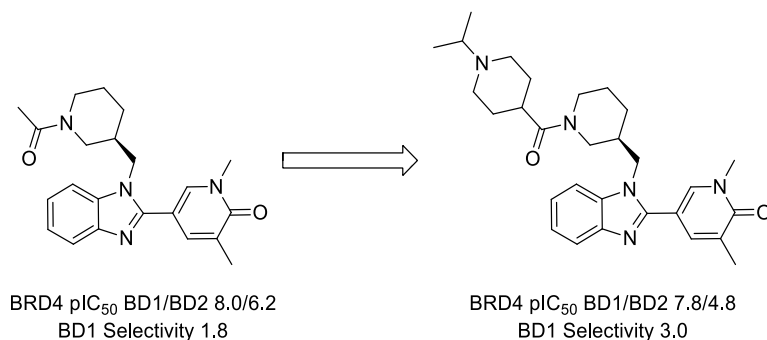
A	Alanine
Ac	Acetyl
AlphaScreen	Amplified Luminescent Proximity Homogenous Assay
AMP	Artificial Membrane Permeability
ApoA1	Apolipoprotein A1
Asn	Asparagine
Asp	Aspartic Acid
BET	Bromodomain and Extra C- Terminal
BRD	Bromodomain
D	Aspartic Acid
d	Doublet
Da	Daltons
DCM	Dichloromethane
DMF	<i>N,N</i> -Dimethylformamide
DMSO	Dimethylsulfoxide
DNA	Deoxyribonucleic Acid
DSF	Differential Scanning Fluorimetry
ESI	Electrospray Ionisation
EtOAc	Ethyl Acetate
EtOH	Ethanol
F	Phenylalanine
For	Formic acid
Gln	Glutamine
GPCRs	G-protein Coupled Receptors
GSK	GlaxoSmithKline
H	Histidine
h	Hour
HAT	Histone Acetyltransferases
HDAC	Histone Deacetylases
His	Histidine
HpH	High pH
HPLC	High Performance Liquid Chromatography
HRMS	High Resolution Mass Spectrometry
Hz	Hertz
I	Isoleucine
IVC	<i>In vitro</i> Clearance
J	Coupling Constant

K	Lysine
KAc	Acetyl Lysine
L	Leucine
LCMS	Liquid Chromatography Mass Spectrometry
LLE	Lipophilic Ligand Efficiency
M	Molar Concentration
m	Multiplet
MDAP	Preparative Mass Directed HPLC
Me	Methyl
MeOH	Methanol
min	Minutes
mL	Millilitres
mmol	Millimolar
mol	Mole
mp	Melting Point
mRNA	Messenger Ribonucleic Acid
NMC	NUT Midline Carcinoma
NMR	Nuclear Magnetic Resonance
P	Proline
PFI	Property Forecast Index
pH	$-\text{Log}[\text{H}^+]$
pIC ₅₀	$-\text{Log}[\text{IC}_{50}]$
PTM	Post-translational Modification
Q	Glutamine
R	Arginine
R	General Substituent
RFID	Radio Frequency Identification
RT	Room Temperature
s	Singlet
SAR	Structure Activity Relationship
SGC	Structure Genomics Consortium
S _N 2	Nucleophilic Substitution Second Order
S _N Ar	Aromatic Nucleophilic Substitution
t	Triplet
'Am	Tertiary Amyl
<i>tert</i>	Tertiary
THF	Tetrahydrofuran
TLC	Thin Layer Chromatography
TR-FRET	Time-resolved Förster Resonance Energy Transfer

Tyr	Tyrosine
UV	Ultraviolet
V	Valine
W	Tryptophan
wt	Weight
Y	Tyrosine
μM	Micromolar

Abstract

Bromodomain and extra-terminal (BET) proteins have been implicated in a variety of oncological and immunological diseases. However, the domain specific functions of the individual domains of BET proteins, BD1 and BD2 still remain unclear. This work describes the design and development of a BET BD1 selective chemical probe that will have the required BD1 domain selectivity to probe the biological function of this BD1 domain. Initial data mining of an historic benzimidazole series was performed to provide insight into which vectors might provide BD1 selectivity. Four iterations of compounds have been synthesised which aim to take advantage of an amino acid point change between the BD1 and BD2 domains. Two 'lead' compounds have been identified, that maintain excellent potency and have the desired BD1 selectivity. These compounds also have the potential to be utilised *in vivo*. Consequently, these 'lead' compounds are superior to the initial benzimidazole compound from which this project was initiated; historically, production of a compound which is BD1 selective and could also be utilised *in vivo* was not successful. A hypothesis of how BET BD1 selectivity is obtained from these compounds is disclosed, and is rationalised with the aid of computational methods and X-ray crystallography.



1.0 Introduction

1.1 Epigenetics

The human genome consists of approximately 20,000 – 25,000 genes, which are contained in every cell nuclei.¹ When expressed, a gene provides the genetic information that is transcribed into messenger ribonucleic acid (mRNA). This mRNA molecule is then processed in an editing method known as splicing, during which introns (mRNA segments which are not to be expressed) are removed from the transcript and the remaining mRNA (exons) is joined together. In this way, one gene can code for a diverse range of proteins. The mature mRNA molecule can then be translated into a functional protein by the ribosome, resulting in an observable phenotype. Each cell can express and suppress a unique subset of the genome, providing differentiation in cell appearance and function. This differentiation in gene expression is a result of modifications made to the deoxyribonucleic acid (DNA), which do not change the inherited DNA sequence of the cell. This phenomenon is referred to as ‘Epigenetic regulation’.² The epigenetic state of a cell is constantly changing, and the packaging of DNA is modified in response to environmental cues. As such, environmental factors such as diet, lifestyle, and illness all have an effect on the gene expression within a cell, and thus effect its phenotype.² Epigenetic misregulation has been implicated in a number of diseases in which environmental factors have a profound effect. These include cancer, immune mediated diseases, and neurological disorders.² Consequently, there have been significant efforts to develop epigenetic therapeutics to treat such diseases.³

Approximately two metres of DNA is contained within each human cell.⁴ In order to accommodate this DNA, it is tightly coiled around histone proteins (Figure 1).

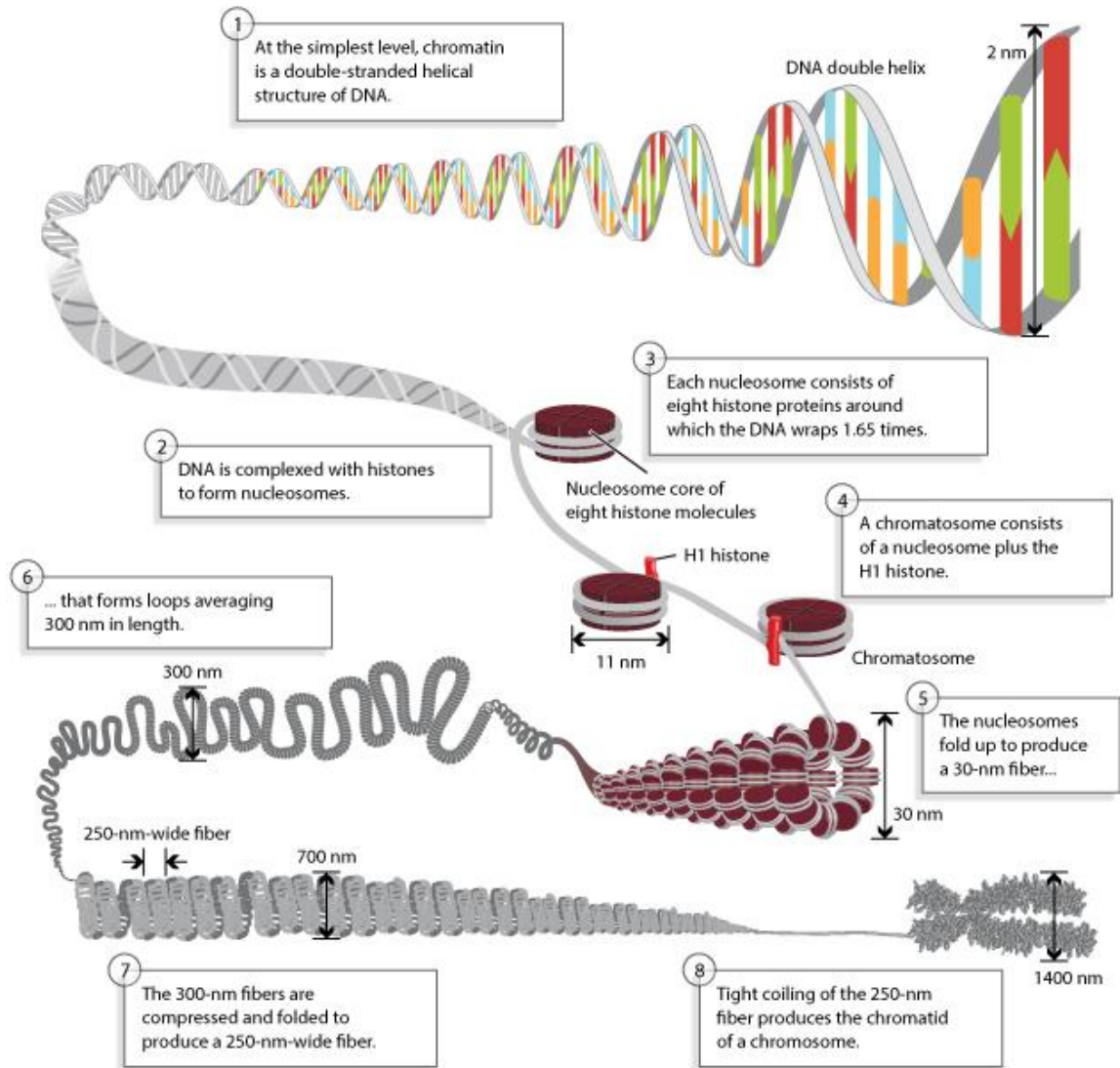


Figure 1: The process of DNA packaging into the form of chromosomes.⁴ (permission to use image granted by author). Formation of a DNA-histone complex leads to production of nucleosomes which fold up tightly to produce fibres which can be packaged into a cell.

This DNA–histone double-stranded, helical complex is known as chromatin. (Figure 1:1). The histone family of proteins – H1, H2A, H2B, H3, and H4 – are positively charged in order to tightly complex the negatively charged DNA backbone. A repeating unit of chromatin consists of approximately 146 base pairs of DNA wrapped around a protein octamer formed from two each

of H2A, H2B, H3, and H4 histone proteins; this is known as a nucleosome (Figure 1:2).⁴ This equates to the DNA strand wrapping around the octamer approximately 1.65 times (Figure 1:3). An additional H1 histone protein binds a further 20 base pairs, and as such each histone complex has two full turns of DNA wrapped around it. This complex is known as a chromatosome (Figure 1:4). Each nucleosome can then fold up to produce a fibre which is eventually tightly coiled into the chromatid of a chromosome (Figure 1:6-8).

In this tightly packaged state, the DNA strand is inaccessible to the proteins responsible for its transcription or replication, and thus protein synthesis cannot occur. For these processes to take place, the chromatin must be uncoiled to allow the DNA strand to be accessed by regulatory proteins. The timing and location of the uncoiling of the DNA strand is controlled by chemical signalling. An example of a chemical signal is a histone modification, whereby the *N*-terminal tails can be chemically altered by post-translational modifications (PTMs). Common PTMs include methylation, acetylation, phosphorylation, and ubiquitination.⁵ These PTMs are located along the chromatin strand, and form the epigenetic code.

There are three main types of protein which are involved in regulating the epigenetic code: 'reader', 'writer', and 'eraser' proteins (Figure 2). The regulation of the epigenetic code is a dynamic process, whereby PTMs are added by 'writer' proteins, and removed by 'eraser' proteins (Figure 2). Different 'writer', 'eraser', and 'reader' proteins exist for each PTM. For example, in the case of histone acetylation, the 'writer' protein histone acetyltransferases (HAT) acetylate the lysine residues of histone proteins. In contrast, histone deacetylases (HDACs) are 'eraser' proteins that deacetylate the lysine residues. The acetylation of lysine residues on histone proteins neutralises their positive charge, which weakens the electrostatic interaction of the histone protein to the negatively charged DNA strand, and loosens the packaging of the chromatin.⁶ This allows regulatory proteins to access the DNA strand.⁶ Additionally, 'reader' proteins such as

bromodomain-containing proteins mediate protein–protein interactions with histones by recognising acetylated lysine (KAc) residues.⁷ This interaction starts a cascade of signal transduction which drives substrate recruitment and the formation of the protein complexes necessary for transcription. In this way, the epigenetic code is the key signal for the regulation of gene expression.

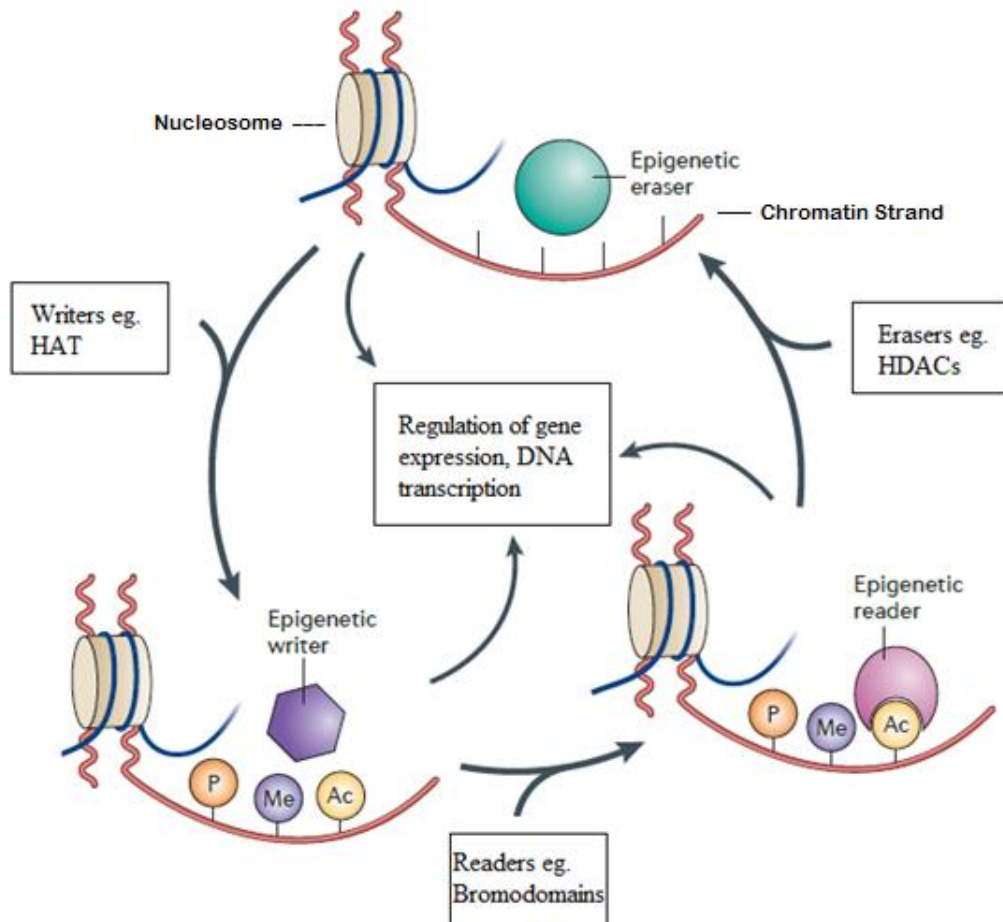


Figure 2: There are three types of epigenetic regulator proteins: ‘writers’, ‘erasers’ and ‘readers’.⁷

1.2 Bromodomains

The bromodomain (BRD) is a conserved structural motif found in many epigenetic ‘reader’ proteins. There are approximately 46 human bromodomain-containing proteins that contain between one and six bromodomain motifs. There are at least 57 structurally unique bromodomains that are divided into eight families based on their similarity (Figure 3).⁸

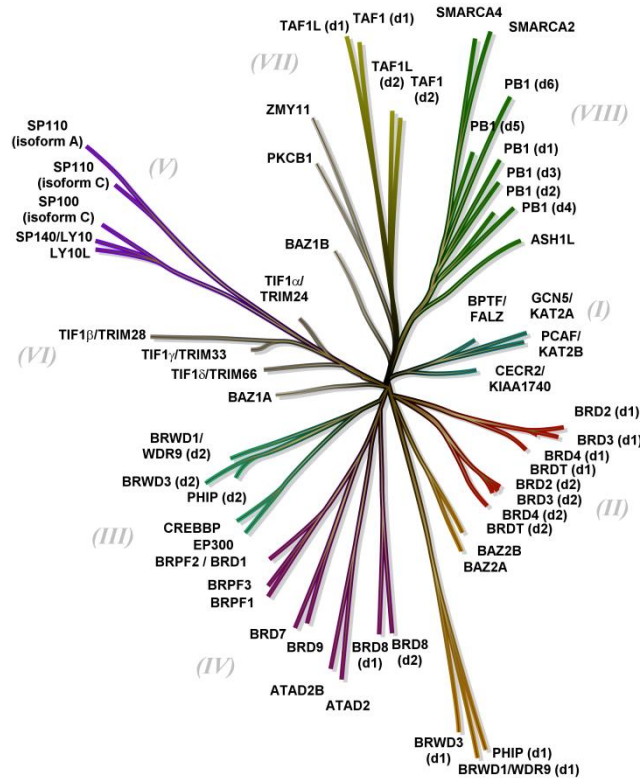


Figure 3: The bromodomain phylogenetic tree, consisting of 57 unique bromodomains within eight families.⁹

Each bromodomain contains approximately 110 amino acids.⁸ The secondary structure of a bromodomain consists of four alpha helices (αZ , αA , αB , and αC) bundled together to form the “bromodomain fold” (Figure 4). These helices are joined together by the short BC loop and the longer, more flexible ZA loop.¹⁰ Situated between the ZA and BC loops is a hydrophobic pocket

which is the binding site of the KAc group. Within this pocket, the carbonyl oxygen of the lysine acetyl group forms a key hydrogen bond with the side chain amide nitrogen of the asparagine 140 (Asn140) residue. An additional interaction between the KAc and the tyrosine 97 (Tyr97) residue *via* a water molecule is also present.¹⁰ This water molecule is part of a conserved water network that is consistently found within the KAc binding pocket of bromodomains.

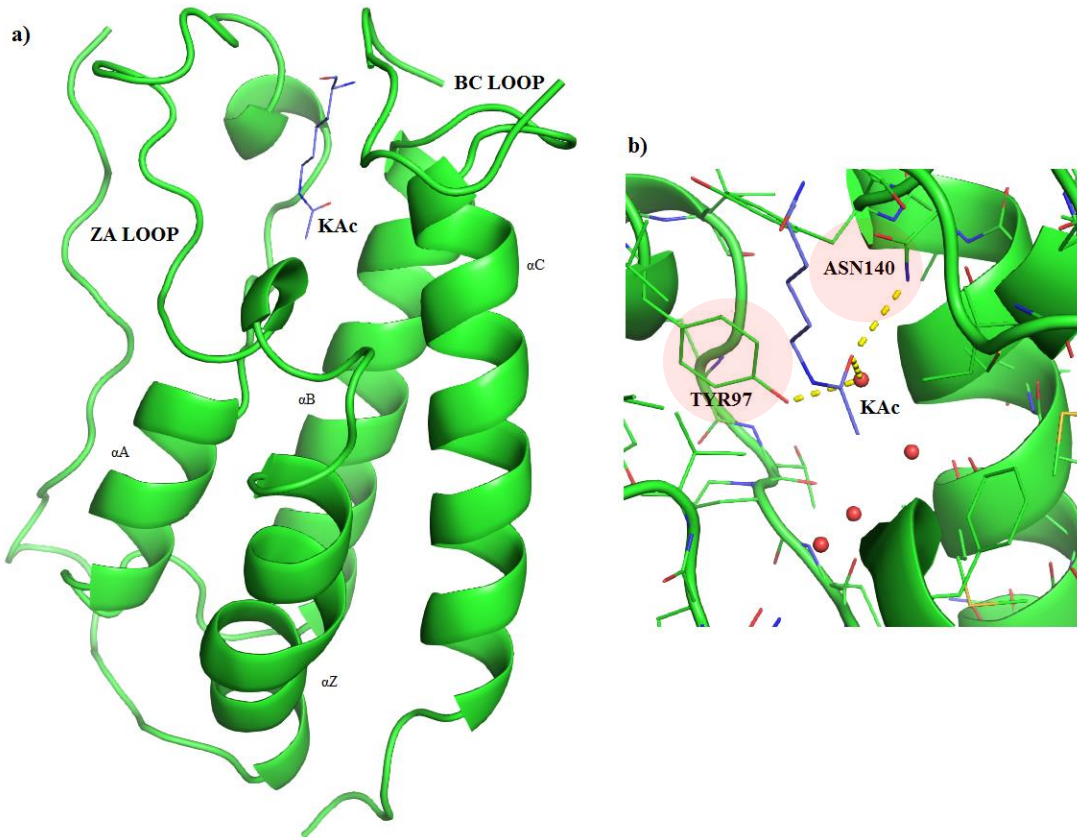


Figure 4: a) Co-crystal structure of an acetylated lysine residue and the BRD4 BD1 bromodomain. The secondary structure of a bromodomain contains four left-handed alpha helices: αZ , αA , αB , and αC . These are joined together by the BC and ZA loops to form the “bromodomain fold”. b) water network (shown in red). (PDB code = 3uvw)

Some of the most studied bromodomain containing proteins are the Bromo- and Extra-terminal domain (BET) protein family. The BET family contains four proteins: of which the BRD2, BRD3,

and BRD4 are ubiquitously expressed, and the BRDT protein which is solely expressed in the testis.¹¹ Each BRD protein contains two highly conserved amino-terminal bromodomains, BD1 and BD2, and a carboxy extra terminal domain (Figure 5).



Figure 5: The four BET proteins: BRD2, 3, 4, and T. The number of amino acids present in the primary structure is highlighted.

1.3 Bromodomain inhibitors

Over the last decade, a vast number of small molecule BET bromodomain inhibitors have been developed.³ This has led to a better understanding of the bromodomain mode of action in gene regulation and their role in disease. Abnormal BET protein function has been implicated in the development of several cancers, inflammatory diseases, and neurological disorders.² As well as their use as biological tool compounds, a number of BET bromodomain inhibitors have been advanced to clinical trials as therapeutics.³

The first reported small molecule BET bromodomain inhibitors, I-BET762 **1** and (+)-JQ1 **2** were reported by Nicodeme and co-workers at GlaxoSmithKline in early 2011, and Filippakopoulos and co-workers in late 2010, respectively (Figure 6).^{5,8} In both cases, the inhibitor can bind either the BD1 or the BD2 domain of each of the four family members, BRD2, BRD3, BRD4, and BRDT. Thus, the compounds are termed pan-BET inhibitors. I-BET762 is currently in Phase I/II clinical trials for the treatment of NUT midline carcinoma (NMC).³

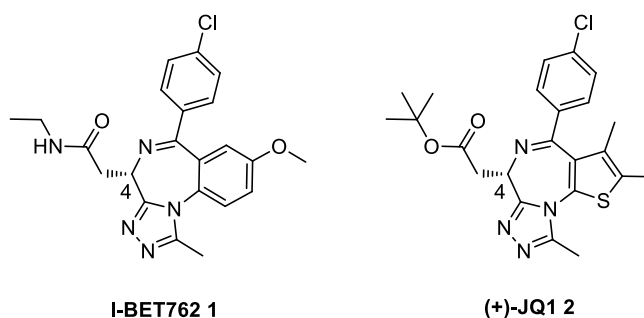


Figure 6: I-BET762 **1** and (+)-JQ1 **2** were the first reported bromodomain inhibitors.

I-BET762 **1** was discovered during efforts to find a small molecule up-regulator of the protein Apolipoprotein A1 (ApoA1), which has been implicated in the protection against atherosclerosis.^{5, 12-13} At the time, the mode of action and molecular target of this mechanism were unknown and, as such, a phenotypic screen was required to initiate the programme. A phenotypic screen is a high-throughput assay method that utilises a biological effect as an output parameter; this is useful when the biological target is unknown. A cell-based reporter assay was used to identify small molecules which could enhance ApoA1 expression. This assay utilised a cell-line containing an ApoA1 luciferase reporter gene. A hit was identified from the reporter assay and, without knowledge of the molecular target, lead optimisation resulted in the discovery of I-BET762 **1**, which showed an EC₅₀ value of 700 nM in the ApoA1 reporter assay. Lead optimisation highlighted that the benzodiazepine core was essential for activity, and that a variety of stereochemically defined groups projecting from the 4-position were tolerated, and could be used to modulate the physicochemical properties of the molecules.

Subsequently, the molecular target of I-BET762 **1** was identified. Initial profiling against panels of known therapeutic targets such as kinases, G-protein coupled receptors (GPCRs), and ion channels gave no suggestion of the mode of action, and as a result a chemo proteomics approach was utilised.^{5, 13} A solid phase support containing fixed I-BET762 **1** was used in an affinity

chromatography experiment, in which HepG2 cell lysates were passed through the column. Several proteins were consistently shown to be retained by the active matrix. An inactive control which contained the enantiomer of I-BET762 **1** showed no evidence of similar protein retention. LCMS/MS studies identified proteins BRD2, BRD3, and BRD4 as the biological targets. Once the targets were identified, development of target specific assays could be achieved. In a biochemical time-resolved Förster resonance energy transfer (TR-FRET) assay, I-BET762 **1** showed IC₅₀ values from 32.5 – 42.5 nM across proteins BRD2, BRD3, and BRD4. In an *in vivo* mouse model, I-BET762 **1** has been shown to suppress the expression of key pro-inflammatory genes.¹⁴ Additionally, it has been demonstrated that I-BET762 **1** inhibits cell growth in a panel of tumour cell lines.¹⁴ I-BET762 **1** also exhibits a good pharmacokinetic profile: high *in vitro* permeability (167 nm s⁻¹), high solubility in all physiologically relevant vehicles tested (> 3 mg mL⁻¹), low cytochrome P450 isoform potencies (IC₅₀ > 33 μM), and low *in vitro* liver microsomes and hepatocyte clearance in all relevant species (CL_i < 1.7 mL min⁻¹ g⁻¹).¹³ On April 3rd 2013, I-BET762 **1** became the first BET inhibitor to enter clinical trials,¹⁵ where it is currently in Phase I/II for the treatment of NUT midline carcinoma and for other haematological malignancies (NCT01587703 and NCT01943851, respectively).

(+)-JQ1 **2** was discovered by Filippakopoulos and co-workers by data mining of published literature.⁸ A Mitsubishi Pharmaceuticals patent revealed that thienodiazepines have affinity for the BRD4 BET protein.¹⁶ (+)-JQ1 **2** and its enantiomer were designed by utilising available SAR and molecular modelling. An AlphaScreen (Amplified Luminescent Proximity Homogenous Assay) in which fluorescence is measured as a function of ligand binding, showed (+)-JQ1 **2** has IC₅₀ values of 33 nM (BRD4 BD1) and 77 nM (BRD4 BD2). The selectivity of (+)-JQ1 **2** for the BET proteins was observed by implementing a binding assay based on differential scanning fluorimetry (DSF). Binding of (+)-JQ1 **2** increased the thermal stability of all bromodomains of

the BET protein family, with no significant stability shifts observed with non-BET bromodomains, indicating selectivity for the BET family. (+)-JQ1 **2** has been shown to inhibit growth tumour cells lines, and *in vivo* activity has been demonstrated in mouse models of NMC, metabolic disease,¹⁷ and acute myeloid leukemia.¹⁸

X-ray crystal structures of I-BET762 **1** and (+)-JQ1 **2** crystallised in BRD2 BD2 are available. Both compounds exhibit very similar binding interactions whereby the methyltriazole moiety acts as the KAc mimetic (Figure 7). One of the nitrogen atoms of the triazole ring is involved in a hydrogen bond to the conserved Asn residue, while the adjacent nitrogen atom makes a water-mediated hydrogen bond to the Tyr residue. The methyl substituent of the triazole ring occupies a hydrophobic pocket. The aromatic rings of each compound occupy the ZA channel, sitting between the α Z and α A helices. The chlorophenyl substituent interacts with the WPF shelf region, which consists of a tryptophan (W), proline (P), and phenylalanine (F) residue. Designing small molecules which interact with the WPF shelf region is a common method of increasing binding affinity and selectivity over non-BET bromodomains as this motif is unique to BET proteins.^{14, 19}

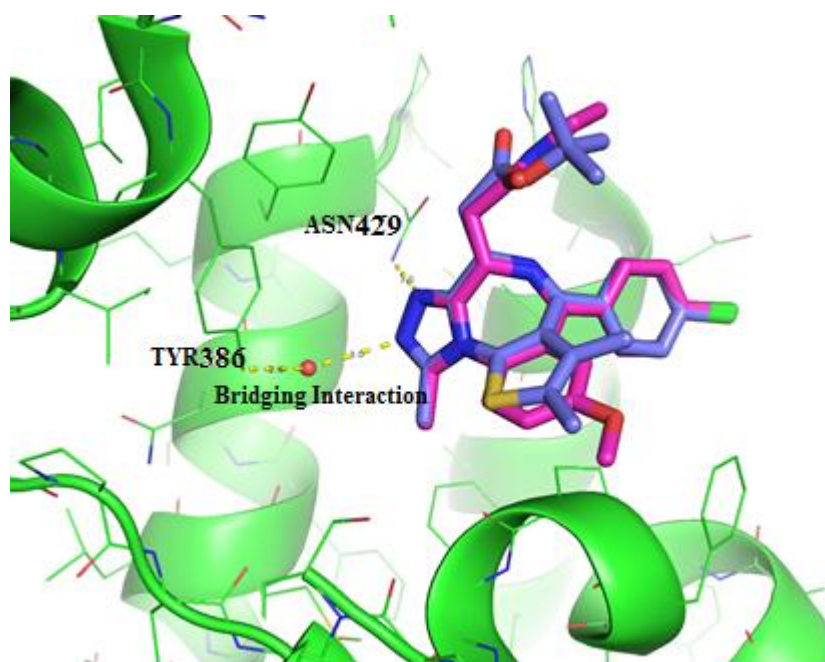


Figure 7: An overlay of X-ray crystal structures of I-BET762 **1** (pink) and (+)-JQ1 **2** (purple) co-crystallised in BRD2 BD2. The methyl triazole moiety acts as the KAc mimetic, forming the key interactions to the Asn and Tyr residues. (PDB codes = 5dfc, 3oni)

Following the discovery of I-BET762 **1** and (+)-JQ1 **2**, the reported number of BET inhibitors developed as potential epigenetic therapeutics has significantly increased, with a number of small molecules progressed into the clinic. As of June 2018, there are 16 small molecule BET inhibitors undergoing clinical trials. In addition, a large number of small molecule bromodomain chemical probes used to aid biological evaluation have been disclosed.^{3, 15} This has led to the discoveries of structurally diverse KAc mimetics, and novel motifs which can interact with the ZA channel and WPF shelf. Early examples include *o*-diazepine **3**,²⁰ *o*-azepine **4**,²¹ isoxazole **5**,²² 2-thiazolidinone **6**,²³ and pyrrolopyridinone **7**²⁴⁻²⁵ (Figure 8). Each of these compounds have a KAc mimetic which interacts with the KAc binding site by forming a hydrogen bond to asparagine 140, and a water-mediated hydrogen bond to tyrosine 97, in an analogous fashion to I-BET762 **1** and (+)-JQ1 **2**.

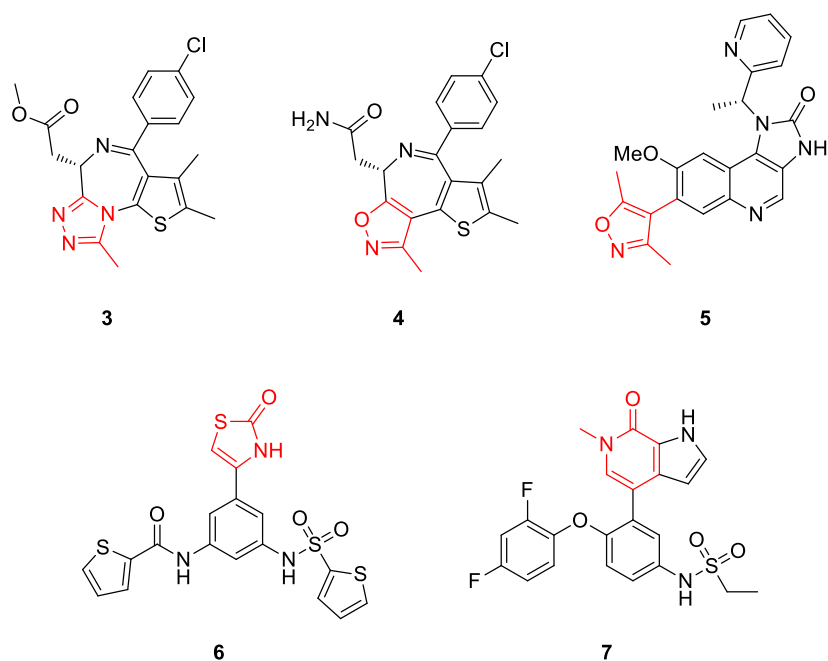


Figure 8: Reported BET inhibitors with a diverse range of KAc mimetics, including γ -diazepine **3**,²⁰ γ -azepine **4**,²¹ isoxazole **5**,²² 2-thiazolidinone **6**,²³ and pyrrolopyridinone **7**.²⁴⁻²⁵ The KAc mimetic is highlighted in red.

1.3.1 BD1/BD2 selective BET inhibitors

The majority of reported BET bromodomain small molecule binders are pan-BET inhibitors. However, results from current clinical trials suggest that pan-BET inhibition can result in associated toxicity effects such as fatigue, anaemia, hyponatraemia, low blood platelet count, and gastrointestinal effects.²⁶ To improve the therapeutic window – the range of doses which achieve the greatest therapeutic benefit, without also generating unwanted side-effects – it has been hypothesised that selective inhibition of the BD1 or BD2 BET bromodomains would be a useful strategy to minimise such side effects related to pan inhibition.²⁶⁻²⁷

However, there is minimal understanding of the domain specific function of the BD1 and BD2 bromodomains due to a lack of appropriate, selective molecular tools. In relation to this, it has

been suggested that selective inhibition of either the BD1 or BD2 bromodomain can induce differentiated gene expression not reported with pan-BET small molecule inhibitors.²⁸

A small number of BD2 selective molecules have been reported. The most advanced domain selective compound is RVX-208 **8**, developed by scientists at Resverlogix (Figure 9).²⁹ This compound was shown to be an up-regulator of ApoA1 in phenotypic assays, and until GSK's Nature publication in 2010, its mode of action was unknown.¹² Upon the discovery that I-BET762 **1** upregulated ApoA1 protein *via* inhibition of the BET family of bromodomains, it was hypothesised that RVX-208 **8** acted through the same mechanism. This was confirmed by both Resverlogix³⁰ and the Structure Genomics Consortium (SGC).²⁹ Furthermore, both groups carried out thermal denaturation assays to show that RVX-208 **8** preferentially binds to the BD2 domain of BRD2, BRD3, and BRD4. Resverlogix reported TR-FRET BRD3 IC₅₀ values of 3.1 μM (BD1) and 0.28 μM (BD2); the SGC reported AlphaScreen BRD3 IC₅₀ values of 87 ± 10 μM (BD1) and 0.510 ± 0.041 μM. The SGC publication attempts to provide insight into the observed selectivity for the BD2 domain. By comparing the co-crystal X-ray structures of RVX-208 **8** in BRD4 BD1 and BRD2 BD2, it is observed that the binding modes are almost identical. In BRD2 BD2, the carbonyl oxygen and one of the nitrogen atoms of the quinazolinone ring system act as the KAc mimetic, forming a bidentate interaction with the conserved Asn429 (Figure 10). The commonly observed water-mediated interaction with Tyr386 is also present. Interestingly, RVX-208 **8** does not occupy the WPF shelf in either case. However, in BRD2 BD2, the domain unique residue His433 is directed into the KAc binding site, packing against the phenyl ring of RVX-208 **8**. It is suggested that this could result in the tighter binding affinity of RVX-208 for BD2 domains. RVX-208 **8** is currently in Phase III clinical trials for the treatment of cardiovascular disease.

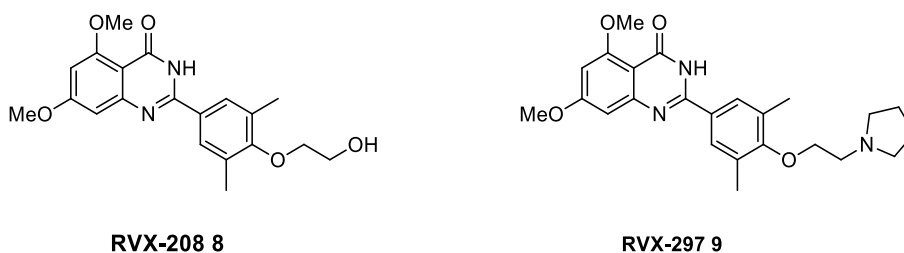


Figure 9: Reported BD2 selective inhibitors RVX-208 8, RVX-297 9.^{29, 31-32}

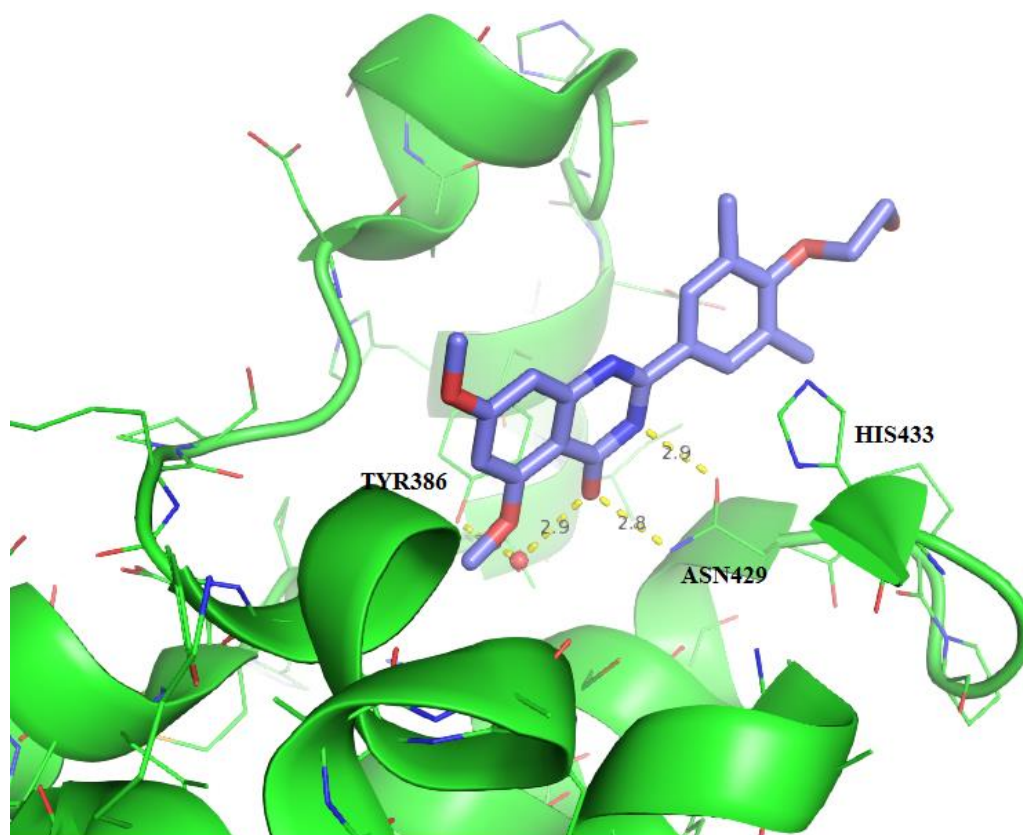


Figure 10: An X-ray structure of RVX-208 8 co-crystallised in BRD2 BD2, with BRD2 numbering. (PDB code = 4mr6)

RVX-297 9, also developed by Resverlogix,³¹ is structurally related to RVX-208 8 (Figure 9). RVX-297 9 is a 4-quinazolinone derivative with an alkylpyrrolidine side chain off the dimethyl substituted phenyl ring. Analogous to the RVX-208 8 publications, RVX-297 9 shows significant shifts in the thermal denaturation assay for the BD2 domains relative to BD1, indicating increased

BD1 selective small molecule inhibitors have also been reported. In 2013, Zhou and co-workers disclosed diazobenzene MS611 **13**, which shows BD1 selectivity (Figure 12).^{28,34} This compound and related analogues have been shown to achieve up to 100-fold selectivity over the BD2 bromodomain, however it is unclear where this BD1 bias arises from. Additionally, this level of bias is insufficient to probe the biological function of the BET BD1 bromodomain. Olinone **14**, which was reported in 2014, has a BRD4 BD1 IC₅₀ of 3.4 μM, with no BRD4 BD2 activity detected (Figure 12).³⁴

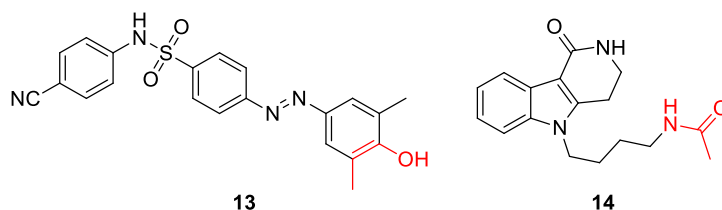


Figure 12: Reported BET BD1 selective inhibitors MS436 **13**,²⁸ olinone **14**. The KAc mimetics are highlighted in red.

BET inhibitors with single isoform selectivity have also been disclosed. Wohlwend *et al.* have disclosed acylpyrrole **15**, a BRD4 BD1 selective inhibitor that has 10-fold bias over other members of the BET family.³⁵ Xanthine derivative **16** has a 10-fold bias for BRD4 BD1 over the other BD1 domains (BRD4 BD1 IC₅₀ 5 μM) with no identifiable BD2 binding (Figure 13).³⁶ The related publication hypothesises that a hydrogen bond between the triazolo fragment and a conserved aspartic acid (Asp) residue, could be stabilised more in BRD4 BD1 by the ZA loop, which exhibits differing dynamics across the BET family, and thus differing levels of stabilisation. More recently, Zhou *et al.* reported a series of BRD4 isoform selective inhibitors developed *via* a structure-based design approach.³⁷ The group analysed available X-ray crystal structures of

known BRD4 inhibitors and produced a pharmacophore model, leading to a fragment merging and elaboration based approach. Exemplars from this work include diazobenzenes **17** and **18** (Figure 13), which, when tested in a TR-FRET assay, displayed 30 – 60-fold BRD4 selectivity over BRD2, 50 – 90-fold selectivity over BRD3, and 70 – 120-fold selectivity over BRDT. No selectivity was exhibited between BRD4 BD1 and BD2 domains.

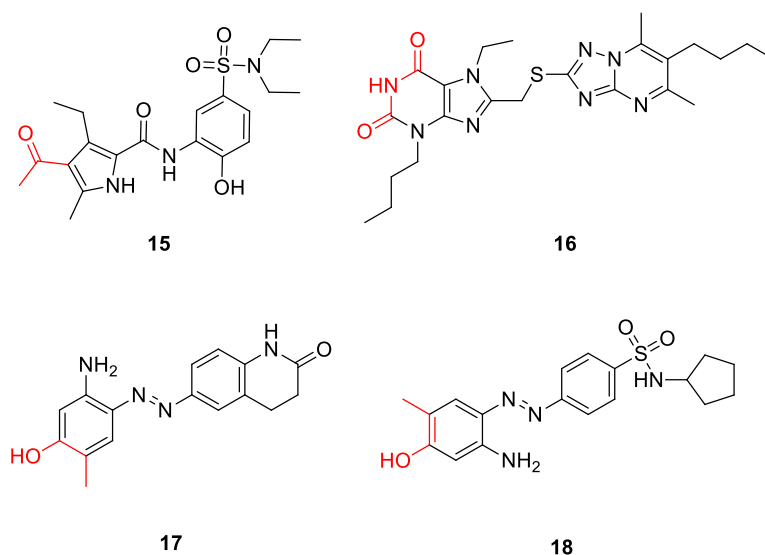


Figure 13: BRD4 isoform selective inhibitors acyl pyrrole **15**, xanthine **16**, and diazobenzenes **17** and **18**.

Significant work has been achieved by Ciulli *et al.*, who have taken a chemical biological approach to establish BET sub-family selectivity. The group have developed a “bump-and-hole” strategy, which was first disclosed in 2014 (Figure 14).³⁸ The method involves developing a series of analogues of known pan-BET ligands bearing a sterically bulky “bump” that complements a “hole” on a mutant bromodomain protein. All bromodomains in the BET family contain a conserved leucine residue in the ZA loop (Leu94 in BRD4 BD1) that can be mutated to the smaller residue alanine, thus generating a “hole” in the protein. A methyl ester analogue of I-BET762 **1**,

ET **19**, was generated also possessing a functionalised methylene side-chain with a stereodefined ethyl group to act as the “bump” (Figure 14). Full profiling of the selectivity of **19** for mutant bromodomains relative to wild type was achieved by isothermal calorimetry for all eight BET proteins. This profiling highlighted that binding selectivity for the mutant versus wild type bromodomain can be achieved, with selectivities of up to 540-fold and no less than 30-fold observed across the BET protein family. This work highlights an alternative engineered method to achieve BET sub-family selectivity by utilising single point change mutant BET proteins.

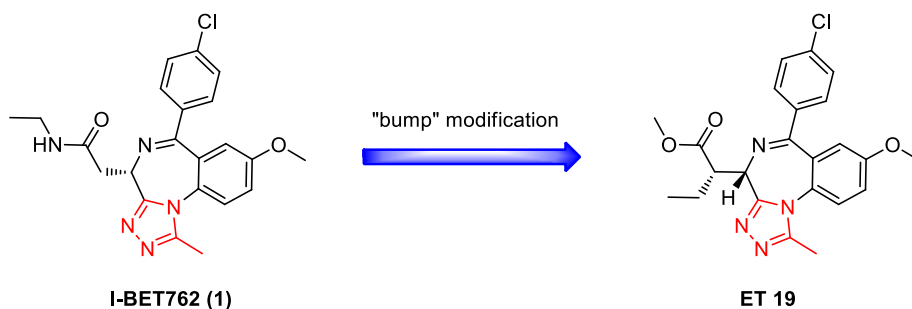


Figure 14: The “bump-and-hole” strategy developed by Ciulli *et al.* utilises analogues of known BET inhibitors.³⁸⁻⁴⁰

Ciulli *et al.* have further developed this strategy, synthesising alternate analogues for I-BET762 **1**, that target different protein vectors, which also show isoform selectivity *via* the “bump-and-hole” approach.³⁹ Most recently, the group have optimised their “bump-and-hole” strategy,⁴⁰ introducing a leucine/valine mutation rather than the more disruptive leucine/alanine mutation previously disclosed. A lead optimisation effort guided by the SAR of known benzodiazepine analogues led to the generation of 9-ME-1 **20**, a methyl ester variant of I-BET762 **1**, that also contains a stereodefined methyl substituent acting as the “bump” (Figure 15). 9-ME-1 **20** shows > 100-fold selectivity for the L/V mutant over wild type bromodomain proteins. This probe has been used to investigate and compare the roles of the first and second bromodomains in chromatin binding. To date, this has been a challenging task due to the availability of high quality, domain

selective chemical probes, and so Ciulli's chemical biology approach has proved significant. The experiments performed with 9-ME-1 **20** highlighted the importance of the BD1 domain in all BET proteins for the function of chromatin recognition. It was shown that the BD2 domain has varying levels of importance in chromatin recognition, while that BRD4 BD2 is essential for gene expression; it was hypothesised that this protein is needed for the recruitment of non-histone proteins. Ciulli *et al.* have delivered a useful methodology to probe the specific functions of the BD1 and BD2 domains, without the development of highly domain selective tool molecules.

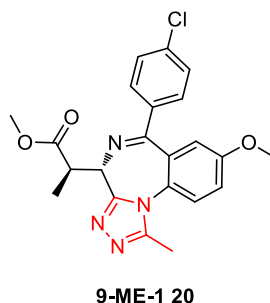


Figure 15: An optimised “bump-and-hole” strategy led to the development of 9-ME-1 **20**, which was utilised in experiments probing domain specific functions.⁴⁰

The difficulty in designing a compound which is truly selective (> 1000-fold) for BD1 or BD2 arises from the structural similarity of the BD1 and BD2 domains. This challenge is highlighted by the small number of selective BET BD1 or BD2 probes which have been reported in literature. Within the BET binding pocket, the BD1 and BD2 domains have 100% sequence homology.³² When considering residues adjacent to the binding pocket, the domains differ in amino acid sequence at only five positions (Table 1).³²

Amino Acid Point Change	BRD2 BD1/BD2	BRD3 BD1/BD2	BRD4 BD1/BD2	BRDT BD1/BD2
1	I162/V435	I122/V397	I146/V349	I115/V357
2	D160/H433	D120/H395	D144/H437	D113/H355

3	K107/A380	K67/A342	K91/A384	K60/A302
4	Q101/K374	Q61/K336	Q85/K378	R54/N296
5	R100/Y373	Y60/Y335	Q84/Y377	Q53/Y295

Table 1: The differences in BET BD1 and BD2 primary structure.³²

Although subtle, the changes in the BD1 and BD2 bromodomain structure have the potential to be exploited in the development of domain specific small molecule inhibitors. Utilisation of the available literature and crystallographic data will potentially allow for the development of truly selective (> 1000-fold) BET BD1 chemical probes. Such probes are essential to fully understand the domain specific function of the BD1 (and BD2) bromodomains, and have the potential to progress as therapeutics which avoid the toxicity profile associated with pan-BET inhibition.

1.4 Chemical probes

A chemical probe can be defined as a small molecule which can reversibly or irreversibly bind to a particular biological target in a selective manner, and can interrogate the biological system of interest to determine target function. Although they have the potential to be developed into therapeutics, the characteristics of a chemical probe and a drug can differ. Parameters for a desired chemical probe have been described by Bunnage and co-workers (Figure 16).

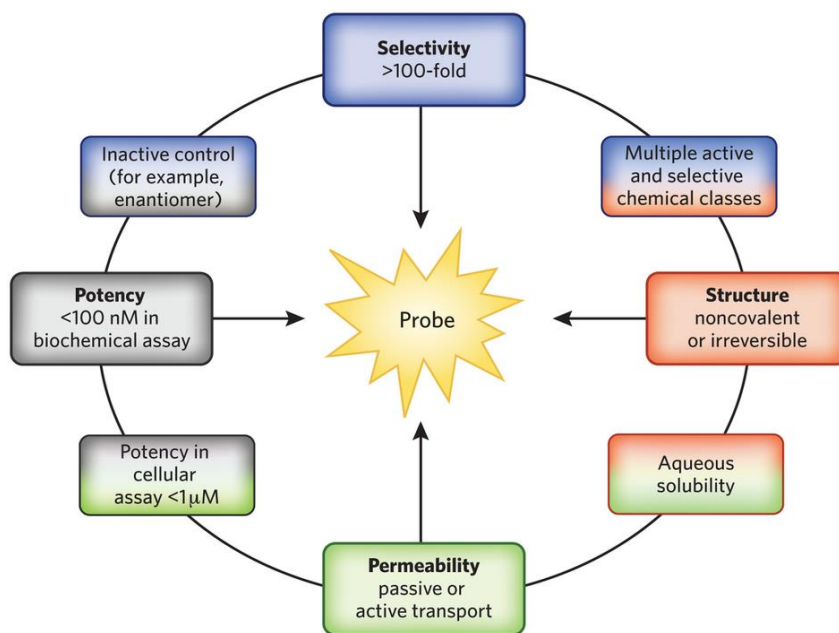


Figure 16: Bunnage and co-workers report the general characteristics required of a useful chemical probe.⁴¹

For a chemical probe to be utilised in assessing the function of a biological target, it is essential that it can reach the site of action. Consequently, permeability is a key consideration when designing a chemical probe; it is important that evidence is generated to support cell permeability. This parameter can be measured directly by permeability assays, or indirectly *via* whole-cell potency assays. If a chemical probe is intended for *in vivo* purposes, aqueous solubility also becomes important with regard to accessing the site of action. If permeability is considered a prerequisite for a quality chemical probe, the next consideration is target engagement and potency

at the site of action. Potency can be assessed *via* biochemical and cellular assays. Biochemical assays provide a simple view of potency, and can only confirm that the probe is engaging the target. Whole-cell phenotypic assays provide a more in-depth analysis of target engagement and efficacy. The selectivity profiles of a chemical probe and a drug have very different criteria. A chemical probe is used to investigate the phenotypic effect and function of a specific biological target, and it is thus imperative that it has high selectivity for that target to have confidence in correlating the target of interest to the observed phenotype. By contrast, a therapeutic often does not need as strict a selectivity profile. A drug must be efficacious and safe, but this may be achieved without strict selectivity. In fact, 'safe' promiscuity may be warranted to achieve high efficacy. While it is desirable to have high selectivity, it is certain that a chemical probe will have some off-target effects. Consequently, it is recommended to build a chemical tool kit of structurally orthogonal probes to allow for cross-validation. A structurally related inactive control compound is also useful for this purpose. If these criteria can be adhered to, a chemical probe can be a powerful tool in identifying and validating target function, with the prospect of therapeutic development.

2.0 Proposed Work

The aim of this project is to develop a truly selective (>1000 fold) BET BD1 bromodomain chemical probe. Ideally, the probe will have the required physicochemical properties to be capable of *in vivo* studies. A suitable probe will allow elucidation of the biological function of the BET BD1 bromodomain. As yet, no truly selective BET BD1 chemical probes at the (>1000-fold) level noted above have been disclosed in the literature. This will be of significant interest to the scientific community as little is known about the domain specific functions of the BD1 bromodomain. If this can be understood, it will aid the development of therapeutics targeting BET proteins.

The parameters for a BET BD1 selective chemical probe have been adapted from Bunnage's work.⁴¹ In particular, a TR-FRET biochemical pIC₅₀ and Whole Blood Monocyte chemoattractant protein-1 (hWB MCP-1) cell based pIC₅₀ of > 7 (IC₅₀ < 100 nM) are desired, this will ensure sufficient target engagement and efficacy. Crucially, 1000-fold selectivity over the BET BD2 domain is required. This is a result of emerging data from elsewhere in our laboratory where BET BD2 selective inhibitors are being developed.⁴² In this related programme, it has been shown that less than 1000-fold selectivity is insufficient to ensure engagement of only the second domain. As a result, this knowledge has been adapted for the BET BD1 domain probe. Additionally, 100-fold selectivity over non-BET bromodomains is desired. Such a selectivity profile will ensure that when utilised to probe the function of the BD1 domain, any biological effect observed can be attributed to the BET BD1 domain, and not to other related bromodomains. Sufficient potency and selectivity is key to enable association between *in vitro* and *in vivo* findings. Finally, in conjunction with high affinity and selectivity, it is desired that the probe has high cell permeability and solubility. This will allow it to be used *in vivo* studies to generate useful pharmacokinetic and pharmacodynamic data.

The starting point for this project is a historic BET ‘benzimidazole’ series developed within our laboratories⁴³ An example from the series is benzimidazole **21**, a highly profiled pan-BET bromodomain inhibitor. A key structural feature of benzimidazole **21** is the pyridone ‘warhead’ which acts as the KAc mimetic as can be seen in the crystal structure of **21** in the BRD4 BD1 binding region (Figure 17 (a)). The di ether motif extends into a region known as the WPF shelf (Figure 17 (b)). Additionally, benzimidazole **21** extends into the ZA channel, which is situated between the α Z and α A helices of the bromodomain (Figure 17 (c)). The morpholine substituent extends into solvent.

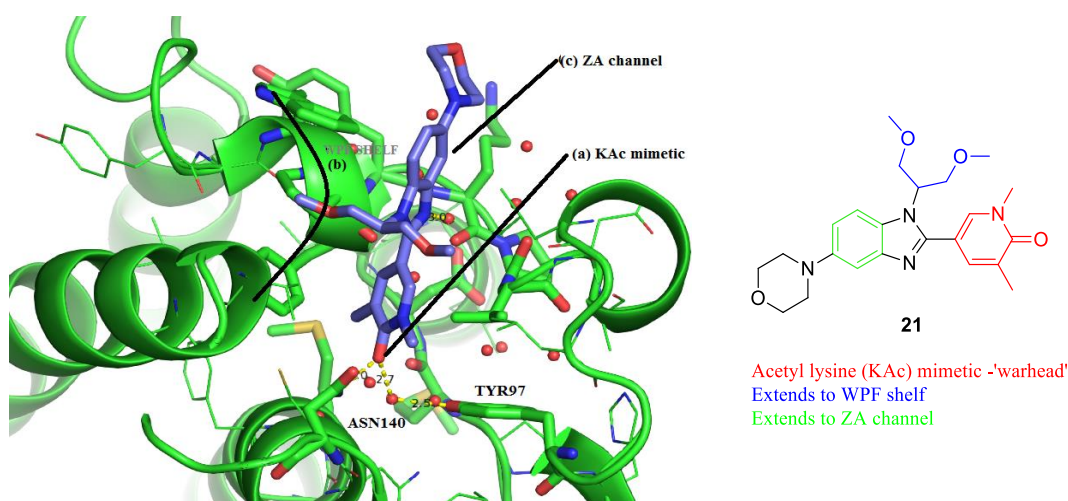


Figure 17: X-ray crystal structure of benzimidazole **21** co-crystallised in BRD4 BD1. (a) key interaction of the KAc mimetic with Asn140 (a), (b) interactions of the WPF shelf (c) ZA channel.

During the development of the benzimidazole series, over 1500 compounds were designed and synthesised to produce relevant SAR. The series was ultimately terminated by GSK when Boehringer Ingelheim released a patent covering the structure of the benzimidazole compounds.⁴⁴ Data mining of the GSK series highlighted that several of the compounds show inherent BD1

bromodomain selectivity. As a result, this series was chosen for further development in this project. Therefore, all known data on the benzimidazole series was interrogated using the Spotfire visualisation software to highlight SAR relevant to BD1 selectivity. It was envisaged that existing SAR could generate hypotheses for the next generation of analogues which could ultimately lead to a high quality chemical probe.

By developing a high-quality BET BD1 selective chemical probe, the source of this BD1 selectivity would also be investigated, with a view to developing further understanding in this overarching area. The source of BD1 selectivity for the benzimidazole series has not previously been investigated. This could aid the design of the BD1 selective series, whilst also generating knowledge for future generations of BET BD1 and BD2 selective chemical probes. In order to achieve this aim, both computational methods and x-ray crystallography will be used.

3.0 Results and Discussion

3.1 Spotfire visualisation of the benzimidazole series

In order to identify which substituents of the benzimidazole core were already providing BD1 selectivity, Spotfire analysis of historic compounds was undertaken. Initially, the benzimidazole motif with the pyridone ‘warhead’ was treated as the ‘core’ structure **22**, as much of data available was for this scaffold. Each vector from the benzimidazole was treated as a different R–group vector (Figure 18).

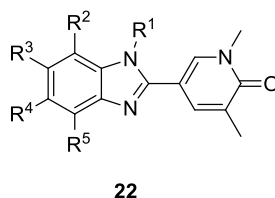
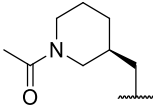
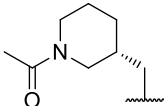
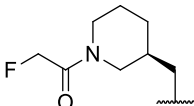
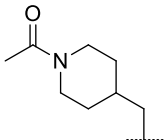
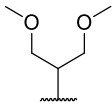


Figure 18: R–group analysis was carried out on the benzimidazole series **22**, constituting five R group vectors.

Analysis of the R1 vector, which extends out to the WPF shelf region, was carried out where R2 – R5 were hydrogen. This showed that capped piperidine motifs were consistently providing BD1 selectivity by significantly increasing BD1 potency, while BD2 potency is marginally increased (Table 2). Acetyl–capped piperidine **23** shows 1.8 log units selectivity for BRD4 BD1 over BD2 (Entry 1, Table 2). Interestingly, acetyl-capped piperidine **24**, the enantiomer of **23**, has a lower BD1 selectivity, at 1.2 log units (Entry 2, Table 2). The regioisomer of **24**, acetyl-capped piperidine **26**, maintains BD1 selectivity at 1.7 log units, but has a significantly decreased BRD4 BD1/BD2 potency of 6.8/5.1. This comparison highlights that ‘meta’ substitution of the acetyl-piperidine ring is the preferred substitution pattern for this substituent. Fluorinated acetyl-capped piperidine **25** also exhibits good BD1 selectivity at 1.7 log units, indicating that substitution from the acetyl group is tolerated. The diether motif present in benzimidazole **27** provides 1.1 log units

of selectivity at BD1 (Entry 5, Table 2). Where R1 is a methyl group, BD1 bias is still maintained with benzimidazole **28** showing 0.9 log units selectivity for BRD4 BD1 over BD2, however this compound has low potency ($pIC_{50} < 6$) (Entry 6, Table 2). This supports the previously mentioned strategy of accessing the WPF shelf to increase potency (Section 1.3). Certain shelf groups provide potency but not sufficient selectivity. For example, a benzylic shelf group provides no BD1 selectivity while having potency at BRD4 BD1/BD2 in the desired space (pIC_{50} 7.6/7.2) (Entry 7, Table 2). Sulfone shelf groups were shown to not be potent ($pIC_{50} < 6$) and have no selectivity for BD1 over BD2 (Entry 8, Table 2).

Entry	Compound Number	R1 (WPF shelf group) ^a	BRD4 BD1/BD2 pIC_{50}	BD1 Selectivity
1	23		8.0/6.2	1.8
2	24		7.5/6.3	1.2
3	25		7.7/5.9	1.8
4	26		6.8/5.1	1.7
5	27		7.4/6.3	1.1

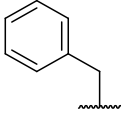
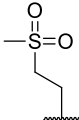
6	28	-CH ₃	5.7/4.8	0.9
7	29		7.6/7.2	0.4
8	30		5.7/5.4	0.3

Table 2: ^aWhere R2 – R5 = H. Results of data mining of compounds functionalised at the R1 position. Green denotes ‘good’ selectivity of 1.5 – 1.8 log units; amber denotes ‘moderate’ selectivity of 0.9-1.4 log units; red denotes ‘minimal’ selectivity of 0.3 – 0.8 log units. The potency data disclosed is the mean of at least 2 test occasions.

Match-pair analysis of the R5 vector indicated that addition of a chloro- or methoxy-substituent can further increase BD1 selectivity (Figure 19). In this analysis, R2 – R4 were set as hydrogen, and the R1 vector was varied to a pyran, acetyl piperidine, and diether motif.

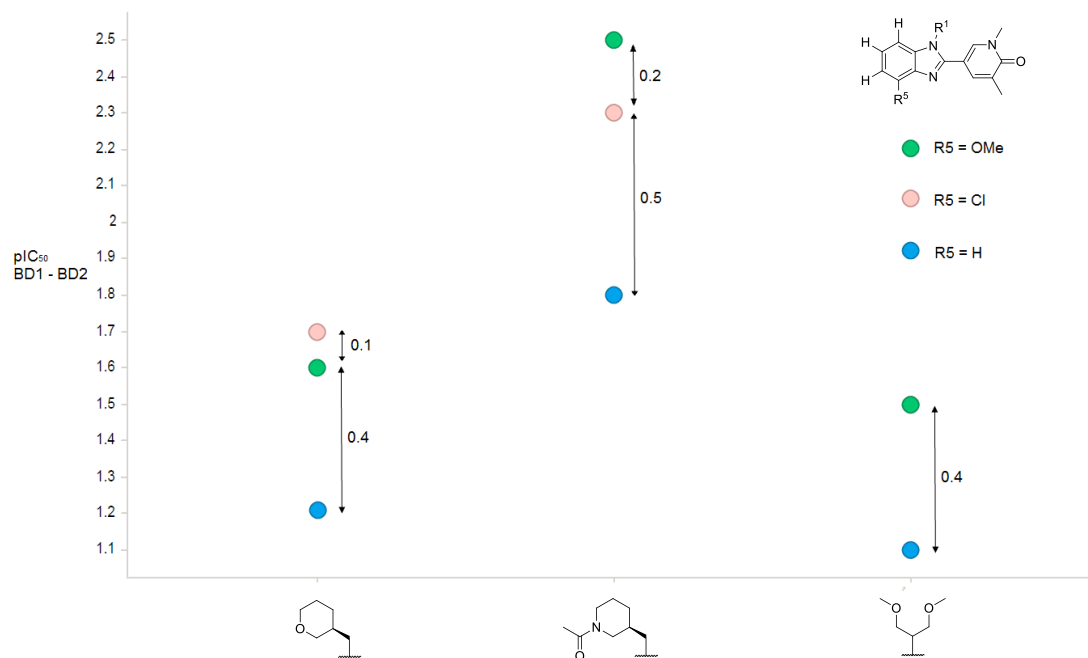


Figure 19: Match-pair analysis of the R5 vector.

A match-pair analysis of the R4 vector was carried out. In this instance, vectors R2, R3, and R5 were set as hydrogen, and various R1 groups were selected. From this data, it was noted that addition of a 4-*N*-methylpiperazine moiety could provide a further jump in selectivity of up to 0.4 log units (Figure 20).

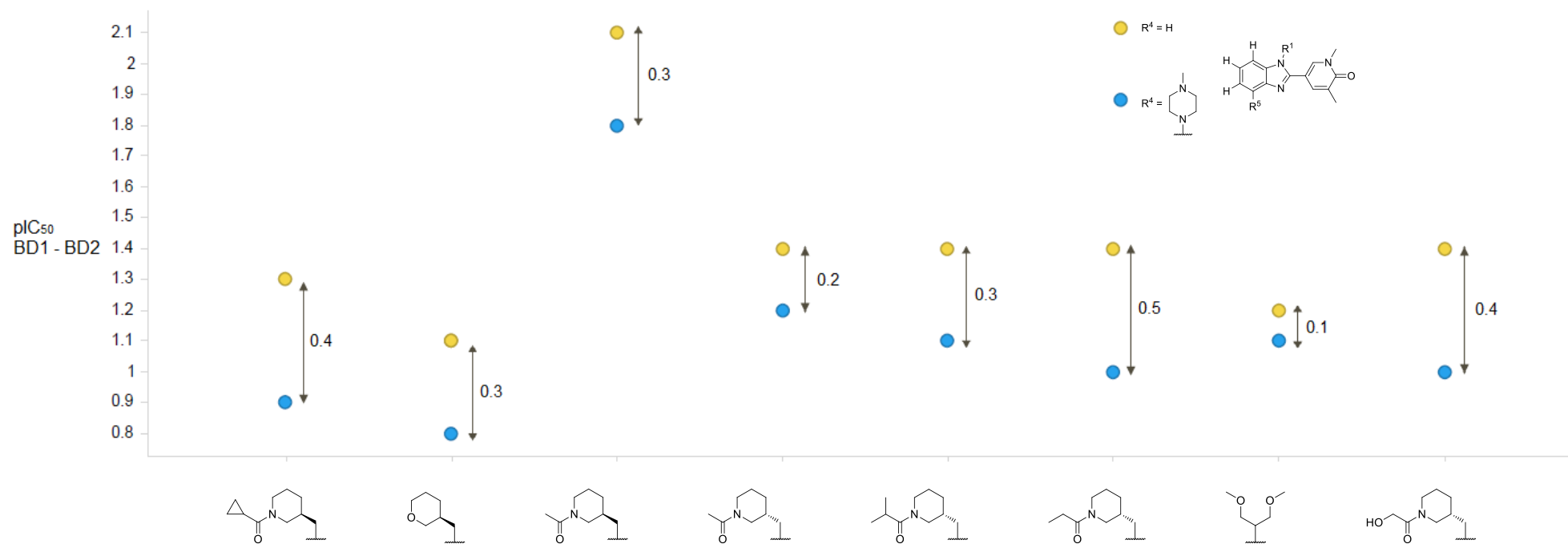


Figure 20: Match-pair analysis of the R4 vector.

Although it was found that addition of a 4-*N*-methylpiperazine substituent at the R4 position provides a small increase in BD1 selectivity, investigation of this vector was down prioritised. Incorporation of bulky heterocyclic rings to the benzimidazole core will add significantly to the molecular weight of this series, which is already close to 500 amu. It was envisaged that the R1 substituent would also add molecular weight to the series, and so this vector was prioritised over the R4 vector.

It was decided that the R1 and R5 vectors were the key areas of interest for generating further SAR and selectivity for BD1. Each vector and relevant motif will be analysed in turn in order to determine what it is providing BD1 selectivity. Analogues will be synthesised in efforts to further increasing BD1 selectivity over BD2.

3.2 Functionalising the R5 vector

Spotfire analysis had shown that where R5 is a chloro- or methoxy-substituent, an increase in BD1 selectivity is observed. In order to further investigate what parameters are driving this effect, and with the aim of increasing the selectivity window, further analogues were designed that varied electronics, size, and polarity (Figure 21). The acetyl-piperidine motif was chosen as the preferred R1 substituent, as it had previously been shown to exhibit good BD1 selectivity.

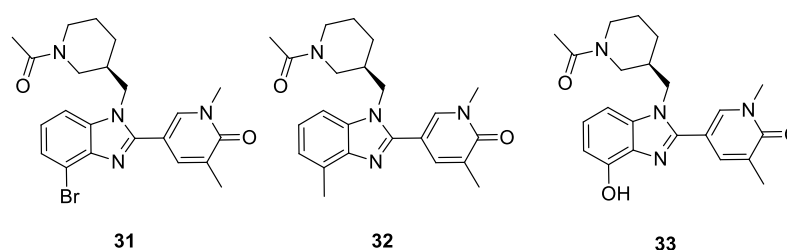
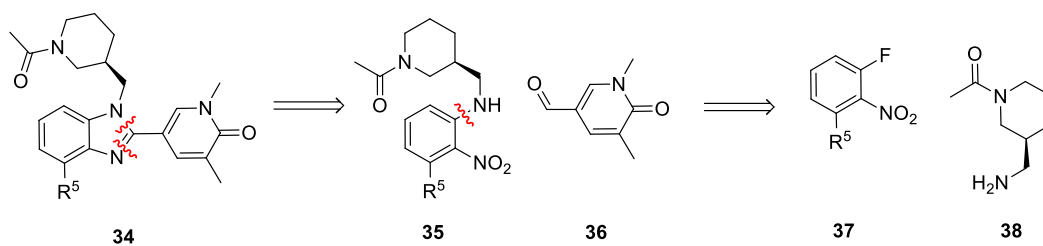


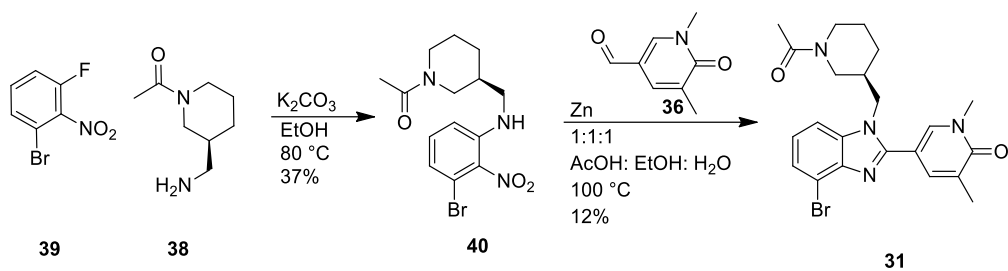
Figure 21: Target analogues varying at the R5 position.

It was known that the target benzimidazoles could be made in two key steps. An initial nucleophilic aromatic substitution (S_NAr) reaction would install the amine **38**, followed by a one-pot nitroreduction and cyclisation to form the benzimidazole core (Scheme 1).



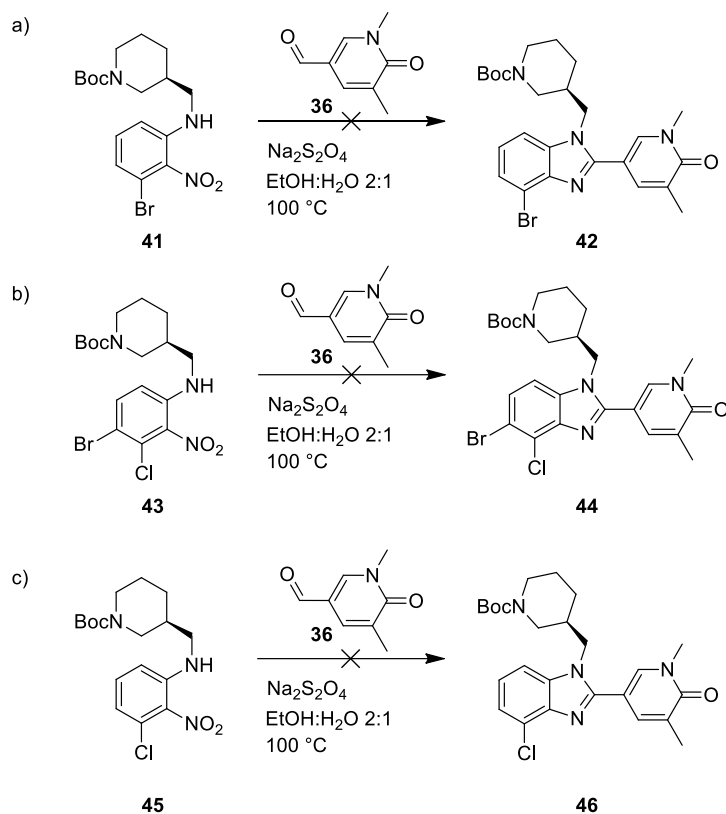
Scheme 1: Retrosynthetic analysis of target compounds varying at R5.

With this in mind, the synthesis of benzimidazole **31** was achieved in two steps (Scheme 2). An S_NAr reaction carried out in ethanol gave nitro aniline **40** in a low yield (37%). A subsequent zinc-promoted nitroreduction and cyclisation of nitro aniline **40** with aldehyde **38** yielded the desired benzimidazole **31** in 12% yield.



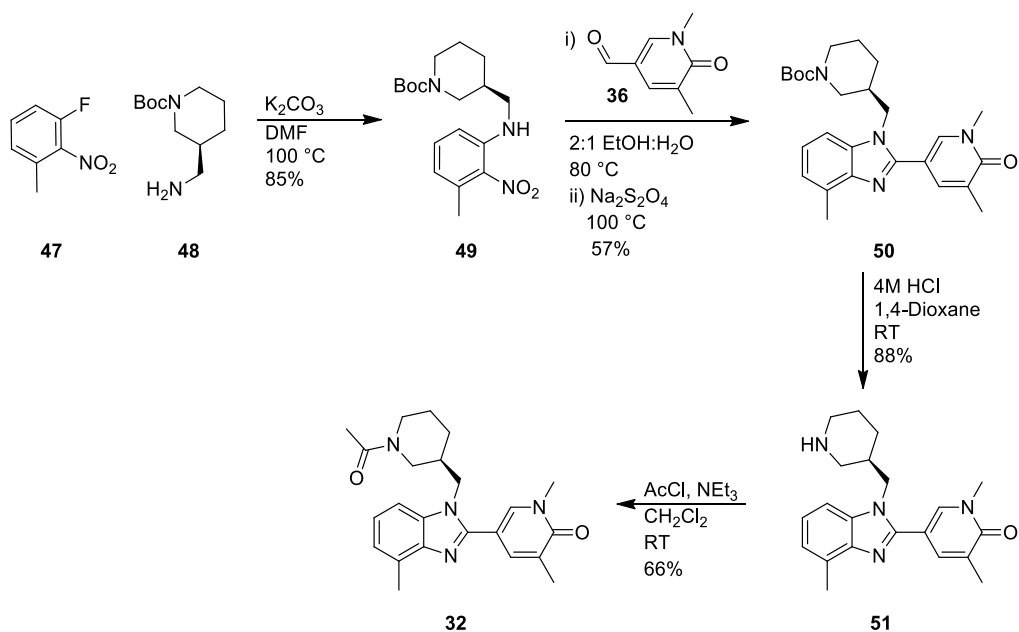
Scheme 2: Synthesis of compound **31**.

Given the low yields, optimisation of the route was necessary. Historically, the cyclisation was performed using sodium dithionite as the reducing agent,⁴⁵ whereby a nitro aniline, aldehyde **36**, and sodium dithionite were added simultaneously to the solvent and then heated to 100 °C (Scheme 3). However, attempts utilising these conditions showed no conversion to the desired product, and only starting material could be observed by LCMS (Scheme 3, (a) and (b)). An exact substrate from a historic synthesis was replicated,⁴⁵ and where previously it yielded benzimidazole **46**, no product was observed (Scheme 3, (c)).



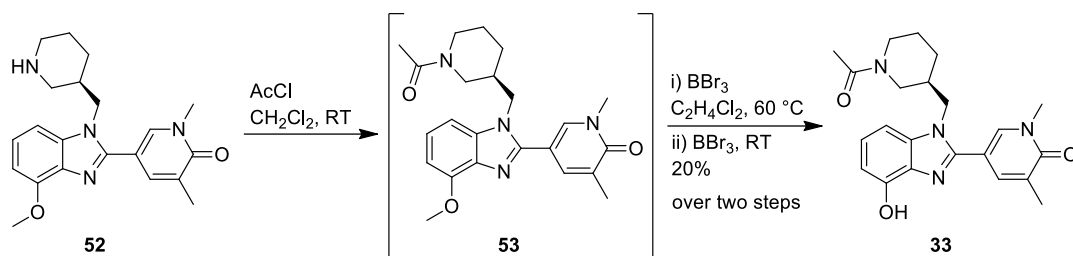
Scheme 3: Attempted benzimidazole formation using sodium dithionite.

The S_NAr was optimised on an analogue where R5 is a methyl substituent (Scheme 4). It was found that utilising *N,N*-dimethylformamide (DMF) as a solvent instead of EtOH greatly increased the yield for this S_NAr reaction. For the nitro reduction and cyclisation step, it was found that pre-mixing the aldehyde and amine at 80 °C, prior to the addition of the sodium dithionite at 100 °C, yielded the cyclised product **50** in a moderate 57 % yield. Cyclised product **50** was then treated with hydrochloric acid solution to remove the *tert*-butyloxycarbonyl (Boc) protecting group, and subsequently acetylated with acetyl chloride to yield desired benzimidazole **32** in moderate yield.



Scheme 4: Synthesis of benzimidazole **32** was achieved in four steps, utilising the optimised cyclisation conditions.

The synthesis of phenol analogue **33** was achieved in a similar manner, utilising methoxy intermediate **52**, which had previously been synthesised for another purpose (see Scheme 12). Boron tribromide was employed to demethylate the methoxy substituent, revealing phenol analogue **33** (Scheme 5).



Scheme 5: Synthesis of phenol analogue **33**.

Once analogues **31** - **33** had been synthesised, they were submitted for biological testing by means of a BRD4 FRET assay, and the data was compared with historic benzimidazole compounds (Table 3).

Entry	Compound	R5	BRD4 BD1/BD2 FRET pIC ₅₀	Selectivity
1	23	H ^a	8.0/6.2	1.8
2	31	Br	7.0/5.6	1.4
3	32	Me	7.3/5.1	2.2
4	33	OH	7.8/5.6	2.2
5	54	Cl ^a	7.5/5.2	2.3
6	55	OMe ^a	7.7/5.2	2.5
7	56^a	NH ₂ ^a	7.2/5.6	1.6

Table 3: Potency data for R5 functionalised analogues. ^aHistoric compounds.⁴⁵ The potency data disclosed is the mean of at least 2 test occasions.

Relative to benzimidazole **23**, all R5 substituents currently tested decrease in BD1 and BD2 potency (Table 3). Interestingly, BD2 potency drops further than BD1 potency, giving an increased selectivity window. It is currently unclear why this is the case. Synthesis of more R5 substituted analogues would be useful to generate a more appreciable SAR. It is thought that functionalisation of the R5 group can be used in conjunction with another vector if it is thought a further increase in BD1 selectivity or modulation of physicochemical properties is required.

3.3 Investigation of an amino acid point change between BD1 and BD2

As previously discussed, there are only a few point changes of amino acid sequence at the BD1 and BD2 domains. One such point change close to the binding site is an aspartic acid (Asp) residue in BD1 and a histidine (His) residue in BD2 (Figure 22). An aspartic acid at physiological pH exists in its carboxylate form (pKa 3.9), while a histidine residue can exist in its protonated form at physiological pH (pKaH 6.0). As such, this point change could have a significant effect on the binding of ligands in this region.

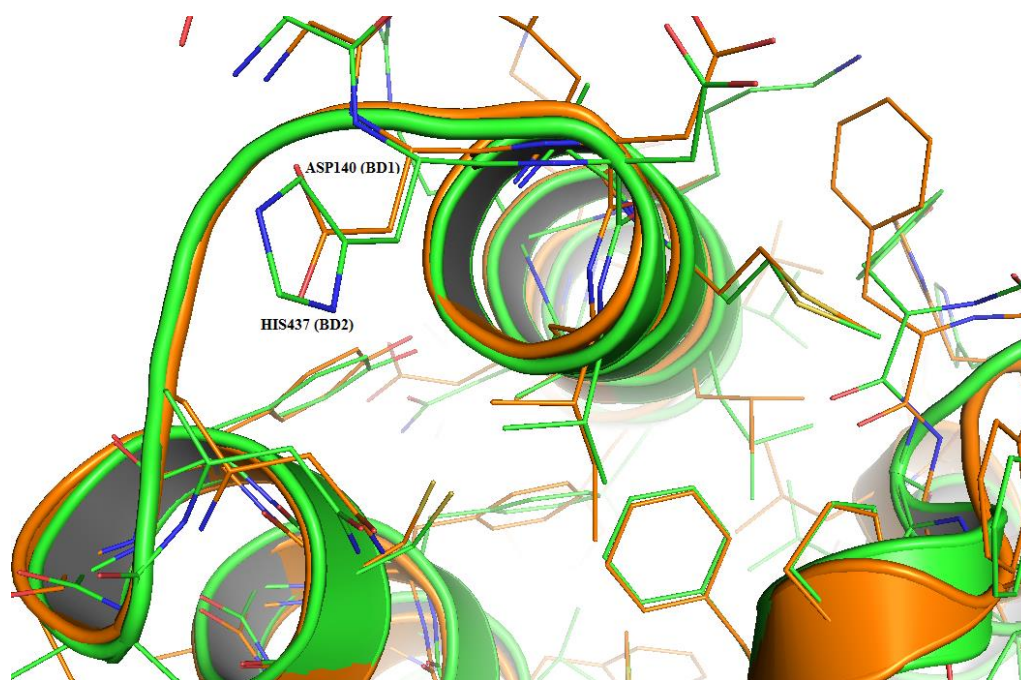


Figure 22: Overlaid X-ray crystal structures of BRD4 BD1 and BD2 with BRD4 numbering. The point change of Asp140 (BD1) to His437 (BD2) is highlighted. (PDB codes = 2oss, 2dww)

An X-ray crystal structure of benzimidazole **57**, which has an acetyl piperidine motif at R1, showed that this motif does not appear to interact with the WPF shelf, but instead the acetyl group points out towards the His433 in BRD2 BD2 (Figure 23).

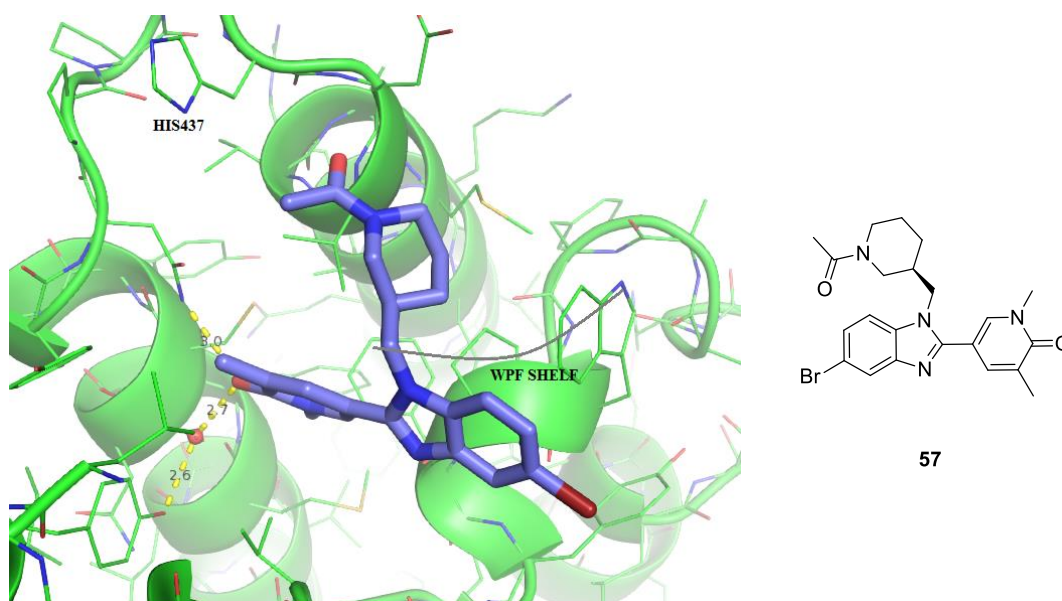


Figure 23: X-ray crystal structure of benzimidazole **57** co-crystallised in BRD2 BD2 shows that the acetyl piperidine motif is directed towards His433.

It was hypothesised that further derivatising a benzimidazole molecule by extending from the acetyl piperidine with a basic group, that would be charged at physiological pH, would result in a favourable interaction with the Asp residue in BD1, and an unfavourable interaction with His in BD2. An initial amine functionalised target **58** was chosen to test this hypothesis (Figure 24). This target was generated from the overlaying of crystal structures of related benzimidazole compounds with the BD1 domain, to determine a suitable linker length.

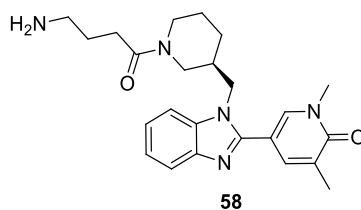
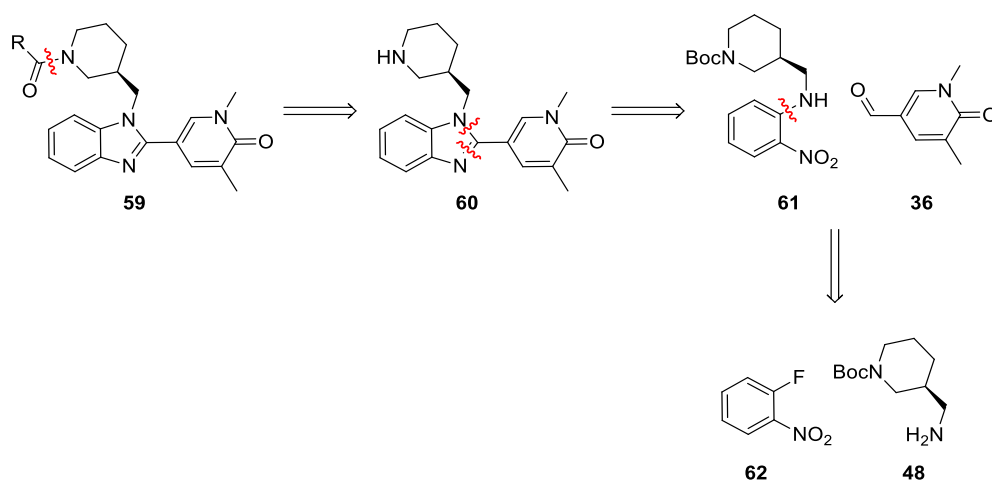


Figure 24: First generation amine functionalised target molecules.

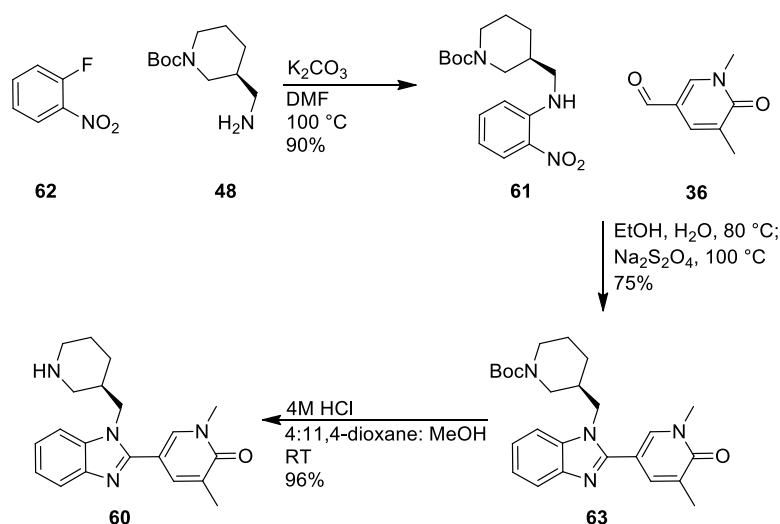
3.3.1 Synthesis of amine functionalised benzimidazoles

It was envisaged that amine functionalised targets could be synthesised in a similar fashion to previous compounds *via* an initial S_NAr reaction followed by a one-pot nitro reduction and cyclisation to generate the benzimidazole core (Scheme 6). The amide functionality would be introduced at the final step by an amide coupling between benzimidazole **60** and the amine functionalised carboxylic acid coupling partner (Scheme 6). This route would allow for late stage derivatisation and rapid synthesis of analogues.



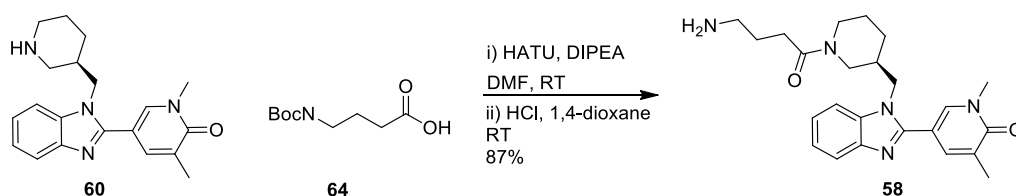
Scheme 6: Retrosynthetic analysis of amine functionalised target molecules.

Synthesis of the benzimidazole core **60** was achieved in three steps (Scheme 7). An S_NAr reaction to couple nitrophenyl **62** and amine **48** gave nitro aniline **61** in excellent yield. A sodium dithionite promoted nitro reduction and cyclisation with aldehyde **36**, followed by a Boc deprotection produced benzimidazole core **60** in good overall yield.



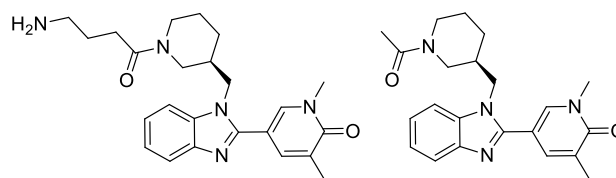
Scheme 7: The synthesis of key benzimidazole intermediate **60** was achieved in three steps.

The initial target **58** was synthesised by an amide coupling between amine **60** and a suitable carboxylic acid coupling partner, and subsequent Boc deprotection. Use of hexafluorophosphate azabenzotriazole tetramethyl uronium (HATU) reagent and DMF gave **58** in good yield after Boc deprotection and purification by mass-directed auto-prep (MDAP) (Scheme 8).



Scheme 8: Benzimidazole **58** was synthesised *via* HATU promoted amide coupling.

Benzimidazole **58** was submitted to the BRD4 TR-FRET assay, testing against BRD4 BD1 and BD2. A MCP-1 cell potency assay was also carried out, to assess the correlation between biochemical and cell-based potency. ChromLogD_{7.4} values were also measured (Table 4).



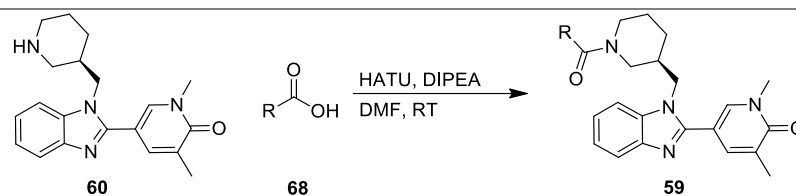
Compound	58	23
BRD4 BD1/BD2 pIC₅₀	7.8/5.6	8.0/6.2
Selectivity BD1–BD2	2.2	1.8
hWB MCP-1 pIC₅₀	6.3	-
ChromLogD_{7.4}	1.18	2.20

Table 4: Biological data of amine target **58** compared to acetyl piperidine **23**. The potency data disclosed is the mean of at least 2 test occasions.

Benzimidazole **58** does provide an increased selectivity window compared to benzimidazole **23**. Benzimidazole **58** has a lower BD1 and BD2 potency compared to benzimidazole **23**; the increase in selectivity derives from an increased relative drop in BD2 potency. In a cell-based assay, benzimidazole **58** had a markedly lower potency of 1.5 log units relative to the biochemical TR-FRET assay. This may be explained by the relatively low ChromLogD_{7.4}, and possible low permeability into cells. This initial result was encouraging, as it highlights that increased BD1 selectivity can be derived from amine functionality, supporting the initial hypothesis.

To further probe the hypothesis, a second pool of amine functionalised benzimidazoles was designed. Benzimidazoles **65**, **66**, and **67** were designed to test the effect of reduced hydrogen bond donors, linker length, and aromaticity on BD1 selectivity, respectively.

In a similar fashion to **58**, each compound was synthesised by a HATU promoted amide coupling of amine **60** and a corresponding carboxylic acid coupling partner **68**, followed by Boc deprotection if required (Table 5). All three reactions show excellent conversion to desired product; the low reported yields arise from poor recovery of free amine compounds during purification by reverse phase chromatography.



Entry	Compound	Acid	Conditions	% Yield
1	65		2 h ^a	47
2	66		2 h	23 ^b
3	67		17 h ^a	19 ^c

Table 5: Synthesis of second generation amine functionalised benzimidazoles.^aAdditional carboxylic acid was added at 1 h. ^bYield over two steps after subsequent Boc deprotection. ^cIsolated as the formic acid salt.

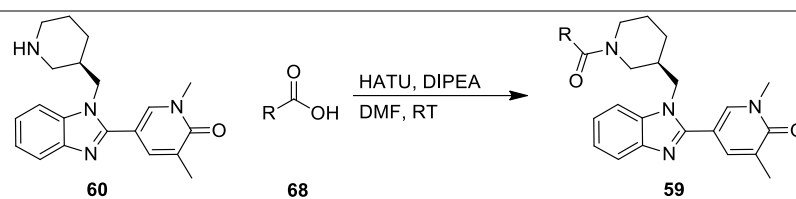
These three final compounds were then submitted for biological testing, in an analogous manner to benzimidazole **58** (Table 6).

Compound	65	66	67	58
BRD4				
BD1/BD2	8.0*/5.8*	7.9/6.0	7.0/4.9	7.8/5.6
pIC₅₀				
Selectivity				
BD1–BD2	2.2	1.9	2.2	2.2
hWB MCP-1				
pIC₅₀	6.8	6.3	-	6.3
ChromLogD_{7.4}	1.48	1.21	1.30	1.18

Table 6: Biological data of second generation benzimidazole compounds. The potency data disclosed is the mean of at least 2 test occasions, for n=1 data, this is stated by *.

Benzimidazole **65** was designed to remove hydrogen bond donors from the molecule, to determine if this influences BD1 selectivity and cell potency. Comparing to benzimidazole **58**, it has the same BD1 selectivity, but increased BD1 and BD2 potency. Furthermore, the MCP-1 cell potency has increased by 0.5 log units, at 6.8, compared to 6.3 for benzimidazole **58**. Benzimidazole **66** has an additional CH₂ moiety compared to benzimidazole **58**, to examine the effect of increased linker length on BD1 potency and selectivity. Indeed, there is an increase in BD1 and BD2 potency, but a slight drop in BD1 selectivity relative to benzimidazole **58**. Finally, benzimidazole **67** contains an aromatic imidazole group, to compare sp² to sp³ hybridised functional groups. Benzimidazole **67** has the same selectivity window as **58**, but a BRD4 BD1 potency of only 7.0, which is at the lower limit of desired efficacy range. Consequently, no further investigation of this molecule was undertaken.

While benzimidazoles **58**, **65**, and **66** had an increased BD1 selectivity compared to acetyl-substituted benzimidazole **23**, they all contained a flexible alkyl linker. It was thought that by rigidifying this linker, a more directional interaction with the aspartic acid or histidine could be achieved. Consequently, a lower entropic penalty could result in an increase BD1 potency, whilst lowering BD2 potency. As such, six-membered heterocycles **69** – **74** were synthesised by HATU-promoted amide coupling to test this theory (Table 7).



Entry	Compound	Acid	Conditions	% Yield
1	69		1 h	40
2	70		1 h	25 ^a
3	71		1 h	58

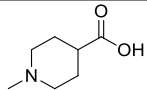
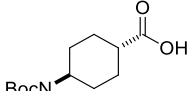
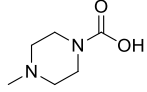
4	72		1 h	28
5	73		1 h	3 ^a
6	74		1 h	36

Table 7: Synthesis of N-heterocyclic third generation benzimidazole compounds. ^aYield over two steps after subsequent Boc deprotection.

In a similar fashion, benzimidazoles **69** – **74** were submitted for biological testing (Table 8).

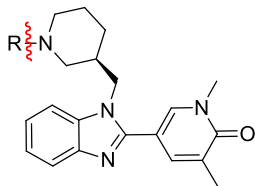
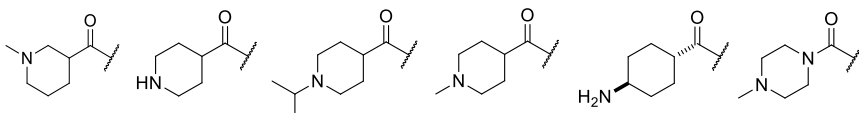
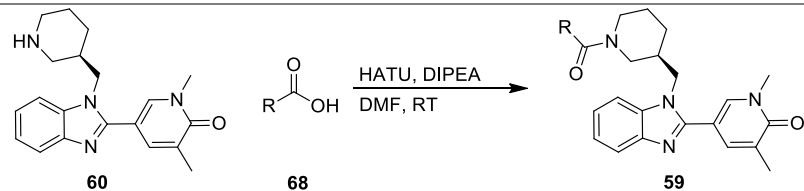
						
R=						
						
Compound	69^a	70	71	72	73	74
BRD4						
BD1/BD2	6.8/5.1	7.5/4.9	7.8/4.8	7.7/4.8	7.9/5.1	7.0/4.6
pIC₅₀						
Selectivity						
BD1–BD2	1.7	2.6	3.0	2.9	2.8	2.4
hWB MCP-1 (cell) pIC₅₀	6.8*	5.9	7.1	6.8	6.5	6.6
ChromlogD_{7.4}	1.68	1.30	1.69	1.46	1.40	2.12

Table 8: Biological data of third generation N-heterocyclic benzimidazoles. ^aSubmitted as a diastereomeric mixture. The potency data disclosed is the mean of at least 2 test occasions, for n=1 data, this is stated by *.

Analysis of the biological data shows that all benzimidazoles in this generation of compounds, except benzimidazole **69**, have an increased BD1 selectivity relative to the acetyl piperidine motif in compound **23**. Regarding benzimidazole **69**, this was submitted for test as a

diastereomeric mixture, which could explain the lower BD1 selectivity. However, its lower BD1 potency meant that there was no further investigation of this compound. Benzimidazole **70** was designed to have an alternative nitrogen substitution pattern to **69**, and has a good BD1 potency (BRD4 BD1 pIC₅₀ 7.5), and a good BD1 selectivity of 2.6 log units. However, it exhibits a large drop in potency when measured in cells, with a MCP-1 pIC₅₀ of 5.9, a 1.6 log unit drop off from the biochemical assay. Benzimidazoles **71** and **72** were designed to cap the nitrogen of the piperidine ring, to remove a hydrogen bond donor. Benzimidazoles **71** and **72** show excellent BD1 potency (BRD4 BD1 pIC₅₀ 7.8 and 7.7, respectively). Benzimidazole **72** has a BD1 selectivity of 2.9 log units, which is close to the desired window of 3.0 log units. Indeed, benzimidazole **71** has a BD1 selectivity of 3.0 log units, and thus is within the desired window of selectivity. With regards to the cell-based assay, benzimidazole **71** has good cell potency (hWB MCP-1 pIC₅₀ 7.1) that exceeds the desired criteria. Benzimidazole **72** also exhibits good cell-based potency (hWB MCP-1 pIC₅₀ 7.8), albeit it below the desired figure of 7.0. Benzimidazole **73** also contains a six-membered ring, but now contains a primary amine as the basic functionality. This benzimidazole also exhibits excellent BD1 potency (BRD4 BD1 pIC₅₀ 7.9), and BD1 selectivity at 2.8 log units. However, compared to benzimidazoles **71** and **72**, it has a larger drop-off between biochemical and cell-based potency measurements (hWB MCP-1 pIC₅₀ 6.5). Finally, benzimidazole **74** contains a piperazine based heterocycle, as an alternative to the piperidine motif previously used. Benzimidazole **74** exhibits a lower BD1 potency than its counterparts (BRD4 BD1 pIC₅₀ 7.0), and a lower BD1 selectivity at 2.4 log units; it exhibits good cell-based potency, with only a small drop-off between biochemical and cell-based measurements (hWB MCP-1 pIC₅₀ 6.6). However, its BD1 potency is at the lower limit of the desired criteria, and thus was not further investigated. This iteration of compounds highlights that use of nitrogen containing heterocycles as basic functionality in the benzimidazole series is a strategy for yielding BET BD1 selectivity.

With the knowledge of nitrogen containing heterocycles in hand, a fourth pool of compounds was designed which contained heterocycles of different ring sizes to investigate if changing the ring size could affect BD1 selectivity and potency. These were again synthesised by HATU-promoted amide coupling of amine **60** and a suitable carboxylic acid coupling partner **68** (Table 9).



Entry	Compound	Acid	Conditions	% Yield
1	75		20 h ^a	30 ^b
2	76		66 h	26 ^b
3	77a, 77b		1 h	11 ^{b,c}
4	78		0.5 h	34
5	79		1 h	41

Table 9: Synthesis of fourth generation benzimidazole compounds. ^aAdditional carboxylic acid was added after 16 h. ^bYield over two steps after subsequent Boc deprotection. ^cYield of each diastereomer over three steps after Boc deprotection and diastereomer separation by chiral purification.

Table 10 summarises the biological and physical data of benzimidazoles **75** – **79**.

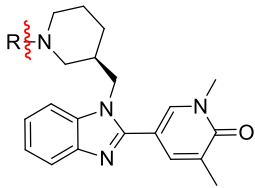
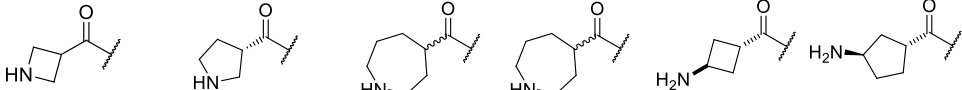
						
R =						
						
Compound	75	76	77a	77b	78	79
BRD4						
BD1/BD2	8.0/6.0	7.6/5.3	7.3/4.9	7.5/4.8	7.9/5.4	7.7/5.0
pIC₅₀						
Selectivity						
BD1–BD2	2.0	2.3	2.4	2.7	2.5	2.7
hWB MCP-1						
pIC₅₀	6.2	6.0	5.7	5.7	6.7	6.0
ChromLogD_{7.4}	1.15	1.25	1.37	1.44	1.24	1.35

Table 10: Biological data of fourth generation benzimidazole compounds. The potency data disclosed is the mean of at least 2 test occasions.

Compared to acetyl piperidine benzimidazole **23** (Figure 25), benzimidazoles **75** – **79** all have an increased BD1 selectivity. However, none of these compounds have an improved selectivity compared to isopropyl and methyl piperidines **71** and **72**. The most selective of this fourth pool of compounds are benzimidazoles **77b** and **79**, which both have a BD1 selectivity of 2.7 log units. Additionally, none of the benzimidazoles **75** – **79** have an improved cell MCP-1 potency relative to compounds **71** and **72**, although all do show activity in this regard. The ChromLogD_{7.4} measurements of these compounds are all relatively low (≤ 1.44). This data shows that nitrogen containing heterocycles of altered ring size are all tolerated, but that six-membered heterocycles provide better BD1 selectivity and cell potency.

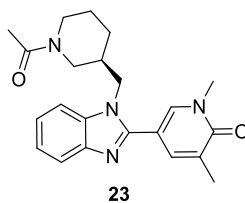


Figure 25: Acetyl piperidine benzimidazole **23**.

With reference to the overall aims of this project, it is desired to design a BD1 selective chemical probe that would have *in vivo* capabilities. From the array of compounds designed, isopropyl and methyl piperidines **71** and **72** are deemed ‘lead’ compounds regarding BD1 biochemical and cell potency, and BD1 selectivity. As such, they were progressed into subsequent assays. Both isopropyl and methyl piperidines **71** and **72** were submitted to *in vitro* metabolic stability assays, to monitor compound metabolism in both liver microsomes and hepatocytes (Table 11). If a chemical probe is to be dosed orally for *in vivo* experiments, it must be able to withstand ‘first pass’ metabolism in the liver.

Compound	71	72
BRD4 BD1/BD2 pIC₅₀	7.8/4.8	7.7/4.8
Selectivity		
BD1–BD2	3.0	2.9
hWB MCP-1 pIC₅₀	7.1	6.8
ChromLogD_{7.4}	1.69	1.46
<i>in vitro</i> microsomes		
mL/min/g liver		
<i>Human</i>	<0.40*	<0.40*
<i>Rat</i>	<0.46*	<0.46*
<i>in vitro</i> hepatocytes		
mL/min/g liver		
<i>Human</i>	<0.45*	<0.45*
<i>Rat</i>	<0.80*	<0.80*
AMP nm s⁻¹	< 3	<3

Table 11: Biological profiles of ‘lead’ benzimidazole compounds **71** and **72**. The data disclosed is the mean of at least 2 test occasions, for n=1 data, this is stated by *.

Isopropyl piperidine **71** and methyl piperidine **72** have good BRD4 BD1 biochemical potency at 7.8 and 7.7, respectively. In each case, the BD1 selectivity is also excellent at 3.0 and 2.9 log units, respectively, almost meeting the criteria set out at the beginning of the project. With regard to whole blood MCP-1 activity, both compounds have good cellular potencies, which would indicate that the compound is able to pass through cell membranes. However, both compounds have a low measured artificial membrane permeability (AMP). This apparent inconsistency cannot currently be explained. Pleasingly, both compounds have low clearance in microsome and hepatocytes in both rat and human species, indicating high metabolic stability. However, if there is a membrane permeability issue as the measured values would

suggest, the low clearance values in hepatocytes may be a product of the compounds not permeating through the cell membrane. Consequently, the hepatocyte clearance values should not be used to draw any valid conclusions about either compound. Nevertheless, the microsomal clearance data gives confidence that both compounds are metabolically stable; as microsomes do not contain a cell membrane, permeability is not an issue. Isopropyl amine **71** has been submitted for *in vivo* pharmacokinetic (PK) assays to generate the first *in vivo* PK profile for this series.

Another key aim of the project was to develop a chemical probe with at least 100-fold selectivity over non-BET bromodomains. Consequently, isopropyl piperidine benzimidazole **71** was submitted for a full-curve Bromoscan screen against a number of such proteins. pIC₅₀ values for BRD2, BRD3, and BRDT were also obtained (Table 12).

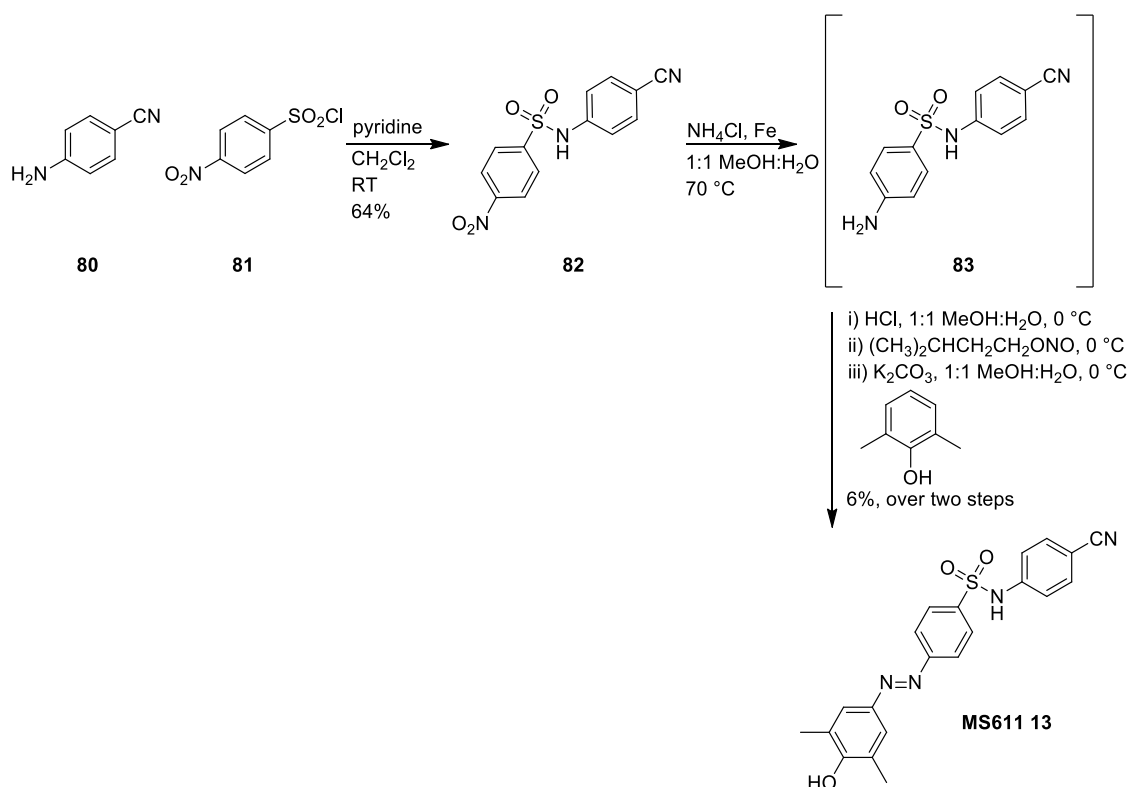
Compound	71
BRD4 BD1/BD2 pIC₅₀ (selectivity)	8.1/5.6 (2.5)
BRD2 BD1/BD2 pIC₅₀ (selectivity)	8.5/5.5 (3.0)
BRD3 BD1/BD2 pIC₅₀ (selectivity)	8.4/5.8 (2.6)
BRDT BD1/BD2 pIC₅₀ (selectivity)	8.1/5.5 (2.6)
ATAD2 pIC₅₀	< 4.50
CECR2 pIC₅₀	< 4.50
EP300 pIC₅₀	5.00
PCAF pIC₅₀	< 4.50

Table 12: Bromoscan data of benzimidazole **71** for selected bromodomains. Full list of proteins tested is available in the appendix (Section 8.0). The potency data disclosed is the mean of at least 2 test occasions.

For all non-BET bromodomains tested, all pIC₅₀ values determined were below the lower limit of the assay (<4.5), except EP300 which has a low pIC₅₀ of 5, which is well within the 100-fold selectivity window desired. For BRD2, BRD3, and BRDT, it was found that benzimidazole **71** is also BD1 selective, with a selectivity value of 2.6 log units for BRD3 and T, and 3.0 log units for BRD2. However, BRD4 BD1 and BD2 pIC₅₀ values were also determined in this assay screen that are different from that of the in-house TR-FRET assay. The in-house TR-FRET assay has shown that benzimidazole **71** has a BRD4 pIC₅₀ of 7.8/4.8 (BD1/BD2), giving a selectivity window of 3.0 log units. However, in the Bromoscan assay, the calculated BRD4 pIC₅₀ values are 8.1/5.6 (BD1/BD2), giving a selectivity window of 2.5 log units. This discrepancy can be explained by the fact that the in-house TR-FRET and out-sourced bromoscan assays use different protocols, but larger n numbers (n = 7 vs n = 2) in the BRD4 TR-FRET assay provide confidence that benzimidazole **71** achieves the desired 1000-fold BD1 selectivity window.

Isopropyl and methyl piperidines **71** and **72** are the ‘lead’ compounds in this project, with superior BD1 selectivity. However, no direct comparison to a literature BD1 chemical probe has been possible, as these compounds are tested in different assays. Consequently, it was decided to synthesis a literature compound with a high BD1 selectivity, and test it in-house to compare to the ‘lead’ benzimidazole compounds. MS611 **13** has been shown to have 100-fold selectivity over the BRD4 BD2 domain.³⁴

The first step in the synthesis of MS611 **13** was a coupling of amine **80** and sulfonyl chloride **81**, to give **82** in reasonable yield (Scheme 9). Next, an iron-promoted nitro reduction yielded intermediate **83**, which was taken through crude to a diazotisation and coupling with 2,6-dimethylphenol, yielding desired compound MS611 **13** in 6% yield over two steps.



Scheme 9: A three-step synthesis of literature BRD4 BD1 compound MS611 **13**.³⁴

With MS611 in hand, it was tested in both the biochemical TR-FRET and cell-based MCP-1 assays, to compare with ‘lead’ compounds **71** and **72** (Table 13).

Compound	71	72	MS611 13
BRD4 BD1/BD2 pIC₅₀	7.8/4.8	7.7/4.8	6.3/5.0
Selectivity BD1-BD2	3.0	2.9	1.3
hWB MCP-1 pIC₅₀	7.1	6.8	5.3*
ChromLogD_{7.4}	1.69	1.46	5.32

Table 13: A comparison of the biological data of MS611 **13** with ‘lead’ benzimidazole compounds **71** and **72**. The potency data disclosed is the mean of at least 2 test occasions, for n=1 data, this is stated by *.

With reference to table 13, MS611 **13** has a significantly lower BRD4 BD1 potency at 6.3 log units compared to benzimidazoles **71** and **72**. Furthermore, it has a lower BD1 selectivity of

1.3 log units. Additionally, MS611 **13** exhibits a low cell-based potency (hWB MCP-1 pIC₅₀ 5.3), which is 1.0 log units lower than the biochemical measurement. MS611 **13** is one of the most selective BRD4 BD1 compounds disclosed in literature.³³⁻³⁴ This data highlights the superiority of benzimidazoles **71** and **72**, and that these compounds provide a higher quality BD1 selective chemical probe to those currently available in the literature.

3.3.2 Investigating the hypothesis of BD1 selectivity in the amine functionalised benzimidazole series

It was observed that relative to acetyl piperidine **23**, BD1 pIC₅₀ is decreased or maintained for each compound from the iterations of benzimidazoles tested. On first inspection, this suggests that the hypothesised interaction with the Asp residue is not being formed, as an increased BD1 pIC₅₀ would be expected due to the formation of a strong ionic interaction. This suggests a basic substituent may not be required for BD1 selectivity. To investigate this theory, three benzimidazoles, **84**, **85**, and **86**, which are functionalised from the acetyl piperidine motif but do not contain a basic nitrogen, were designed (Figure 26).

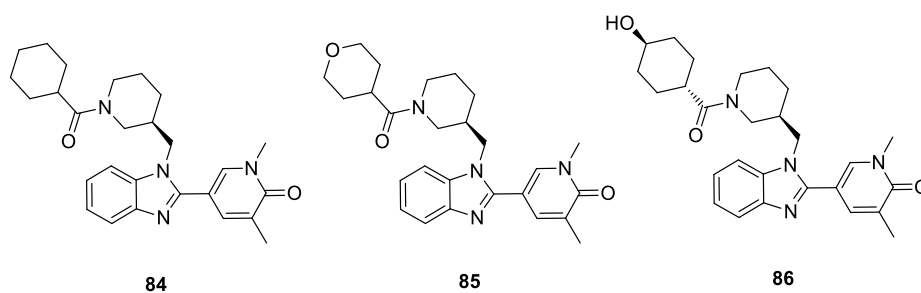
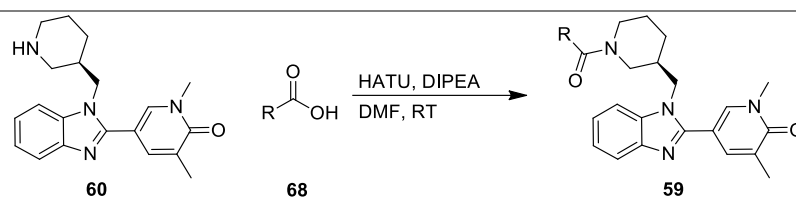


Figure 26: Benzimidazoles **84**, **85** and **86** do not contain a basic nitrogen atom.

These were synthesised in an analogous fashion to previous final compounds (Table 14).



Entry	Compound	Acid	Conditions	% Yield
1	84		1 h	40
2	85		1 h	41
3	86		1 h	45

Table 14: Synthesis of benzimidazoles **84** – **86**.

Benzimidazoles **84**, **85** and **86** were then compared to previously synthesised benzimidazoles **71** and **72**, and the non-functionalised acetyl piperidine benzimidazole **23** (Table 15).

Compound	23	71	72	84	85	86
BRD4 BD1/BD2 pIC₅₀	8.0/6.2	7.8/4.8	7.7/4.8	6.9/4.9	6.7/4.5	6.7/4.8
Selectivity BD1–BD2	1.8	3.0	2.9	2.0	2.2	1.9
hWB MCP-1 pIC₅₀	-	7.1	6.8	5.7	6.2	6.0
ChromLogD_{7.4}	2.20	1.69	1.46	4.52	2.71	2.18

Table 15: Comparison of the biological data for benzimidazoles **84** – **86** with amine functionalised benzimidazoles **71** and **72**, and acetyl piperidine benzimidazole **23**. The potency data disclosed is the mean of at least 2 test occasions.

Cyclohexyl, pyran, and alcohol benzimidazoles **84**, **85**, and **86** have a significantly lower BD1 pIC₅₀ when compared to benzimidazoles **23**, **71**, and **72**. When comparing the five functionalised compounds, BD1 pIC₅₀ is increased (between 0.8 and 1.1 log units) upon addition of a basic nitrogen atom. Contrastingly, BD2 pIC₅₀ remains similar in all five compounds. It was originally thought that as BD1 pIC₅₀ is lower for piperidines **71** and **72** relative to acetyl functionalised benzimidazole **23**, that a favourable interaction with the Asp residue is not occurring. However, it is now hypothesised that incorporation of the six-membered ring warrants an energy penalty in all cases, but that incorporation of a basic nitrogen atom allows for a favourable interaction with the Asp residue, which results in the increased potency of piperidines **71** and **72** relative to cyclohexyl **84**, pyran **85** and alcohol **86**. A crystal structure of benzimidazole **71**, co-crystallised in BD1 will reveal if the basic functionality results in a favourable interaction with the Asp residue.

To probe this hypothesis further, benzimidazoles **87** - **90** were designed, whereby the basicity of the piperidine has been reduced (Figure 27). It was thought that reducing the basicity of the piperidine ring would decrease BD1 pIC₅₀ and further solidify the idea that a basic nitrogen is required for an Asp residue interaction and, in turn, BD1 potency.

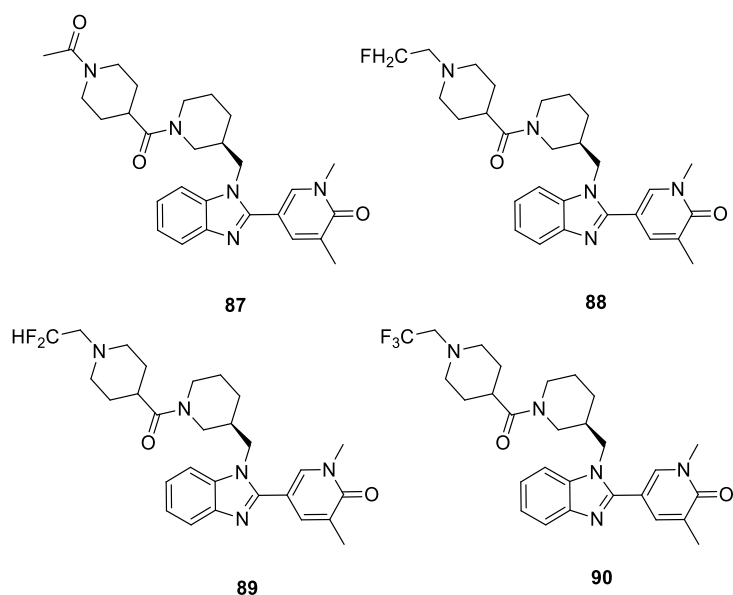
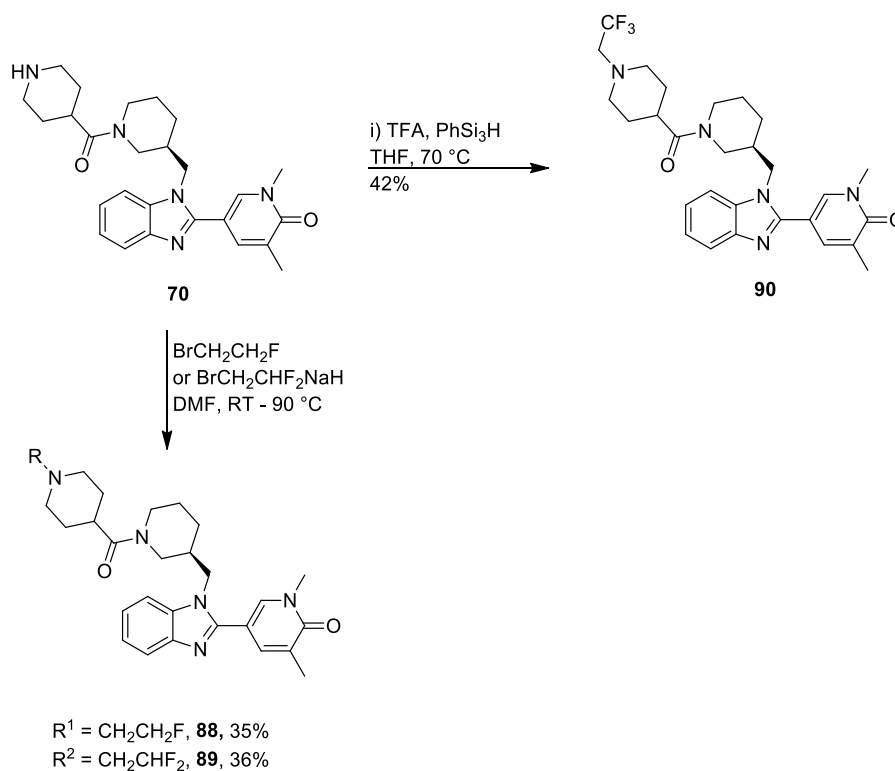


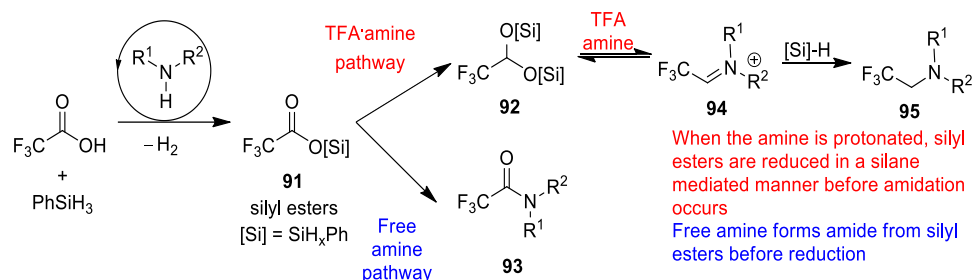
Figure 27: Benzimidazoles **87** - **90** contain a nitrogen atom with reduced basicity.

Acetyl-capped benzimidazole **87** was again synthesised by a HATU-promoted amide coupling of amine **70** and the corresponding carboxylic acid coupling partner. Mono- and difluoroethylated benzimidazoles **88** and **89** were accessed in one step from piperidine benzimidazole **70** by alkylation (Scheme 10). Trifluoroethylated benzimidazole **90** was also accessed in one step from piperidine benzimidazole **70** using catalyst-free trifluoroethylation conditions developed by the Denton group.⁴⁶ Piperidine benzimidazole **70** was heated with trifluoroacetic acid (TFA) and phenylsilane in tetrahydrofuran (THF) at 70 °C, and incomplete conversion to the desired benzimidazole **90** was observed after 17 hours. Additional equivalents of TFA and phenylsilane were added to the reaction which led to complete conversion; **90** was isolated in 42% yield (Scheme 10).



Scheme 10: Syntheses of **88**, **89**, and **90** were all achieved *via* intermediate **70**.⁴⁶

Denton *et al.* undertook mechanistic investigations in order to determine a pathway for the trifluoroethylation of secondary amines.⁴⁶ Indeed, they showed that the reaction does not proceed *via* a silane-mediated amidation followed by amide reduction, but rather by amine-catalysed dehydrogenative silyl ester **91** formation, followed by silane-mediated reduction to afford silyl acetals and hemiacetals **92** (Scheme 11). In the presence of acid, these species can undergo reductive amination to generate a highly reactive iminium species **94**, which is then reduced by phenylsilane to generate the desired amine **95**. Interestingly, the stoichiometry of TFA is an important consideration to prevent a competitive amidation reaction promoted by free amine to generate amide **93**.



Scheme 11: Proposed pathway of trifluoroethylation.⁴⁶

The biological data of benzimidazoles **87** - **90** is presented below (Table 16).

Compound	87	88	89	90
BRD4 BD1/BD2 pIC₅₀	6.5/4.6	7.6/4.7	6.8/4.6	6.3/4.6
Selectivity BD1–BD2	1.9	2.9	2.2	1.7
hWB MCP-1 pIC₅₀	5.7	7.2	6.3	5.8
ChromLogD_{7,4}	2.23	2.52	3.22	4.21
cpKa[H]	-	7.4 ^a	6.2 ^a	5.4 ^a

Table 16: Biological data of benzimidazoles **87**– **90**. ^aCalculated values. The potency data disclosed is the mean of at least 2 test occasions.

Benzimidazoles **87** - **90** have a decreased BD1 pIC₅₀ relative to amine functionalised compounds **71** and **72**, and comparable BD1 pIC₅₀'s to pyran, cyclohexyl and alcohol benzimidazoles **84** - **86**. This agrees with the hypothesis that a basic nitrogen is required for BD1 potency *via* an Asp residue interaction. Having stated this, monofluorinated

benzimidazole **88** has a comparable BD1 pIC₅₀ to isopropyl and methyl piperidines **71** and **72**. Additionally, **87** - **90** have comparable BD2 pIC₅₀'s to other benzimidazoles synthesised, indicating that a basic nitrogen does not impact BD2 potency.

The pKa[H] values of the nitrogen on the piperidine ring were calculated for benzimidazoles **71** and **72**, and the fluorinated series. These values were compared to the measured BD1 potencies (Figure 28). There is a notable trend in the increase of BD1 potency, and thus selectivity, with increase in pKa[H] of the nitrogen on the piperidine ring in the fluorinated series. The fact that the monofluorinated is tolerated in BD1, but the di- and trifluorinated species are not, is again indicative of the importance of the basicity of the nitrogen atom in maintaining BD1 potency.

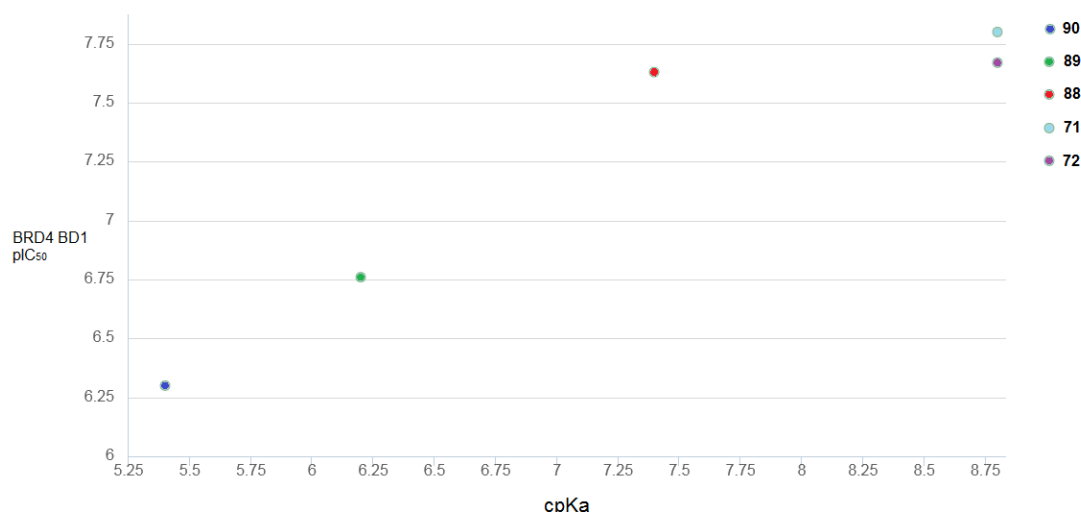


Figure 28: Plot of calculated pKa[H] values for the piperidine ring vs. BRD4 BD1 potency.

3.3.2.1 Computational efforts and X-ray crystallography used towards the understanding of BD1 selectivity

In the BD2 domain, it is known that the His residue can exist in “open” and “closed” forms. A co-worker without our laboratories has undertaken computational work to understand if there is an energy difference between the “open” and “closed” forms, and if this can be taken

advantage of to impact BD2 potency, and thus increase BD1 selectivity.⁴⁷ In the “closed” form, the His residue interacts with the backbone of the gatekeeper residue; in the “open” form, it is involved in a water-mediated interaction with the conserved Asn residue that interacts with the KAc and mimetics. It was hypothesised that functionalising the acetyl piperidine with a bulky motif would result in an unfavourable interaction with the His residue in BD2, forcing it into an unfavourable conformation, which would decrease BD2 pIC₅₀ and result in increased BD1 selectivity. Initially, available X-ray crystal structures were analysed to determine in what conformation the His was crystallised.⁴⁷ The majority of X-ray structures appear to have His in a “closed” orientation, and this was, therefore, assumed to be the energetically preferred conformation. It was thus hypothesised that by functionalising the acetyl piperidine, a steric clash with the His residue would force it into the energetically disfavoured “open” conformation, which would decrease BD2 potency. Metadynamic calculations were performed in order to understand how the free energy of the system varied with changing the His conformation.⁴⁷ Calculations on the Apo BRD4 BD2 protein were performed. The free energy profile obtained using as collective variables the chi1 and chi2 torsional angle of the His is represented in Figure 29, where chi1 and chi2 denote different torsion angles of the His side chain (Table 17). It was shown that the system in the open (C) and closed (A) conformations have similar energies and are, thus, equally observable.

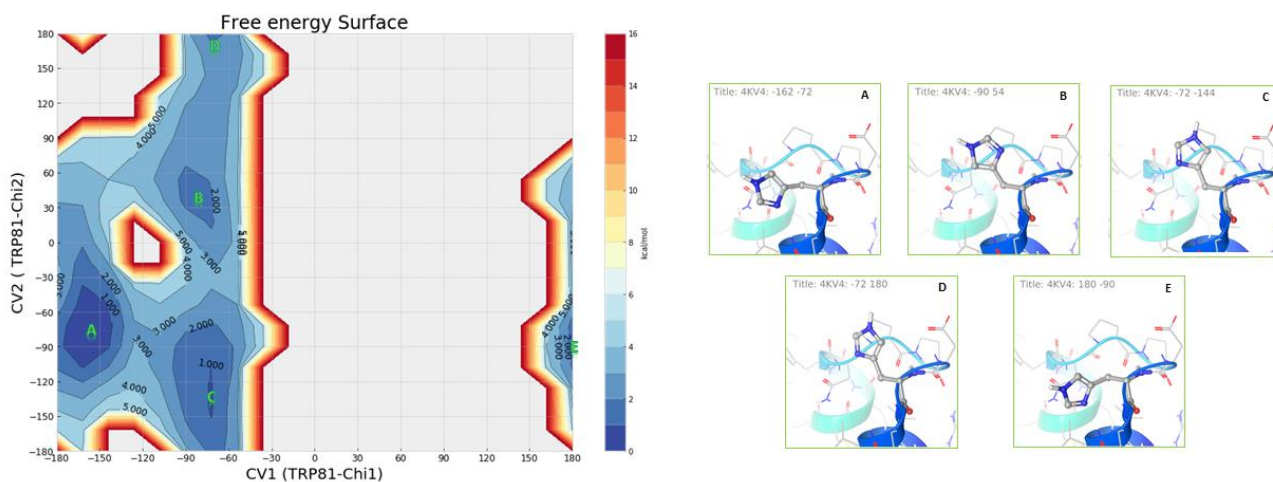


Figure 29: Free energy plot of conformations of the His residue in the BD2 domain. (A) represents the ‘closed’ conformation; (C) represents the ‘open’ conformation.⁴⁷

	Energy	Chi1/ Chi2
	kcal/mol	(torsion angle)
A	-73.71	-162.0/ -72.0
B	-72.01	-90.0/ 54.0
C	-72.80	-72.0/ -144.0
D	-72.02	-72.0/ 180.0
E	-70.81	180.0/ 18.0

Table 17: Chi1 and Chi2 represent the torsion angles of the His side chain. Conformations A–E represent energy minima.⁴⁷

From these results, it was thought that the decrease in BD2 pIC₅₀ was not due to the conformational changes of the His residue. To better understand this, benzimidazole **58** was submitted for X-ray crystallography, co-crystallised in BRD2 BD2 (Figure 30). When this crystal structure is overlaid with the crystal structure of the non-functionalised acetyl

benzimidazole **57**, it is evident that the amine has displaced a water molecule. This water molecule is involved in a bridging interaction between the His and Asn residues.

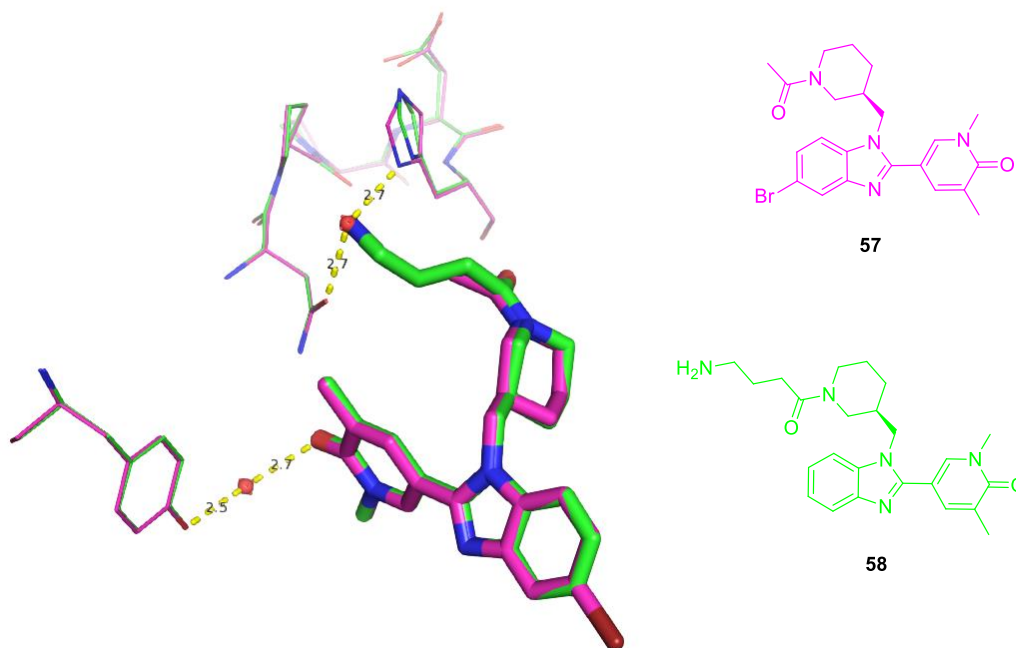


Figure 30: An overlay of X-ray crystal structures of benzimidazoles **57** and **58**, co-crystallised in BRD2 BD2. The amine moiety has displaced a water molecule involved in an interaction between the His and Asn residues.

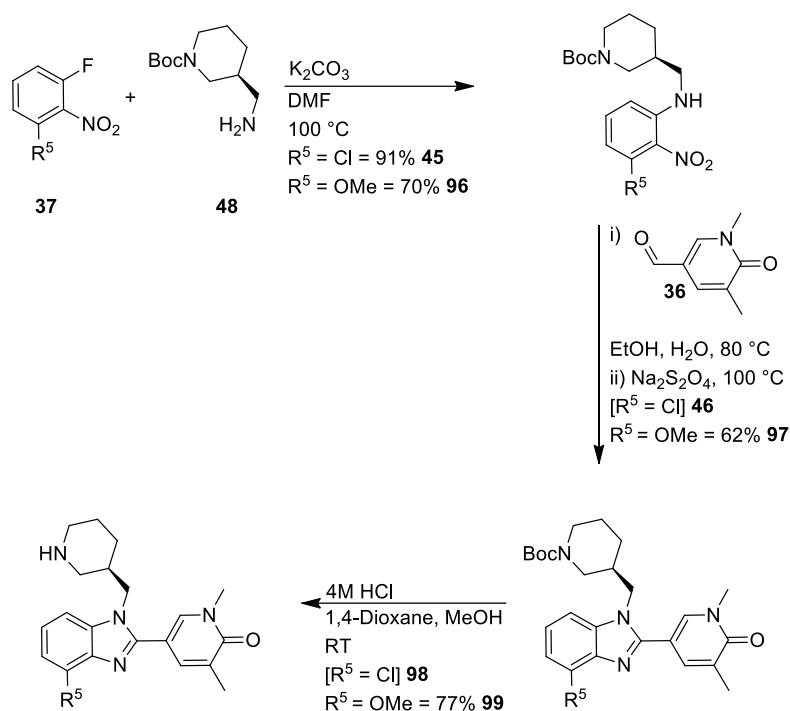
It is thought that this displacement of a water molecule, and disruption of the His–Asn interaction may be the cause for the decrease in BD2 pIC₅₀. However, it is surmised that an amine group is not required to displace the water: with reference to Table 15, benzimidazoles **84 - 86** which do not contain a basic nitrogen have comparable BD2 pIC₅₀ values to **71** and **72**.

These results have led to a modification and solidification of the hypothesis. With reference to the BD1 domain, it is thought that incorporation of a basic amine substituent in the form of a carbon chain or ring results in the formation of an ionic interaction between the protonated amine and the Asp residue. However, there is not an expected increase in BD1 potency, due

to an energy penalty for incorporation of the bulky carbon chain or ring. This is explained by comparison of piperidine benzimidazoles **71** and **72** with benzimidazoles **84** - **86**. A higher BD1 pIC₅₀ is observed in compounds which contain a basic nitrogen. This is further exemplified by benzimidazoles **87** - **90**, which contain a nitrogen atom with reduced basicity; these compounds have pIC₅₀ values comparable to compounds which do not contain a basic nitrogen. With reference to BD2, a water-mediated interaction between a His and Asn residue is disrupted by displacement of the bridging water molecule. This is observed in the crystal structure of benzimidazole **58** in BRD2 BD2. When compared to the amine functionalised benzimidazoles, benzimidazoles **84** - **90** have comparable BD2 pIC₅₀ values, and so it is thought an amine is not required for displacement of this water.

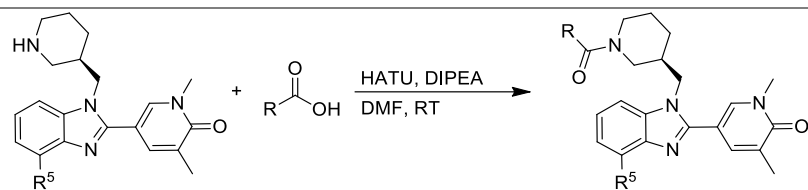
3.4 Dual functionalisation of the benzimidazole core

It was decided to further functionalise benzimidazoles **58**, **69**, and **70** by substituting at the R5 position, to investigate if the BD1 selectivity window could be further increased (see Section 3.2). Both the chloro- and methoxy-motifs were chosen as they had previously provided increased BD1 selectivity relative to a hydrogen atom. The chloro- and methoxy-functionalised intermediates were synthesised in a similar fashion to benzimidazole **60** (Scheme 12). An S_NAr coupling, one pot cyclisation, and Boc deprotection yielded benzimidazoles **98** and **99** in good yield. The chloro-substituted core **98** was taken forward crude to the amide coupling step.



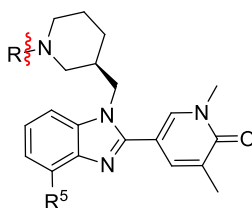
Scheme 12: The syntheses of key benzimidazole intermediates **98** and **99** were achieved in three steps.

Amide couplings were again utilised to give the final compounds **100** - **103** (Table 18).



Entry	Compound	R5	Acid	Conditions	% Yield
1	100	OMe		0.5 h	31 ^a
2	101	Cl		1 h	20 ^a
3	102	Cl		1 h	74
4	103	OMe		1 h	53 ^a

Table 18: Amide couplings yielded final compounds **100–103**. ^aYield over two steps after subsequent Boc deprotection.



Compound	100	101	102 ^a	103
R5	OMe	Cl	Cl	OMe
BRD4 BD1/BD2	7.8*/5.2*	7.4/4.9	6.6*/5.0*	7.1*/4.4*
pIC ₅₀				
Selectivity	2.6	2.5	1.6	2.7
BD1 – BD2				
ChromLogD _{7.4}	1.25	1.76	2.17	1.37

Table 19: Biological data of final compounds **99–102**. ^aCompound submitted as diastereomeric mixture. The potency data disclosed is the mean of at least 2 test occasions, for n=1 data, this is stated by *.

With reference to benzimidazole **58**, addition of a chloro- or methoxy-substituent at R5 provides an increase in the BD1 selectivity window (0.4 and 0.3 log units, respectively). Addition of the chloro-substituent results in a significant drop in BD1 pIC₅₀ (7.8 to 7.4 log units for **101**). Addition of a chloro-substituent to methyl piperidine benzimidazole **69** to give compound **102** provided no significant increase in the selectivity window. Finally, addition of a methoxy-substituent to give piperidine benzimidazole **103** provided a decrease in BD1 and BD2 pIC₅₀ (7.1 and 4.4, respectively). In this case, the BD1 pIC₅₀ has decreased by 0.4 log units relative to the piperidine benzimidazole **70**, and is at the lower limit of desired BD1 pIC₅₀. The BD1 selectivity of **103** is similar to its match-pair **70**, and so addition of a methoxy substituent to the R5 position does not provide any benefit for BD1 selectivity. Substitution at the R5 position increases the ChromLogD_{7.4} in all cases.

The exemplars show that there is no significant increase in BD1 selectivity upon addition of an R5 substituent, and none of these compounds have the desired 3.0 log unit selectivity window. Benzimidazoles **101** – **103** also show that addition of an R5 substituent can decrease BD1 pIC₅₀. Furthermore, substitution with a chloro or methoxy unit does not provide any significant increase in permeability. As a result, substitution at the R5 position was not considered further in this programme.

3.5 Investigating an alternative core structure

An interesting factor of the benzimidazole series is the inherent BD1 selectivity of the benzimidazole core. Table 2, entry 6 shows that with only a methyl substituent placed at R1, benzimidazole **28** is 0.9 log units selective for BD1 over BD2, with BRD4 BD1/BD2 pIC₅₀ values of 5.7/4.8. Previous work at GSK investigated the synthesis of indole core compounds as potential BET inhibitors.⁴⁸ This work includes indole compound **104**, which has an acetyl piperidine as an R1 substituent. Notably, in comparison to benzimidazole **23**, indole **104** has lost BD1 selectivity as BD1 potency has been maintained, while BD2 potency has increased (Figure 31).

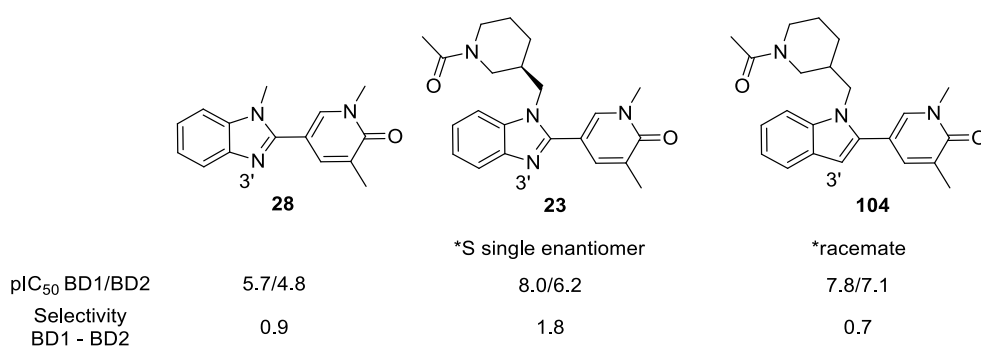
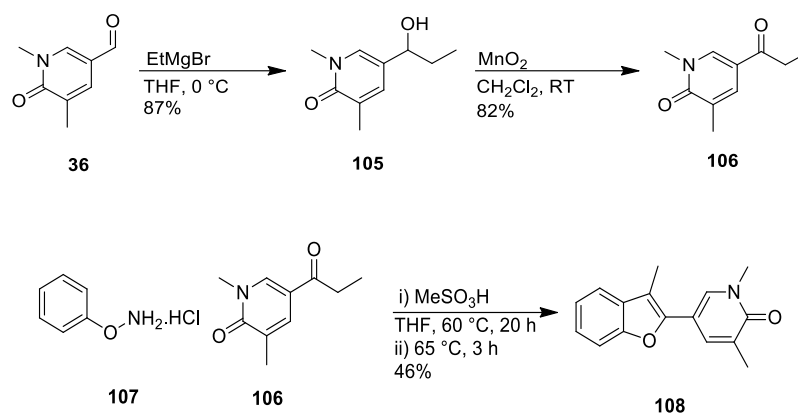


Figure 31: Comparison of the BD1 selectivity of the benzimidazole and indole cores. The potency data disclosed is the mean of at least 2 test occasions.

It was hypothesised that the nitrogen H-bond acceptor at the 3-position is critical to the selectivity of the benzimidazole core. Contrastingly, a CH donor at this position in indole **104** improves BD2 potency. Indole **104** was submitted as the racemate, and so it cannot be ruled out that the change to BD1 selectivity could be impacted by this. However, it is thought that the arrangement of the water networks in BD1 and BD2 differ in this region of binding. Additional studies in our laboratory have been initiated to further understand how the water network in BD1 and BD2 are affected by this point change to the core.⁴⁷

Due to its increased electronegativity, oxygen is a better H-bond acceptor than nitrogen. Consequently, it was decided to synthesise a compound with a benzofuran core that had an available benzimidazole match-pair. This would allow for comparison of the potency and selectivity. The benzimidazoles synthesised in this project have relatively low ChromLogD_{7.4} values (< 2), and it was thought that this may be the reason for the low AMP permeability values of benzimidazoles **71** and **72**. Consequently, switching from a benzimidazole to benzofuran core may be a strategy to increase the ChromLogD_{7.4}, and thus the AMP permeability values of this series. Additionally, if it were possible to switch from a benzimidazole to a benzofuran core, whilst maintaining the excellent BD1 selectivities observed, the series would no longer fall under the remit of the benzimidazole patent released by Boehringer Ingelheim⁴⁴, and thus this would be a novel BET pharmacophore. Benzofuran **108**, which has a methyl substituent at R1, was chosen as the initial target. This would result in a simple three step synthesis, and a suitable match-pair was available through benzimidazole **28**.

The first step in the synthesis of benzofuran **108** was a Grignard addition of ethylmagnesium bromide into aldehyde **36**, generating alcohol **105** in good yield (Scheme 13). Oxidation of alcohol **105** with manganese dioxide yielded ketone **106** in good yield. Finally, following the work of Tomkinson *et al.*, an acid-promoted Fischer indole-type coupling of phenylhydroxylamine **107** and ketone **106**, which undergoes [3,3]-sigmatropic rearrangement as a key step,⁴⁹ yielded benzofuran **108** in moderate yield, following purification by MDAP.



Scheme 13: Synthesis of benzofuran **108**.

Through comparison of the cores, benzimidazole **28** and benzofuran **108** can be seen to have the same BD1 selectivity window of 0.9 log units (Table 20). However, benzofuran **108** is 0.5 log units more potent at BD1 and BD2. Additionally, as predicted, benzofuran **108** has a higher ChromLogD_{7.4} than benzimidazole **28**. This parameter could be crucial in the development of a lead compound, as the currently profiled benzimidazole compounds have a relatively low ChromLogD_{7.4} and subsequent low AMP permeability. However, this increased ChromLogD_{7.4} is reflected in the Lipophilic Ligand Efficiency (LLE) values.⁵⁰ LLE is a parameter which links lipophilicity to potency and can be used to compare compounds with different ChromLogD_{7.4} and pIC₅₀ values. A lower relative LLE value indicates that lipophilicity is driving a given increased pIC₅₀ value. In this case, benzofuran **108** has a higher BD1 and BD2 potency compared to benzimidazole **28**, but it also has a higher ChromLogD_{7.4} value. Benzofuran **108** has a lower LLE parameter than benzimidazole **28** and so indicates that the increased potency is driven by an increased lipophilicity.

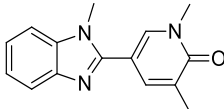
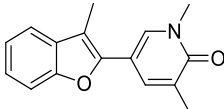
Core	benzimidazole	benzofuran
Compound		
	28	108
BRD4 BD1/BD2	5.7/4.8	6.2*/5.3*
Selectivity BD1–BD2	0.9	0.9
ChromLogD_{7.4}	2.30	5.40
LLE	3.64	2.93

Table 20: A comparison of the data of benzimidazole **28** and benzofuran **108**. The potency data disclosed is the mean of at least 2 test occasions, for n=1 data, this is stated by *.

It may be possible to further develop a lead compound by substituting the core from a benzimidazole to benzofuran, to increase the ChromLogD_{7.4} and AMP permeability. This data highlights that having a heteroatom placed at this position is beneficial for BD1 selectivity, and the synthesis of a new benzofuran core could be of importance when tuning the physicochemical properties of future lead compounds.

To further investigate the utility of a benzofuran core, targets which combine the benzofuran core with the most BD1 selective R1 substituents have been designed (Figure 32). It is believed that the BD1 potency and selectivity can be maintained, whilst increasing the ChromLogD_{7.4}. Predicted ChromLogD_{7.4} values have been calculated (cChromLogD_{7.4}). Benzofuran **109** and **110** have significantly increased ChromLogD_{7.4} values relative to the comparative benzimidazoles (Figure 32).

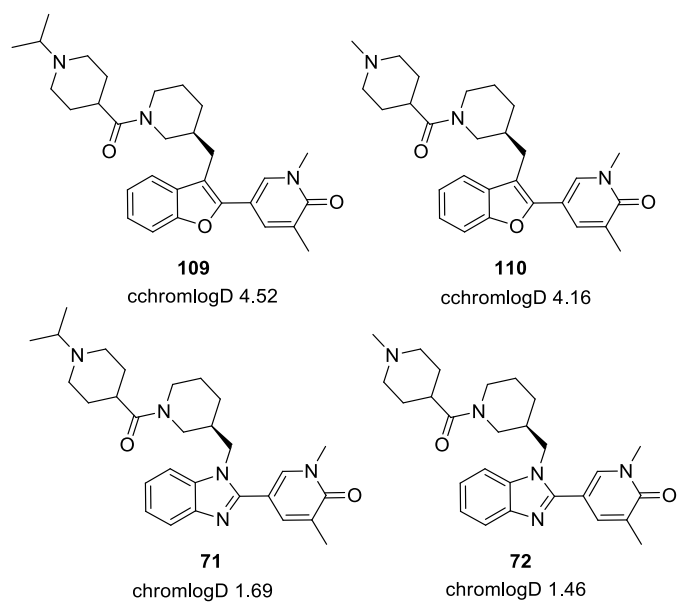
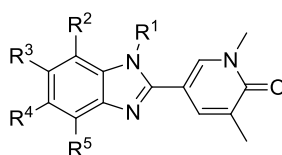


Figure 32: Benzofuran targets **109** and **110** have increased calculated ChromLogD_{7,4} values compared to benzimidazoles **71** and **72**.

4.0 Conclusions

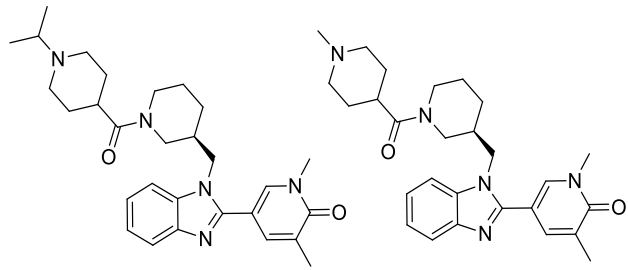
Considerable progress has been made in the development of a BET BD1 selective chemical probe. Initial data mining of a historic benzimidazole series provided insight into substituent vectors and motifs which were shown to provide BD1 selectivity; namely the R1 and R5 vectors. A chloro- and methoxy-substituent at the R5 position provided an increase in BD1 selectivity relative to hydrogen. Initial investigations into derivatising at the R5 vector provided no substituent which yielded a greater selectivity window than a chloro or methoxy motif.



22

Figure 33: Generic benzimidazole structure **22**.

A crystal structure of piperidine benzimidazole **57** co-crystallised in BRD2 BD2 showed that the piperidine R1 group is directed towards a key point change in the BD1 and BD2 domains, which is close to the active site. It was thought that the change from an Asp residue in BD1 to a His residue in BD2, could be utilised to provide BD1 selectivity. It was hypothesised that functionalising the acetyl piperidine ring with basic functionality would extend out towards this point change. This would result in a favourable interaction with the Asp residue in BD1, and an unfavourable interaction with the His residue of BD2. Four iterations of benzimidazole targets were synthesised, with benzimidazoles **71** and **72** showing high BD1 selectivity, of 3.0 and 2.9 log units respectively. Both compounds have an encouraging ‘lead’ profile, with excellent biochemical potency, good cell-based activity, and desirable BD1 selectivity (Table 21).



Compound	71	72
BRD4 BD1/BD2 pIC₅₀	7.8/4.8	7.7/4.8
Selectivity BD1–BD2	3.0	2.9
hWB MCP-1 pIC₅₀	7.1	6.8
ChromLogD_{7.4}	1.69	1.46
<i>in vitro</i> microsomes		
mL/min/g liver		
<i>Human</i>	< 0.40*	< 0.40*
<i>Rat</i>	< 0.46*	< 0.46*
<i>in vitro</i> hepatocytes		
mL/min/g liver		
<i>Human</i>	< 0.45*	< 0.45*
<i>Rat</i>	< 0.80*	< 0.80*
AMP nm s⁻¹	< 3	< 3

Table 21: Benzimidazoles **71** and **72** have an encouraging biological profile. The data disclosed is the mean of at least 2 test occasions, for n=1 data, this is stated by *.

Isopropyl piperidine benzimidazole **71** was also tested in a Bromoscan full curve assay panel, to test against other BET and non-BET bromodomains. It showed high selectivity in all cases, the highest non-BET pIC₅₀ of 5.0 for EP300 being well within the desired 100-fold selectivity window.

A hypothesis regarding the source of BRD4 BD1 selectivity was constructed. Analogues which did not contain a basic nitrogen on the R1 substituent were synthesised, and showed lower BD1 pIC₅₀ values than those with a basic nitrogen, indicating the formation of a favourable interaction with the Asp residue of BD1. A crystal structure to confirm this is anticipated. A crystal structure of benzimidazole **58**, the initial amine functionalised

compound that was synthesised, co-crystallised in BRD2 BD2, showed that the basic nitrogen displaces a water molecule involved in a bridging interaction between His and Asn residues. It is thought that this explains the decrease in BD2 potency. Additionally, it is observed that compounds which do not contain a basic nitrogen have similar BD2 pIC₅₀ values to those that do, indicating that a basic nitrogen is not required for water displacement.

A small series of bifunctionalised compounds, which have substituents at the R1 and R5 positions, were synthesised. Analysis of the data showed that further functionalisation with an R5 substituent provided slight increase in BD1 selectivity. Given that the desired selectivity profile has been achieved with benzimidazoles **71** and **72**, this series was not progressed further in this programme.

Investigations into a benzofuran core as an alternative to the benzimidazole structure were initiated. A match-pair analysis was conducted by synthesising the first benzofuran based BET inhibitor, which showed comparable BD1 selectivity to its benzimidazole counter-part. However, the benzofuran core exhibits a higher ChromLogD_{7.4} value, which could be important in tuning the physicochemical properties of the series, whilst also moving the project out with the reaches of a benzimidazole patent published by Boehringer Ingelheim.⁴⁴

This project has been successful in delivering a BET BD1 chemical probe with a superior BD1 selectivity compared to current literature probes. Further profiling of the lead compounds by *in vivo* PK studies will be required to fully established the utility of these molecules as BET BD1 chemical probes.

5.0 Future Work

The functionalisation of the R1 position with basic substituents has been validated as a method of increasing BET BD1 potency. Benzimidazole **71** is the furthest progressed compound, having been submitted to *in vitro* clearance and Bromoscan assays. As there is an apparent disconnect between compound permeability, cellular potency, and *in vitro* clearance, this compound has been submitted for *in vivo* PK analysis. This study will generate data to understand blood and renal clearance of the compound, compound half-life, mean residence time of the drug in the systemic circulation, and bioavailability. The data gained from this study will build confidence in the ability of **71** to be utilised for *in vivo* efficacy models, and determine if it can be dosed orally.

It is anticipated that a crystal structure of benzimidazole **58** co-crystallised in BRD4 BD1 will be solved. It is hoped that this will provide evidence of an ionic interaction between the amine substituent and the Asp residue of BD1. This will support the hypothesis that an amine substituent can provide BD1 potency, while lowering BD2 potency by displacing a water molecule.

Future work could also include the exploration of more R5 substituents. Given the rapid progress of benzimidazoles **71** and **72**, work to find a R5 substituent with superior BD1 selectivity to methoxy or chloro group was not advanced further within this programme. Production of more analogues of this type may allow SAR for this vector to be generated, which could be used to explain the increased BD1 selectivity observed for these substituents.

Work was initiated into the exploration of alternative cores to the benzimidazole motif. This involved investigating a previous indole-based series synthesised elsewhere in the laboratory,⁴⁸ which showed lower BD1 selectivity than its benzimidazole match-pair. This is an intriguing discovery, as it highlights the potential need for a heteroatom at this position in order to maintain BD1 selectivity. An aim of this project was to investigate the source of BD1 selectivity in the benzimidazole series. Accordingly, further modelling and computational

6.0 Experimental

Solvents used were anhydrous and reagents purchased from commercial suppliers were used as received unless otherwise indicated.

Reactions were monitored by thin layer chromatography (TLC) or liquid chromatography–mass spectroscopy (LCMS). Product spots were visualized under UV light ($\lambda_{\text{max}} = 254 \text{ nm}$) and/or by staining with potassium permanganate.

Nuclear Magnetic Resonance (NMR) spectroscopy. Proton (^1H), carbon (^{13}C) and fluorine (^{19}F) (when appropriate) spectra were recorded in deuterated solvents at ambient temperature using standard pulse methods on a Bruker AV-400 or Bruker AV-500 ($^1\text{H} = 400 \text{ MHz}$, $^{13}\text{C} = 101 \text{ MHz}$ or 176 MHz , $^{19}\text{F} = 376 \text{ MHz}$). Chemical shifts are reported in ppm to the nearest 0.01 ppm, and are referenced to residual solvent peaks. Coupling constants are quoted to the nearest 0.1 Hz and multiplicities are described as singlet (s), doublet (d), triplet (t), quartet (q), quintet (quin), sextet (sxt), septet (sept), br. (broad), and multiplet (m).

IR spectra were obtained on a Perkin Elmer Spectrum 1 machine. Absorption maxima (ν_{max}) are reported in reciprocal centimeters (cm^{-1}) and are described as strong (s), medium (m), weak (w), and broad (br).

Liquid Chromatography Mass Spectroscopy (LCMS) was conducted on an Acquity UPLC CSH C18 column (50 mm x 2.1 mm i.e. 1.7 μm packing diameter) at 40 °C eluting with either: Method A (HpH) – 10 mM ammonium bicarbonate in water adjusted to pH 10 with ammonia solution (solvent A) and acetonitrile (solvent B). The gradient (A:B) employed was from 99:1 to 0:100 over 2 min.

Method B (For) – 0.1% v/v solution of formic acid in water (solvent A) and 0.1% v/v solution of formic acid in acetonitrile (solvent B). The gradient (A:B) employed was from 97:3 to 3:97 over 2 min.

The UV detection is a summed signal from wavelength of 210 nm to 350 nm. The mass spectra were recorded on a Waters ZQ spectrometer using electrospray positive and negative mode. The scan range was 100 to 1000 AMU, the scan time was 0.27 sec, and the inter-scan delay was 0.10 sec.

Preparative mass directed HPLC (MDAP) was conducted on an Xselect CSH C18 column (150 mm x 30 mm i.d. 5 µm packing diameter) at ambient temperature. The solvents employed were 10 mM ammonium bicarbonate adjusted to pH 10 with ammonia in water (solvent A) and acetonitrile (solvent B). The UV detection is a summed signal from wavelength of 210 nm to 350 nm. Mass spectra were recorded on Waters ZQ mass spectrometer using alternate-scan positive and negative electrospray ionization. The software used was *MassLynx* 3.5 with *FractionLynx*.

Purification by Combiflash® EZ prep HPLC machine was conducted on an Xselect CSH C18 column (100 mm x 30 mm i.d. 5 µm packing diameter) at ambient temperature. The solvents employed were 10 mM ammonium bicarbonate adjusted to pH 10 with ammonia in water (solvent A) and acetonitrile (solvent B). The CombiFlash® Rf uses RFID (Radio Frequency Identification) technology to automate the setting of the parameters for purification runs and fraction collection. The system is equipped with a UV variable dual-wavelength and a Foxy® fraction collector enabling automated peak cutting, collection, and tracking.

Column chromatography was conducted on a Combiflash® Rf, automated flash chromatography system, from Teledyne Isco using disposable, normal, or reverse phase, SPE Redisep or Grace cartridges (4 g to 330 g). The CombiFlash® Rf uses RFID (Radio Frequency

Identification) technology to automate the setting of the parameters for purification runs and fraction collection. The system is equipped with a UV variable dual-wavelength and a Foxy® fraction collector enabling automated peak cutting, collection, and tracking.

Chiral purification chromatography was conducted on a Chiralpak IBN-5 (250 x 30 mm, 5 micron) column at 42.5 mL/min. The system uses UV Diode Array at 280 nm.

ESI (+) high resolution mass spectra (HRMS) were obtained on a Micromass Q-ToF 2Hybrid quadrupole time-of-flight mass spectrometer, equipped with a Z-spray interface, over a mass range of 100 – 1100 Da, with a scan time of 0.9 s and an interscan delay of 0.1 s. Reserpine was used as the external mass calibrant ($[M+H]^+ = 609.2812$ Da). The Q-ToF 2 mass spectrometer was operated in W reflectron mode to give a resolution (FWHM) of 16000–20000. Ionisation was achieved with a spray voltage of 3.2 kV, a cone voltage of 50 V, with cone and desolvation gas flows of 10–20 and 600 L/h, respectively. The source block and desolvation temperatures were maintained at 120 °C and 250 °C, respectively. The elemental composition was calculated using MassLynx v4.1 for the $[M+H]^+$. An Agilent 1100 Liquid Chromatograph equipped with a model G1367A autosampler, a model G1312A binary pump, and a HP1100 model G1315B diode array detector was used.

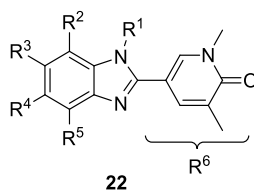
The method used was generic for all experiments. All separations were achieved using a Phenomenex Luna C18 (2) reversed phase column (100 x 2.1 mm, 3 µm particle size). Gradient elution was carried out with the mobile phases as (A) water containing 0.1% (v/v) formic acid and (B) acetonitrile containing 0.1% (v/v) formic acid. The conditions for the gradient elution were initially 5% B, increasing linearly to 100% B over 6 minutes, remaining at 100% B for 2.5 min then decreasing linearly to 5% B over 1 min, followed by an equilibration period of 2.5 min prior to the next injection. The flow rate was 0.5 mL/min,

temperature controlled at 35 °C with an injection volume of between 2 to 5 μ L. All samples were diluted with DMSO (99.9%) prior to LCMS analysis.

Isolute® phase separator cartridges are fitted with a hydrophobic Teflon frit. These were used to separate organic solvent from aqueous phase under gravity.

Spotfire Visualisation Method

All data analysis of historic benzimidazole compounds was carried out using Microsoft Excel and TIBCO Spotfire software. The data set of 1544 benzimidazole compounds was first analysed in Microsoft Excel using the Helium platform. All available biological data was sought out using the Helium function “get biological data”. Selectivity for each compound was then calculated by performing $BD1\ pIC_{50} - BD2\ pIC_{50}$ as an excel function. Next, R group analysis was carried out on the benzimidazole core as follows:



This data set was opened in Spotfire software to analyse each individual R group relative to selectivity.

Table 2 plot: To analyse the R1 vector, a bar chart of “RX” versus “Row count” (i.e. number of compounds) was produced. A filter was applied to include compounds which had the pyridone “warhead” as the R6 substituent only using the “Filter to” function. A filter was then applied individually to each R2 – R5 vector, in order to show compounds that have this substituent as a hydrogen atom only by use of the “Filter To” function. With these filters applied, a scatter plot of “R1” vs “BD1 – BD2” (BD1 selectivity) was generated. Each R1 substituent present was analysed to look at its BD1 selectivity, and from this, **Table 2** was generated.

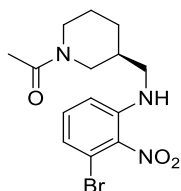
Figure 19 plot: To analyse the R5 vector, a bar chart of “RX” versus “Row count” (i.e. number of compounds) was produced. A filter was applied to include compounds which had the pyridone “warhead” as the R6 substituent only using the “Filter to” function. A filter was then applied individually to each R2 – R4 vector, in order to show compounds that have this substituent as a hydrogen atom only by use of the “Filter To” function. Additionally, a filter

was applied to the R1 vector to remove compounds which have this substituent as a hydrogen atom by use of the “Filter Out” function. With these filters applied, a scatter plot of “R5” vs “BD1 – BD2” (BD1 selectivity) was generated. All R5 substituents were analysed, and the chloro- and methoxy-substituents were observed as having exemplars with BD1 selectivity (> 1.1). The data set was then filtered to compounds with either a hydrogen atom, chlorine atom, or methoxy- substituent at R5. A scatter plot of “R1” versus “BD1 – BD2” (BD1 selectivity) was then generated to identify which R1 substituted compounds had three data points and could be included in the match-pair analysis. The three R5 substituents were differentiated by applying a colour filter: blue for a hydrogen atom, pink for a chlorine atom, and green for the methoxy-substituent. Compounds which only had one data point were filtered out using the “Filter Out” function. From this, **Figure 19** was generated.

Figure 20 plot: To analyse the R4 vector, a bar chart of “RX” versus “Row count” (i.e. number of compounds) was produced. A filter was applied to include compounds which had the pyridone “warhead” as the R6 substituent only using the “Filter to” function. A filter was then applied individually to each R2, R3, and R5 vector, in order to show compounds that have this substituent as a hydrogen atom only by use of the “Filter To” function. Additionally, a filter was applied to the R1 vector to remove compounds which have this substituent as a hydrogen atom by use of the “Filter Out” function. With these filters applied, a scatter plot of “R4” vs “BD1 – BD2” (BD1 selectivity) was generated. All R4 substituents were analysed, and the 4-*N*-methylpiperazine was chosen as a representative of a small series of 6-membered heterocycles which had exemplars with BD1 selectivity (> 0.8). The data set was then filtered to compounds with either a hydrogen atom or 4-*N*-methylpiperazine motif at the R4 vector. A scatter plot of “R1” versus “BD1 – BD2” (BD1 selectivity) was then generated to identify which R1 substituted compounds had two data points and could be included in the match-pair analysis. The two R4 substituents were differentiated by applying a colour filter: blue for a hydrogen atom and yellow for a 4-*N*-methylpiperazine motif. Compounds which only had one

data point were filtered out using the “Filter Out” function. From this, **Figure 20** was generated.

(S)-1-(3-(((3-bromo-2-nitrophenyl)amino)methyl)piperidin-1-yl)ethan-1-one 40

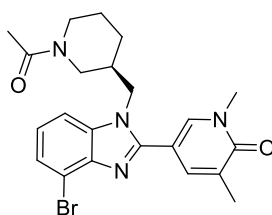


Chemical Formula: C₁₄H₁₈BrN₃O₃
Molecular Weight: 356.22 amu

1-bromo-3-fluoro-2-nitrobenzene **39** (108 mg, 0.493 mmol), (S)-1-(3-(aminomethyl)piperidin-1-yl)ethan-1-one **38** (77.0 mg, 0.493 mmol), potassium carbonate (102 mg, 0.739 mmol) and EtOH (2 mL) were added to a round bottom flask. The reaction mixture was stirred at 80 °C under a nitrogen atmosphere for 20 h. After cooling to RT, the reaction mixture was diluted and partitioned between EtOAc (40 mL) and brine (40 mL), and the phases were separated. The aqueous phase was further extracted with EtOAc (40 mL). The combined organic phases were washed with brine (40 mL), dried by passing through a hydrophobic frit, and the solvent concentrated *in vacuo*. The crude material was purified by normal phase chromatography, eluting with 0 – 100% EtOAc in cyclohexane over 45 CV. Fractions containing the desired product were concentrated *in vacuo* to yield (S)-1-(3-(((3-bromo-2-nitrophenyl)amino)methyl)piperidin-1-yl)ethan-1-one **40** (72 mg, 0.182 mmol, 37% yield) as an orange gum. **LCMS (HpH)**: rt = 1.10 min, [M+H]⁺ 356/358 **¹H NMR δ(400 MHz, CDCl₃)**: *rotamer 1* 7.07 – 7.19 (1H, m), 6.95 – 7.01 (1H, m), 6.73 (1H, d, *J* = 8.3 Hz), 5.59 – 5.73 (1H, m, CH), 4.15 – 4.23 (1H, m), 3.70 – 3.78 (1H, m), 3.09 – 3.26 (2H, m), 2.86 – 3.07 (2H, m), 2.04 (3H, s), 1.86 (2H, m), 1.66 – 1.79 (1H, m), 1.43 – 1.56 (1H, m), 1.27 – 1.36 (1H, m). *rotamer 2* 7.07 – 7.19 (1H, m), 6.89 – 6.95 (1H, m), 6.73 (1H, d, *J* = 8.3 Hz), 5.76 – 5.89 (1H, m), 4.25 – 4.33 (1H, m), 3.61 – 3.70 (1H, m), 3.09 – 3.26 (2H, m), 2.86 – 3.07 (1H, m), 2.66 – 2.75 (1H, m), 2.09 (3H, s), 1.80 – 2.00 (2H, m), 1.66 – 1.79 (1H, m), 1.43

– 1.56 (1H, m), 1.27 – 1.36 (1H, m). ^{13}C NMR δ (101 MHz, CDCl_3) ppm: *additional peaks due to rotamers present* 169.1, 168.9, 143.4, 143.1, 133.0, 132.9, 122.1, 121.7, 116.3, 116.2, 112.3, 50.1, 47.1, 46.1, 45.1, 42.1, 36.3, 34.9, 28.6, 28.3, 26.9, 24.8, 23.8, 21.4, 21.3, 14.1. **HRMS (ESI)** exact mass calculated for $\text{C}_{14}\text{H}_{19}\text{BrN}_3\text{O}_3$ $[\text{M}+\text{H}]^+$ m/z 356.0611, found m/z 356.0604.

(S)-5-(1-((1-Acetylpiperidin-3-yl)methyl)-4-bromo-1H-benzo[d]imidazol-2-yl)-1,3-dimethylpyridin-2(1H)-one 31

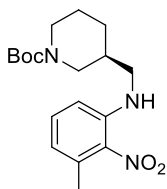


Chemical Formula: $\text{C}_{22}\text{H}_{25}\text{BrN}_4\text{O}_2$
Molecular Weight: 456.36 amu

Zinc (47 mg, 0.724 mmol) and 1,5-dimethyl-6-oxo-1,6-dihydropyridine-3-carbaldehyde **36** (24 mg, 0.157 mmol) were added to a stirring solution of (S)-1-(3-(((3-bromo-2-nitrophenyl)amino)methyl)piperidin-1-yl)ethan-1-one **40** (43 mg, 0.121 mmol) in EtOH (0.2 mL) and acetic acid (0.2 mL). Water (0.2 mL) was then added. The reaction mixture was stirred at 100 °C under a nitrogen atmosphere for 16 h. After cooling to RT, the reaction mixture was concentrated *in vacuo*. The residue was dissolved in 1:1 MeOH:DMSO (1 mL) and purified by MDAP using a solvent system of 10 mM ammonium bicarbonate adjusted to pH 10 with ammonia in water (solvent A) and acetonitrile (solvent B). Fractions containing the desired product were concentrated *in vacuo* to yield (S)-5-(1-((1-acetylpiperidin-3-yl)methyl)-4-bromo-1H-benzo[d]imidazol-2-yl)-1,3-dimethylpyridin-2(1H)-one **31** (7 mg, 15 μmol , 12% yield). **LCMS (HpH)**: $t_r = 0.85$ min, $[\text{M}+\text{H}]^+$ 457/459. ^1H NMR δ (400 MHz, CDCl_3): *rotamer 1* 7.75 – 7.86 (1H, m), 7.40 – 7.56 (2H, m), 7.29 – 7.35 (1H, m), 7.13 – 7.22 (1H, m), 4.01 – 4.41 (3H, m), 3.57 – 3.69 (4H, m), 2.98 – 3.09 (1H, m), 2.50 – 2.58 (1H, m), 2.25 (3H, s), 2.00 – 2.12 (4H, m), 1.46 – 1.70 (2H, m), 1.24 – 1.40 (1H, m), 0.99 –

1.21 (1H, m). *rotamer 2* 7.75 – 7.86 (1H, m), 7.40 – 7.56 (2H, m), 7.29 – 7.35 (1H, m), 7.13 – 7.22 (1H, m), 4.01 – 4.41 (3H, m), 3.57 – 3.69 (4H, m), 3.31 – 3.39 (1H, m), 2.65 – 2.75 (1H, m), 2.25 (3H, s), 2.00 – 2.12 (1H, m), 1.78 (3H, s), 1.46 – 1.70 (2H, m), 1.24 – 1.40 (1H, m), 0.99 – 1.21 (1H, m). ^{13}C NMR δ (101 MHz, CDCl_3): 169.1 (C), 162.7 (C), 151.0 (C), 141.6 (C), 138.4 (CH), 136.0 (C), 135.8 (CH), 129.9 (C), 125.8 (CH), 123.9 (CH), 113.4 (C), 109.4 (CH), 108.6 (C), 47.8 (CH_2), 46.8 (CH_2), 44.9 (CH_2), 38.2 (CH_3), 36.0 (CH), 28.2 (CH_2), 24.7 (CH_2), 21.3 (CH_3), 17.4 (CH_3). HRMS (ESI) exact mass calculated for $\text{C}_{22}\text{H}_{26}\text{BrN}_4\text{O}_2$ $[\text{M}+\text{H}]^+$ m/z 457.1240, found m/z 457.1237.

tert*-Butyl (*S*)-3-(((3-methyl-2-nitrophenyl)amino)methyl)piperidine-1-carboxylate **49*

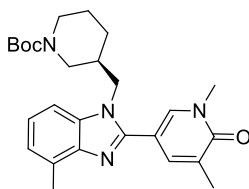


Chemical Formula: $\text{C}_{18}\text{H}_{27}\text{N}_3\text{O}_4$
Molecular Weight: 349.42 amu

1-Fluoro-3-methyl-2-nitrobenzene **47** (250 mg, 1.61 mmol) and potassium carbonate (334 mg, 2.42 mmol) were added to a stirring solution of *tert*-butyl (*S*)-3-(aminomethyl)piperidine-1-carboxylate **48** (345 mg, 1.61 mmol) in DMF (7 mL). The reaction mixture was stirred at 100 °C under a nitrogen atmosphere for 4 h. LCMS analysis showed incomplete conversion to the desired product. Additional *tert*-butyl (*S*)-3-(aminomethyl)piperidine-1-carboxylate **48** (50 mg, 0.23 mmol) was therefore added. The reaction mixture was then stirred at 100 °C under a nitrogen atmosphere for 1.5 h. After cooling to RT, the reaction mixture was concentrated *in vacuo*. The residue was diluted in and partitioned between EtOAc (20 mL) and water (20 mL), and the phases were separated. The aqueous phase was further extracted with EtOAc (20 mL). The combined organic phases were washed with a 5% (by wt) aqueous solution of lithium chloride (30 mL), dried by passing through a hydrophobic frit, and concentrated *in vacuo*. The crude material was then purified

by normal phase chromatography, eluting with 0 – 20% EtOAc in cyclohexane over 16 CV. Fractions containing the desired product were concentrated *in vacuo* and then dried on the high vacuum to yield *tert*-butyl (*S*)-3-(((3-methyl-2-nitrophenyl)amino)methyl)piperidine-1-carboxylate **49** (503 mg, 1.37 mmol, 85% yield) as an orange gum. **LCMS (HPLC)**: *rt* = 1.43 min, [M+H]⁺ 350. **¹H NMR δ(400 MHz, CDCl₃)**: 7.18 – 7.26 (1H, m), 6.65 (1H, d, *J* = 8.3 Hz), 6.59 (1H, br. s), 6.54 (1H, d, *J* = 7.3 Hz), 3.96 (1H, br. s), 3.84 (1H, dt, *J* = 13.2, 4.2 Hz), 3.12 – 3.23 (1H, m), 3.02 – 3.12 (1H, m), 2.87 – 3.00 (1H, m), 2.75 (1H, br. s), 2.47 (3H, s), 1.80 – 1.96 (2H, m), 1.64 – 1.73 (1H, m), 1.47 – 1.56 (1H, m), 1.45 (9H, s), 1.19 – 1.36 (1H, m). **¹³C NMR δ(101 MHz, CDCl₃)**: one *CH₂ peak obscured. 154.8 (C), 143.8 (C), 136.0 (C), 135.7 (C), 133.2 (CH), 119.3 (CH), 111.1 (CH), 79.6 (C), 46.3 (CH₂), 35.5 (CH), 28.7 (CH₂), 28.4 (CH₃), 26.9 (CH₂), 24.3 (CH₂), 21.3 (CH₃) **HRMS (ESI)**. exact mass calculated for C₁₈H₂₇N₃O₄Na [M+Na]⁺ *m/z* 372.2002, found *m/z* 372.1895. ***v*_{max}(solid)**: 3414, 2932, 1686, 1602, 1501, 1148 cm⁻¹.

tert*-Butyl (S)-3-((2-(1,5-dimethyl-6-oxo-1,6-dihydropyridin-3-yl)-4-methyl-1*H*-benzo[*d*]imidazol-1-yl)methyl)piperidine-1-carboxylate **50*

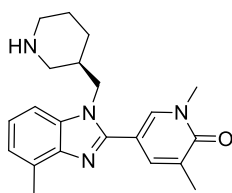


Chemical Formula: C₂₆H₃₄N₄O₃
Molecular Weight: 450.57 amu

tert-Butyl (*S*)-3-(((3-methyl-2-nitrophenyl)amino)methyl)piperidine-1-carboxylate **49** (485 mg, 1.39 mmol), 1,5-dimethyl-6-oxo-1,6-dihydropyridine-3-carbaldehyde **36** (252 mg, 1.67 mmol), EtOH (8 mL), and water (4 mL) were added to a round bottom flask. The reaction mixture was heated to 80 °C, after which sodium dithionite (725 mg, 4.16 mmol) was added. The reaction mixture was stirred at 100 °C under a nitrogen atmosphere for 3 h. After cooling to RT, the reaction mixture was diluted in and partitioned between EtOAc (20 mL)

and water (20 mL), and the phases were separated. The aqueous phase was further extracted with EtOAc (20 mL). The combined organic phases were washed with brine (20 mL), dried by passing through a hydrophobic frit, and concentrated *in vacuo* to yield *tert*-butyl (*S*)-3-((2-(1,5-dimethyl-6-oxo-1,6-dihydropyridin-3-yl)-4-methyl-1*H*-benzo[*d*]imidazol-1-yl)methyl)piperidine-1-carboxylate **50** (393 mg, 0.785 mmol, 57% yield) as a pink solid. **LCMS (HpH)**: 1.15 min, [M+H]⁺ 451 **¹H NMR δ(400 MHz, CDCl₃)**: 7.72 (1H, d, *J* = 2.0 Hz), 7.41 – 7.49 (1H, m), 7.18 – 7.25 (2H, m), 7.06 – 7.15 (1H, m), 4.03 – 4.11 (2H, m), 3.78 – 3.89 (1H, m), 3.65 – 3.67 (3H, m), 2.71 – 2.81 (1H, m), 2.66 – 2.70 (3H, m), 2.44 – 2.55 (1H, m), 2.25 (3H, s), 1.98 – 2.09 (1H, m), 1.67 – 1.78 (1H, m), 1.51 – 1.62 (2H, m), 1.28 – 1.44 (10H, m), 0.98 – 1.11 (1H, m) **¹³C NMR δ(101 MHz, CDCl₃)**: *CH₂ peaks obscured. 162.7 (C), 154.6 (C), 149.5 (C), 142.1 (C), 137.7 (CH), 136.2 (CH), 135.3 (C), 130.0 (C), 129.8 (C), 123.0 (CH), 122.9 (CH), 109.5 (C), 107.6 (CH), 79.7 (C), 47.7 (CH₂), 38.1 (CH₃), 36.4 (CH), 28.5 (CH₂), 28.3 (CH₃), 24.2 (CH₂), 17.4 (CH₃), 16.7 (CH₃). **HRMS (ESI)** exact mass calculated for C₂₆H₃₅N₄O₃ [M+H]⁺ *m/z* 451.2710, found *m/z* 451.2708. **ν_{max}(solid)**: 2973, 2932, 1682, 1270, 1151 cm⁻¹.

(*R*)-1,3-Dimethyl-5-(4-methyl-1-(piperidin-3-ylmethyl)-1*H*-benzo[*d*]imidazol-2-yl)pyridin-2(1*H*)-one 51

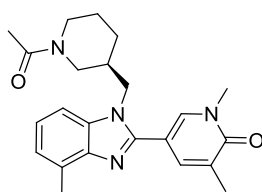


Chemical Formula: C₂₁H₂₆N₄O
Molecular Weight: 350.46 amu

tert-butyl (*S*)-3-((2-(1,5-dimethyl-6-oxo-1,6-dihydropyridin-3-yl)-4-methyl-1*H*-benzo[*d*]imidazol-1-yl)methyl)piperidine-1-carboxylate **50** (379 mg, 0.841 mmol) was dissolved in a solution of hydrochloric acid in 1,4-dioxane (4 M, 4 mL, 16 mmol). The reaction mixture was stirred at RT under air for 1 h. The reaction mixture was diluted with methanol

(20 mL) and then added to a SCX 20 g column (pre-wet with methanol) and allowed to settle by gravity. The column was then washed with methanol (40 mL) under vacuum. Into a separate flask, the column was washed with a solution of ammonia in MeOH (2 M, 80 mL). The filtrate was concentrated *in vacuo* to yield (*R*)-1,3-dimethyl-5-(4-methyl-1-(piperidin-3-ylmethyl)-1*H*-benzo[*d*]imidazol-2-yl)pyridin-2(1*H*)-one **51** (273 mg, 0.740 mmol, 88% yield) as a pink gum. **LCMS (HpH)**: rt = 0.80 min, [M+H]⁺ 351 **¹H NMR δ(400 MHz, CDCl₃)**: 7.73 (1H, s), 7.40 – 7.51 (1H, m), 7.14 – 7.21 (2H, m), 7.03 – 7.09 (1H, m), 3.98 – 4.13 (2H, m), 3.61 (3H, s), 2.86 – 2.92 (1H, m), 2.71 – 2.77 (1H, m), 2.65 (3H, s), 2.52 (1H, td, *J* = 11.4, 2.2 Hz), 2.27 (2H, dd, *J* = 11.7, 9.3 Hz), 2.20 – 2.23 (3H, m), 1.98 – 2.09 (1H, m), 1.53 – 1.63 (2H, m), 1.28 – 1.40 (1H, m), 1.01 – 1.12 (1H, m).

(*S*)-5-(1-((1-Acetylpiperidin-3-yl)methyl)-4-methyl-1*H*-benzo[*d*]imidazol-2-yl)-1,3-dimethylpyridin-2(1*H*)-one 32

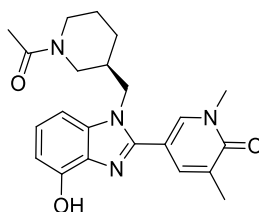


Chemical Formula: C₂₃H₂₈N₄O₂
Molecular Weight: 392.49 amu

Acetyl chloride (6 μL, 0.86 mmol) was added to a stirring solution of triethylamine (0.434 mL, 3.12 mmol) and (*R*)-1,3-dimethyl-5-(4-methyl-1-(piperidin-3-ylmethyl)-1*H*-benzo[*d*]imidazol-2-yl)pyridin-2(1*H*)-one **51** (273 mg, 0.779 mmol) in DCM (6 mL) at RT. The reaction mixture was stirred at RT under a nitrogen atmosphere for 15 minutes. LCMS analysis showed incomplete conversion to desired product. An additional 4 drops of acetyl chloride were added. The reaction mixture was stirred at RT under a nitrogen atmosphere for 15 minutes. The reaction mixture was diluted with and partitioned between DCM (10 mL) and water (20 mL), and the phases were separated. The aqueous phase was further extracted with DCM (20 mL). The combined organic phases were dried by passing through a hydrophobic

frit and concentrated *in vacuo*. The crude material was then purified by normal phase chromatography, eluting with 0 – 6% MeOH in DCM over 25 CV. Fractions containing the desired product were concentrated *in vacuo* and then dried under high vacuum for 30 minutes to yield (*S*)-5-(1-((1-acetylpiperidin-3-yl)methyl)-4-methyl-1*H*-benzo[*d*]imidazol-2-yl)-1,3-dimethylpyridin-2(1*H*)-one **32** (211 mg, 0.511 mmol, 66% yield) as a yellow gum. **LCMS (HPLC)**: rt = 0.81 min, [M+H]⁺ 393 **¹H NMR δ(400 MHz, CDCl₃)**: *rotamer 1* 7.72 (1H, d, *J* = 2.4 Hz), 7.38 – 7.50 (1H, m), 7.18 (2H, s), 7.03 – 7.11 (1H, m), 3.98 – 4.38 (3H, m), 3.55 – 3.67 (4H, m), 2.96 – 3.06 (1H, m), 2.66 (3H, s), 2.45 – 2.53 (1H, m), 2.23 (3H, s), 1.99 – 2.11 (4H, m), 1.49 – 1.70 (2H, m), 1.23 – 1.38 (1H, m), 0.99 – 1.17 (1H, m). *rotamer 2* 7.72 (1H, d, *J* = 2.4 Hz), 7.38 – 7.50 (1H, m), 7.18 (2H, s), 7.03 – 7.11 (1H, m), 3.98 – 4.38 (3H, m), 3.64 (3H, s), 3.28 – 3.36 (1H, m), 2.96 – 3.06 (1H, m), 2.66 (3H, s), 2.45 – 2.53 (1H, m), 2.23 (3H, s), 1.99 – 2.11 (4H, m), 1.49 – 1.70 (2H, m), 1.23 – 1.38 (1H, m), 0.99 – 1.17 (1H, m). **¹³C NMR δ(101 MHz, CDCl₃)**: *additional peaks due to rotamers present* 169.0, 168.6, 162.6, 149.4, 142.0, 137.8, 137.6, 136.3, 135.9, 135.1, 129.9, 129.7, 123.2, 123.1, 123.0, 122.9, 109.3, 107.6, 107.4, 50.5, 49.9, 47.4, 46.7, 44.9, 41.9, 38.1, 38.1, 37.2, 35.9, 28.2, 24.7, 23.9, 21.3, 21.1, 17.4, 17.3, 16.6. **HRMS (ESI)** exact mass calculated for C₂₃H₂₉N₄O₂ [M+H]⁺ m/z 393.2291, found m/z 393.2292. **v_{max}(solid)**: 3387, 2921, 1655, 1614, 1426, 1263 cm⁻¹.

(*S*)-5-(1-((1-Acetylpiperidin-3-yl)methyl)-4-hydroxy-1*H*-benzo[*d*]imidazol-2-yl)-1,3-dimethylpyridin-2(1*H*)-one, Formic acid salt **33**

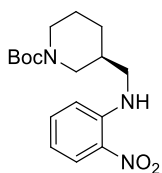


Chemical Formula: C₂₂H₂₆N₄O₃
Molecular Weight: 394.47 amu

Acetyl chloride (9 μ l, 0.120 mmol) was added to a solution of (*R*)-5-(4-methoxy-1-(1-(1-acetylpiperidin-3-yl)methyl)-4-methoxy-1*H*-benzo[*d*]imidazol-2-yl)-1,3-dimethylpyridin-2(1*H*)-one **52** (40 mg, 0.109 mmol) and triethylamine (46 μ L, 0.327 mmol) in DCM (1 mL) at RT. The reaction mixture was stirred for at RT under a nitrogen atmosphere for 1 h. LCMS analysis showed incomplete conversion to desired product. Additional acetyl chloride (9 μ l, 0.120 mmol) was added, and the reaction mixture stirred at RT under a nitrogen atmosphere for 5 h. The reaction mixture was diluted with and partitioned between DCM (20 mL) and brine (20 mL), and the phases were separated. The aqueous phase was further extracted with DCM (2 x 20 mL). The combined organic phases were washed with brine (20 mL), dried by passing through a hydrophobic frit, and concentrated *in vacuo* to yield (*S*)-5-(1-((1-acetylpiperidin-3-yl)methyl)-4-methoxy-1*H*-benzo[*d*]imidazol-2-yl)-1,3-dimethylpyridin-2(1*H*)-one **53** (46 mg, 0.107 mmol). This was used in the next reaction as a crude mixture. Boron tribromide (150 μ L, 1.587 mmol) was added to a stirring solution of (*S*)-5-(1-((1-acetylpiperidin-3-yl)methyl)-4-methoxy-1*H*-benzo[*d*]imidazol-2-yl)-1,3-dimethylpyridin-2(1*H*)-one **53** (40.0 mg, 0.098 mmol) in 1,2-dichloroethane (DCE) (1 mL) at RT under a nitrogen atmosphere. The reaction mixture was stirred at 60 $^{\circ}$ C under a nitrogen atmosphere for 1 h. LCMS analysis showed incomplete conversion to desired product. Additional boron tribromide (150 μ L, 1.587 mmol) was added, and the reaction mixture was stirred at RT under a nitrogen atmosphere for 20 h. LCMS analysis showed incomplete conversion to desired product. Additional boron tribromide (150 μ L, 1.587 mmol) was added, and the reaction mixture was stirred at RT under a nitrogen atmosphere for 1 h. LCMS analysis showed incomplete conversion to desired product. Additional boron tribromide (0.5 mL, 5.29 mmol) was added, and the reaction mixture was stirred at RT under a nitrogen atmosphere for 2 h.

The reaction mixture was quenched by the addition of water (15 mL). The reaction mixture was diluted with and partitioned between DCM (15 mL) and brine (15 mL), and the phases were separated. The aqueous phase was washed with DCM (3 x 20 mL) and 4:1 CHCl₃:IPA (2 x 20 mL). The combined organic phases were dried by passing through a hydrophobic frit, and concentrated *in vacuo*. The residue was dissolved in 1:1 MeOH:DMSO (1 mL) and purified by MDAP, using a solvent system of water containing 0.1% (v/v) formic acid (solvent A) and acetonitrile containing 0.1% (v/v) formic acid (solvent B). Fractions containing the desired product were combined and extracted with 4:1 CHCl₃:IPA (3 x 20 mL). The combined organic phases were dried by passing through a hydrophobic frit, and concentrated *in vacuo*. The residue was placed under high vacuum for 1 h to yield (S)-5-(1-((1-acetylpiperidin-3-yl)methyl)-4-hydroxy-1H-benzo[d]imidazol-2-yl)-1,3-dimethylpyridin-2(1H)-one, formic acid salt **33** (9 mg, 0.019 mmol, 20% yield) as a colourless gum. **LCMS (H₂O)**: rt = 0.49 min [M+H]⁺ 395. **¹H NMR δ(400 MHz, CDCl₃)**: *rotamer 1* 8.14 (1H, s), 7.66 – 7.73 (1H, m), 7.33 – 7.42 (1H, m), 7.24 (1H, t, *J* = 8.1 Hz), 6.82 – 6.96 (2H, m), 3.99 – 4.40 (3H, m), 3.58 – 3.68 (4H, m), 3.01 – 3.10 (1H, m), 2.49 – 2.57 (1H, m), 2.25 (3H, s), 2.05 – 2.14 (1H, m), 2.03 (3H, s), 1.54 – 1.71 (2H, m), 1.28 – 1.43 (1H, m), 1.02 – 1.17 (1H, m), 0.78 – 0.92 (1H, m). *rotamer 2* 8.14 (1H, s), 7.66 – 7.73 (1H, m), 7.33 – 7.42 (1H, m), 7.24 (1H, t, *J* = 8.1 Hz), 6.82 – 6.96 (2H, m), 3.99 – 4.40 (3H, m), 3.58 – 3.68 (4H, m), 3.32 – 3.39 (1H, m), 2.65 – 2.74 (1H, m), 2.25 (3H, s), 2.05 – 2.14 (1H, m), 2.03 (3H, s), 1.54 – 1.71 (2H, m), 1.28 – 1.43 (1H, m), 1.02 – 1.17 (1H, m), 0.78 – 0.92 (1H, m).

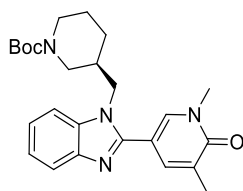
tert*-Butyl (S)-3-(((2-nitrophenyl)amino)methyl)piperidine-1-carboxylate **61*



Chemical Formula: C₁₇H₂₅N₃O₄
Molecular Weight: 335.40 amu

Potassium carbonate (484 mg, 3.50 mmol) and 1-fluoro-2-nitrobenzene **62** (246 μ L, 2.33 mmol) were added to a stirring solution of *tert*-butyl (*S*)-3-(aminomethyl)piperidine-1-carboxylate **48** (500 mg, 2.33 mmol) in DMF (10 mL). The reaction was stirred at 100 °C under a nitrogen atmosphere for 4 h. After cooling to RT, the reaction mixture was concentrated *in vacuo*. The residue was diluted with and partitioned between EtOAc (20 mL) and water (20 mL), and the phases were separated. The aqueous phase was further extracted with EtOAc (20 mL). The combined organic phases were washed with 5% (by wt) aqueous solution of lithium chloride (30 mL), dried by passing through a hydrophobic frit, and concentrated *in vacuo*. The crude material was then purified by normal phase chromatography, eluting with 0 – 20% 3:1 EtOAc in cyclohexane over 16 CV. Fractions containing the desired product were concentrated *in vacuo* to yield *tert*-butyl (*S*)-3-(((2-nitrophenyl)amino)methyl)piperidine-1-carboxylate **61** (763 mg, 2.09 mmol, 90% yield) as an orange gum. **LCMS (HpH)**: *rt* = 1.36 min, [M+H]⁺ 336 **¹H NMR δ (400 MHz, CDCl₃)**: 8.16 – 8.21 (1H, m), 8.07 – 8.15 (1H, m), 7.41 – 7.47 (1H, m), 6.81 – 6.86 (1H, m), 6.62 – 6.69 (1H, m), 3.89 – 4.10 (1H, m), 3.78 – 3.89 (1H, m), 3.22 – 3.33 (1H, m), 3.13 – 3.22 (1H, m), 2.90 – 3.04 (1H, m), 2.64 – 2.90 (1H, m), 1.85 – 2.01 (2H, m), 1.65 – 1.75 (1H, m), 1.45 (10H, s), 1.28 – 1.40 (1H, m). **ν_{max} (solid)**: 3377, 2927, 1684, 1617, 1510, 1417, 1142 cm⁻¹.

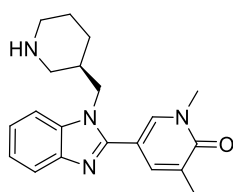
(*S*)-3-((2-(1,5-Dimethyl-6-oxo-1,6-dihydropyridin-3-yl)-1H-benzo[d]imidazol-1-yl)methyl)piperidine-1-carboxylate **63**



Chemical Formula: C₂₅H₃₂N₄O₃
Molecular Weight: 436.55 amu

tert-Butyl (*S*)-3-(((2-nitrophenyl)amino)methyl)piperidine-1-carboxylate **61** (373 mg, 1.11 mmol), 1,5-dimethyl-6-oxo-1,6-dihydropyridine-3-carbaldehyde **36** (202 mg, 1.34 mmol), EtOH (7mL), and water (3.5 mL) were added to a round bottom flask. The reaction mixture was heated to 80 °C, after which sodium dithionite (581 mg, 3.34 mmol) was added. The reaction mixture was stirred at 100 °C under a nitrogen atmosphere for 1 h. After cooling to RT, the reaction mixture was diluted with and partitioned between EtOAc (20 mL) and water (20 mL), and the phases were separated. The aqueous phase was further extracted with EtOAc (20 mL). The combined organic phases were washed with brine (20 mL), dried by passing through a hydrophobic frit, and concentrated *in vacuo*. This was dried on high vacuum for 16 h to yield (*S*)-3-((2-(1,5-dimethyl-6-oxo-1,6-dihydropyridin-3-yl)-1H-benzo[d]imidazol-1-yl)methyl)piperidine-1-carboxylate **63** (383 mg, 0.833 mmol, 75% yield) as a yellow gum. **LCMS (HpH)**: rt = 1.07 min, [M+H]⁺ 437 **¹H NMR δ(400 MHz, CDCl₃)**: 7.73 – 7.78 (2H, m), 7.48 – 7.51 (1H, m), 7.36 – 7.40 (1H, m), 7.28 – 7.34 (2H, m), 4.06 – 4.20 (2H, m), 3.77 – 3.90 (1H, m), 3.65 (3H, s), 2.70 – 2.84 (1H, m), 2.48 – 2.58 (1H, m), 2.25 (3H, s), 1.99 – 2.11 (1H, m), 1.51 – 1.64 (2H, m), 1.35 (11H, m), 0.99 – 1.12 (1H, m). **HRMS (ESI)** exact mass calculated for C₂₅H₃₃N₄O₃ [M+H]⁺ m/z 437.2553, found m/z 437.2552. **v_{max}(solid)**: 2973, 2926, 1652, 1426, 1270, 1142 cm⁻¹.

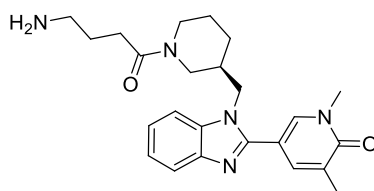
(*R*)-1,3-Dimethyl-5-(1-(piperidin-3-ylmethyl)-1H-benzo[d]imidazol-2-yl)pyridin-2(1H)-one 60



Chemical Formula: C₂₀H₂₄N₄O
Molecular Weight: 336.43 amu

tert-Butyl (S)-3-((2-(1,5-dimethyl-6-oxo-1,6-dihydropyridin-3-yl)-1*H*-benzo[*d*]imidazol-1-yl)methyl)piperidine-1-carboxylate **63** (365 mg, 0.836 mmol) was dissolved in a solution of hydrochloric acid in 1,4-dioxane (4 M, 4 mL, 16 mmol). MeOH (1 mL) was added to aid solubility. The reaction mixture was stirred at RT under air for 1 h. The reaction mixture was diluted with methanol (20 mL) and then added to a SCX 20 g column (pre-wet with methanol) and allowed to settle by gravity. The column was then washed with methanol (80 mL) under vacuum. Into a separate flask, the column was washed with a solution of ammonia in MeOH (2 M, 80 mL). The filtrate was concentrated *in vacuo* to yield (*R*)-1,3-dimethyl-5-(1-(piperidin-3-ylmethyl)-1*H*-benzo[*d*]imidazol-2-yl)pyridin-2(1*H*)-one **60** (283 mg, 0.799 mmol, 96% yield) as a yellow gum. **LCMS (HPLC)**: *rt* = 0.73 min, [M+H]⁺ 337. **¹H NMR δ(400 MHz, CDCl₃)**: 7.77 – 7.82 (1H, m), 7.71 – 7.76 (1H, m), 7.51 – 7.55 (1H, m), 7.35 – 7.41 (1H, m), 7.24 – 7.30 (2H, m), 4.04 – 4.20 (2H, m), 3.63 (3H, s), 2.87 – 2.94 (1H, m), 2.73 – 2.79 (1H, m), 2.51 – 2.60 (1H, m), 2.26 – 2.34 (1H, m), 2.22 (3H, s), 2.00 – 2.20 (2H, m), 1.55 – 1.66 (2H, m), 1.30 – 1.44 (1H, m), 1.03 – 1.18 (1H, m). **¹³C NMR δ(101 MHz, CDCl₃)**: 162.7 (C), 150.4 (C), 142.8 (C), 137.6 (CH), 136.2 (CH), 135.9 (C), 129.8 (C), 122.9 (CH), 122.6 (CH), 119.7 (CH), 110.3 (CH), 109.4 (C), 50.2 (CH₂), 48.2 (CH₂), 46.6 (CH₂), 38.1 (CH₃), 37.3 (CH), 29.0 (CH₂), 25.1 (CH₂), 17.4 (CH₃). **HRMS (ESI)** exact mass calculated for C₂₀H₂₅N₄O [M+H]⁺ *m/z* 337.2029, found *m/z* 337.2026. ***v*_{max}(solid)**: 3366, 2927, 2832, 1651, 1597, 1456 cm⁻¹.

(S)-5-(1-((1-(4-aminobutanoyl)piperidin-3-yl)methyl)-1*H*-benzo[*d*]imidazol-2-yl)-1,3-dimethylpyridin-2(1*H*)-one **58**

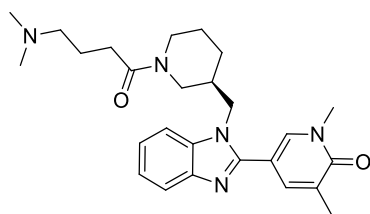


Chemical Formula: C₂₄H₃₁N₅O₂
Molecular Weight: 421.54 amu

DIPEA (587 μ L, 3.36 mmol) was added to a stirring solution of 4-((*tert*-butoxycarbonyl)amino)butanoic acid **64** (137 mg, 0.672 mmol) and HATU (319 mg, 0.840 mmol) in DMF (1.5 mL) at RT. The reaction mixture was stirred at RT under air for 10 minutes, after which a solution of (*R*)-1,3-dimethyl-5-(1-(piperidin-3-ylmethyl)-1H-benzo[d]imidazol-2-yl)pyridin-2(1H)-one **60** (226 mg, 0.672 mmol) in DMF (1.5 mL) was added. The reaction mixture was stirred at RT under air for 4 h. The reaction mixture was diluted with and partitioned between EtOAc (20 mL) and a 5% (by wt) aqueous solution of lithium chloride (20 mL), and the phases were separated. The aqueous phase was further extracted with EtOAc (20 mL). The combined organic phases were washed with 5% (by wt) aqueous solution of lithium chloride (3 x 20 mL), dried by passing through a hydrophobic frit, and concentrated *in vacuo* to yield *tert*-butyl (*S*)-(4-(3-((2-(1,5-dimethyl-6-oxo-1,6-dihydropyridin-3-yl)-1H-benzo[d]imidazol-1-yl)methyl)piperidin-1-yl)-4-oxobutyl) carbamate (371 mg, 0.711 mmol) as a brown gum. This was taken forward crude. *tert*-Butyl (*S*)-(4-(3-((2-(1,5-dimethyl-6-oxo-1,6-dihydropyridin-3-yl)-1H-benzo[d]imidazol-1-yl)methyl)piperidin-1-yl)-4-oxobutyl)carbamate (371 mg, 0.711 mmol) was dissolved in a solution of hydrochloric acid in 1,4-dioxane (4 M, 3 mL, 12 mmol). The reaction mixture was stirred at RT under air for 2 h. The reaction mixture was dissolved in methanol (40 mL) and then added to a SCX 20 g column (pre-wet with methanol) and allowed to settle by gravity. The column was then washed with methanol (80 mL) under vacuum. Into a separate flask, the column was washed with a solution of ammonia in MeOH (2 M, 80 mL). The filtrate was concentrated under a stream of nitrogen to yield (*S*)-5-(1-((1-(4-aminobutanoyl)piperidin-3-yl)methyl)-1H-benzo[d]imidazol-2-yl)-1,3-dimethylpyridin-2(1H)-one **58** (260 mg, 0.586 mmol, 87% yield) as a brown gum. **LCMS (H_pH)**: *rt* = 0.73 min, [M+H]⁺ 422 **¹H NMR δ (400 MHz, CDCl₃)**: 7.74 - 7.87 (2H, m), 7.50 - 7.55 (1H, m), 7.36 - 7.45 (1H, m), 7.29 - 7.35 (2H, m), 4.18 - 4.39 (2H, m), 4.04 - 4.14 (1H, m), 3.64 - 3.70 (4H, m), 3.36 - 3.43 (1H, m), 2.98 - 3.06 (1H, m), 2.75 - 2.80 (1H, m), 2.50 - 2.69 (2H, m), 2.33 - 2.39 (1H,

m), 2.26 (3H, s), 1.95 – 2.14 (2H, m), 1.74 – 1.85 (1H, m), 1.50 – 1.69 (3H, m), 1.00 – 1.39 (3H, m). ^{13}C NMR δ (101 MHz, DMSO- d_6): additional peaks due to rotamers present 170.2, 170.1, 161.7, 150.4, 150.2, 142.4, 142.3, 138.3, 138.2, 136.6, 135.9, 135.8, 127.9, 127.8, 122.2, 121.9, 121.9, 118.8, 111.1, 110.9, 108.1, 79.1, 48.2, 46.9, 46.7, 45.2, 44.3, 41.3, 40.5, 40.5, 38.6, 38.5, 38.2, 37.3, 36.9, 36.1, 29.8, 27.6, 27.4, 24.6, 23.8, 16.8. HRMS (ESI) exact mass calculated for $\text{C}_{24}\text{H}_{32}\text{N}_5\text{O}_2$ [M+H] $^+$ m/z 422.2557, found m/z 422.2555. ν_{max} (solid): 3403, 2927, 2864, 1651, 1603, 1454, 1428 cm^{-1} .

(S)-5-(1-((1-(4-(Dimethylamino)butanoyl)piperidin-3-yl)methyl)-1H-benzo[d]imidazol-2-yl)-1,3-dimethylpyridin-2(1H)-one 65

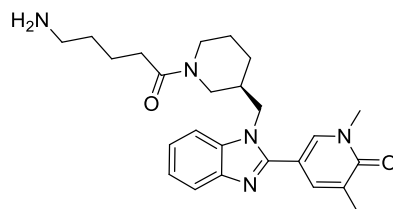


Chemical Formula: $\text{C}_{26}\text{H}_{35}\text{N}_5\text{O}_2$
Molecular Weight: 449.59 amu

DIPEA (78 μL , 0.446 mmol) was added to a solution of 4-(dimethylamino)butanoic acid, hydrochloride (15 mg, 0.089 mmol) and HATU (42 mg, 0.111 mmol) in DMF (0.5 mL) at RT. The reaction mixture was stirred at RT under air for 10 minutes, after which a solution of (R)-1,3-dimethyl-5-(1-(piperidin-3-ylmethyl)-1H-benzo[d]imidazol-2-yl)pyridin-2(1H)-one **60** (30 mg, 0.089 mmol) in DMF (0.5 mL) was added. The reaction mixture was stirred at RT under air for 1 h. LCMS analysis indicated incomplete conversion to desired product. Additional 4-(dimethylamino)butanoic acid, hydrochloride (15 mg, 0.089 mmol) and HATU (42 mg, 0.111 mmol) were added and the reaction mixture was stirred at RT under air for 1 h. The reaction mixture was diluted with and partitioned between 4:1 CHCl_3 : IPA (20 mL) and a 5% (by wt) aqueous solution of lithium chloride (20 mL), and the phases were separated. The aqueous phase was further extracted with 4:1 CHCl_3 : IPA (2 x 20 mL). Solid sodium chloride was added to the aqueous phase to saturate it (about 3 spatulas) and the aqueous phase

was extracted a further two times with 4:1 CHCl₃: IPA (2 x 20 mL). The combined organic phases were dried by passing through a hydrophobic frit, and concentrated *in vacuo*. The residue was dissolved in 1:1 MeOH:DMSO (1 mL) and purified by MDAP, using a solvent system of 10 mM ammonium bicarbonate adjusted to pH 10 with ammonia in water (solvent A) and acetonitrile (solvent B). Fractions containing the desired product were combined and extracted with DCM (2 x 20 mL). The combined organic phases were dried by passing through a hydrophobic frit, and concentrated *in vacuo* to give a colourless gum. This was then placed under high vacuum for 3H to yield (*S*)-5-(1-((1-(4-(dimethylamino)butanoyl)piperidin-3-yl)methyl)-1*H*-benzo[*d*]imidazol-2-yl)-1,3-dimethylpyridin-2(1*H*)-one **65** (20 mg, 0.042 mmol, 47% yield) as a white solid. **LCMS (H_{PLC})**: rt = 0.77 min, [M+H]⁺ 450 **¹H NMR δ(400 MHz, DMSO-*d*₆)**: 7.93 - 8.03 (1H, m), 7.65 - 7.69 (1H, m), 7.55 - 7.65 (2 H, m), 7.18 - 7.30 (2H, m), 4.18 - 4.34 (2H, m), 3.69 - 3.90 (2H, m), 3.59 (3H, s), 2.62 - 2.70* overlapping with H₂O peak (1H, integrates as 2H, m), 2.27 - 2.35 (2H, m), 2.23 (6H, s), 2.11 - 2.19 (5H, m), 1.88 - 2.01 (1H, m), 1.53 - 1.65 (4H, m), 1.16 - 1.34 (3H, m) **¹³C NMR δ(176 MHz, DMSO-*d*₆)**: additional peaks due to rotamers present. 170.1, 170.0, 161.7, 150.4, 150.2, 142.4, 142.3, 138.3, 138.3, 136.7, 136.0, 135.9, 127.9, 127.8, 122.2, 122.0, 121.9, 118.8, 111.1, 111.0, 108.2, 108.2, 66.1, 58.1, 54.9, 48.2, 46.9, 46.7, 45.3, 44.6, 44.6, 44.3, 41.4, 37.4, 36.9, 36.1, 29.8, 29.8, 27.7, 27.6, 24.6, 23.9, 22.3, 22.2, 22.0, 16.8.

(*S*)-5-(1-((1-(5-Aminopentanoyl)piperidin-3-yl)methyl)-1*H*-benzo[*d*]imidazol-2-yl)-1,3-dimethylpyridin-2(1*H*)-one **66**

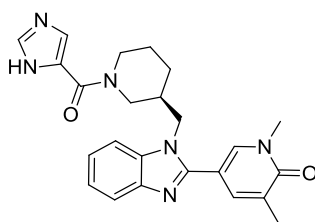


Chemical Formula: C₂₅H₃₃N₅O₂
Molecular Weight: 435.56 amu

DIPEA (78 μ L, 0.446 mmol) was added to a stirring solution of 5-((tert-butoxycarbonyl)amino)pentanoic acid (32 mg, 0.149 mmol) and HATU (71 mg, 0.186 mmol) in DMF (0.5 mL) at RT. The reaction mixture was stirred at RT under air for 10 minutes, after which a solution of (*R*)-1,3-dimethyl-5-(1-(piperidin-3-ylmethyl)-1*H*-benzo[*d*]imidazol-2-yl)pyridin-2(1*H*)-one **60** (50 mg, 0.149 mmol) in DMF (0.5 mL) was added. The reaction mixture was stirred at RT under air for 2 h. The reaction mixture was diluted with and partitioned between EtOAc (20 mL) and a 10% (by wt) aqueous solution of lithium chloride (20 mL), and the phases were separated. The aqueous phase was further extracted with EtOAc (20 mL). The combined organic phases were washed with 10% (by wt) aqueous solution of lithium chloride (2 x 20 mL), dried by passing through a hydrophobic frit, and concentrated *in vacuo* to yield tert-butyl (*S*)-(5-(3-((2-(1,5-dimethyl-6-oxo-1,6-dihydropyridin-3-yl)-1*H*-benzo[*d*]imidazol-1-yl)methyl)piperidin-1-yl)-5-oxopentyl)carbamate (122 mg, 0.228 mmol) as a brown gum. This was taken forward to the next reaction as a crude mixture. (*S*)-(5-(3-((2-(1,5-dimethyl-6-oxo-1,6-dihydropyridin-3-yl)-1*H*-benzo[*d*]imidazol-1-yl)methyl)piperidin-1-yl)-5-oxopentyl)carbamate (122 mg, 0.228 mmol) was added to a solution of hydrochloric acid in 1,4-dioxane (4 M, 5 mL, 20 mmol). MeOH (2 mL) was added to aid solubility. The reaction mixture was stirred at RT under air for 1 h. The reaction mixture was concentrated *in vacuo*. The residue was dissolved in 1:1 MeOH:DMSO (1 mL) and purified by MDAP using a solvent system of 10 mM ammonium bicarbonate adjusted to pH 10 with ammonia in water (solvent A) and acetonitrile (solvent B). Fractions containing the desired product were combined and extracted with DCM (2 x 20 mL). The combined organic phases were dried by passing through a hydrophobic frit, and concentrated *in vacuo* to yield (*S*)-5-(1-((1-(5-aminopentanoyl)piperidin-3-yl)methyl)-1*H*-benzo[*d*]imidazol-2-yl)-1,3-dimethylpyridin-2(1*H*)-one **66** (16 mg, 0.035 mmol, 23% yield) as a white solid. **LCMS (H_pH)**: rt = 0.73 min, [M+H]⁺ 436. **¹H NMR δ (400 MHz, DMSO-*d*₆, VT)**: 7.92 – 8.06 (1H, m), 7.60 – 7.72 (2H, m), 7.52 – 7.60 (1H, m), 7.11 – 7.37 (2H, m), 4.19 – 4.34 (2H, m), 3.79 – 3.92 (1H, m), 3.67 – 3.78 (1H, m), 3.59 (3H, s), 2.62 – 2.91 (4H, m), 2.47 – 2.55* overlapping

DMSO peak (2H, integrates as 7H, m), 2.07 – 2.18 (5H, m), 1.88 – 2.01 (1H, m), 1.54 – 1.64 (2H, m), 1.40 – 1.51 (2H, m), 1.14 – 1.35 (4H, m). ¹³C NMR δ(176 MHz, DMSO-*d*6) ppm: additional peaks due to rotamers present 170.4, 170.1, 170.0, 161.7, 161.7, 150.4, 150.3, 150.2, 142.4, 142.3, 138.3, 138.3, 138.2, 136.7, 136.7, 136.6, 136.0, 135.9, 135.8, 127.9, 127.8, 127.8, 122.2, 122.1, 122.0, 121.9, 121.8, 118.8, 118.7, 111.1, 111.0, 111.0, 108.3, 108.2, 108.1, 49.6, 48.6, 48.3, 47.5, 46.9, 46.7, 46.2, 45.3, 44.2, 41.3, 41.2, 41.2, 37.4, 37.3, 37.1, 36.7, 36.1, 32.7, 32.2, 31.4, 28.4, 27.7, 27.6, 25.0, 24.6, 23.9, 22.2, 22.0, 20.7, 16.8. HRMS (ESI) exact mass calculated for C₂₅H₃₄N₅O₂ [M+H]⁺ m/z 436.2713, found m/z 436.2712.

(S)-5-(1-((1-(1H-Imidazole-5-carbonyl)piperidin-3-yl)methyl)-1H-benzo[d]imidazol-2-yl)-1,3-dimethylpyridin-2(1H)-one, formic acid salt 67

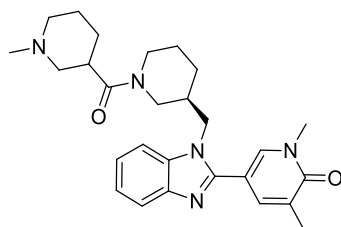


Chemical Formula: C₂₄H₂₆N₆O₂
Molecular Weight: 430.50 amu

DIPEA (130 μL, 0.743 mmol) was added to a stirring solution of HATU (71 mg, 0.186 mmol) and 1H-imidazole-5-carboxylic acid (17 mg, 0.149 mmol) in DMF (0.5 mL) at RT. The reaction mixture was stirred at RT for 10 minutes, after which a solution of (R)-1,3-dimethyl-5-(1-(piperidin-3-ylmethyl)-1H-benzo[d]imidazol-2-yl)pyridin-2(1H)-one **60** (50 mg, 0.149 mmol) in DMF (0.5 mL) was added. The reaction mixture was stirred at RT under a nitrogen atmosphere for 1 h. LCMS analysis showed incomplete conversion to desired product. Additional 1H-imidazole-5-carboxylic acid (17 mg, 0.149 mmol) was added. The reaction mixture was stirred at RT under a nitrogen atmosphere for 16 h. The reaction mixture was diluted with and partitioned between DCM (10 mL) and a 5 % (by wt) aqueous solution of lithium chloride (10 mL), and the phases were separated. The aqueous phase was further

extracted with DCM (2 x 10 mL). The combined organic phases were washed with a 5% (by wt) aqueous solution of lithium chloride (10 mL), dried by passing through a hydrophobic frit, and concentrated *in vacuo*. The residue was dissolved in 1:1 MeOH:DMSO and purified by MDAP using a solvent system of 10 mM ammonium bicarbonate adjusted to pH 10 with ammonia in water (solvent A) and acetonitrile (solvent B). Fractions containing the desired product were combined and extracted with DCM (2 x 20 mL). The combined organic phases were dried by passing through a hydrophobic frit, and concentrated *in vacuo*. LCMS analysis showed purification was unsuccessful. The residue was dissolved in 1:1 MeOH:DMSO and purified by MDAP using a 0.1% v/v solution of formic acid in water (solvent A) and 0.1% v/v solution of formic acid in acetonitrile (solvent B). Fractions containing the desired product were combined and concentrated *in vacuo* to yield (*S*)-5-(1-((1-(1*H*-imidazole-5-carbonyl)piperidin-3-yl)methyl)-1*H*-benzo[*d*]imidazol-2-yl)-1,3-dimethylpyridin-2(1*H*)-one **67**, formic acid salt (14 mg, 0.031 mmol, 19% yield) as a white solid. **LCMS (H_pH)**: rt = 0.72 min, [M+H]⁺ 431 **¹H NMR δ(400 MHz, DMSO-*d*₆)**: 8.12 – 8.43 (1H, m)* formic salt, 7.94 – 8.04 (1H, m), 7.61 – 7.69 (2H, m), 7.53 – 7.59 (1H, m), 7.31 – 7.52 (1H, m), 7.17 – 7.29 (2H, m), 4.24 – 4.43 (4H, m), 3.56 (3H, s), 3.01 – 3.09 (1H, m), 2.83 – 2.94 (1H, m), 2.12 (3H, s), 2.01 – 2.10 (1H, m), 1.57 – 1.70 (2H, m), 1.24 – 1.43 (2H, m), 1.18 – 1.48 (2H, m). **HRMS (ESI)** exact mass calculated for C₂₄H₂₇N₆O₂ [M+H]⁺ m/z 431.2196, found m/z 431.2200. **v_{max}(solid)**: 3398, 3168, 2916, 1653, 1587, 1455, 1428 cm⁻¹.

1,3-Dimethyl-5-(1-(((*S*)-1-(1-methylpiperidine-3-carbonyl)piperidin-3-yl)methyl)-1*H*-benzo[*d*]imidazol-2-yl)pyridin-2(1*H*)-one **69**

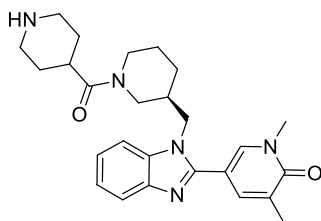


Chemical Formula: C₂₇H₃₅N₅O₂
Molecular Weight: 461.60 amu

DIPEA (130 μ L, 0.743 mmol) was added to a solution of 1-methylpiperidine-3-carboxylic acid (21 mg, 0.149 mmol) and HATU (71 mg, 0.186 mmol) in DMF at RT. The reaction mixture was stirred at RT under air for 10 minutes, after which a solution of (*R*)-1,3-dimethyl-5-(1-(piperidin-3-ylmethyl)-1*H*-benzo[*d*]imidazol-2-yl)pyridin-2(1*H*)-one **60** (50 mg, 0.149 mmol) in DMF (0.5 mL) was added. The reaction mixture was stirred at RT under air for 1 h. The reaction mixture was diluted with and partitioned between EtOAc (20 mL) and a 5% (by wt) aqueous solution of lithium chloride (20 mL), and the phases were separated. The aqueous phase was further extracted with EtOAc (20 mL). The combined organic phases were washed with a 5% (by wt) aqueous solution of lithium chloride (20 mL), dried by passing through a hydrophobic frit, and concentrated *in vacuo*. The aqueous phase was further extracted with DCM (3 x 20 mL). The combined organics were dried by passing through a hydrophobic frit, combined with the first batch, and concentrated *in vacuo*. The residue was dissolved in 1:1 MeOH:DMSO (1 mL) and purified by MDAP using a solvent system of 10 mM ammonium bicarbonate adjusted to pH 10 with ammonia in water (solvent A) and acetonitrile (solvent B). Fractions containing the desired product were combined and extracted with DCM (2 x 30 mL). The combined organic phases were dried by passing through a hydrophobic frit, and concentrated *in vacuo* to yield 1,3-dimethyl-5-(1-(((3*S*)-1-(1-methylpiperidine-3-carbonyl)piperidin-3-yl)methyl)-1*H*-benzo[*d*]imidazol-2-yl)pyridin-2(1*H*)-one **69** (29 mg, 60 μ mol, 40% yield) as a white solid. **LCMS (H_pH)**: rt = 0.83 min, [M+H]⁺ 462. **¹H NMR δ (400 MHz, DMSO-*d*₆, VT)**: 7.96 – 8.01 (1H, m), 7.61 – 7.69 (2H, m), 7.57 (1H, d, *J* = 7.8 Hz), 7.19 – 7.29 (2H, m), 4.19 – 4.35 (2H, m), 3.83 – 3.93 (1H, m), 3.65 – 3.76 (1H, m), 3.59 (3H, s), 2.77 – 2.89* overlapping H₂O peak (1H, integrates as 15H, m), 2.65 – 2.73 (2H, m), 2.52 – 2.61 (2H, m), 2.10 – 2.17 (6H, m), 1.75 – 1.99 (3H, m), 1.14 – 1.63 (8H, m). **¹³C NMR δ (101 MHz, CDCl₃)**: additional peaks due to rotamers present 172.7, 172.6, 162.6, 150.3, 142.9, 142.8, 137.7, 136.0, 135.9, 135.6, 130.1, 129.9, 123.0, 122.7, 120.2, 119.9, 110.1, 110.0, 109.2, 99.9, 58.2, 58.1, 55.6, 47.6, 47.4, 46.6, 46.5, 45.9,

45.8, 45.2, 42.0, 39.6, 39.5, 38.1, 36.3, 36.1, 28.5, 28.2, 27.1, 25.3, 25.2, 25.1, 25.0, 24.9, 17.4,
1.8. $\nu_{\max}(\text{solid})$: 3424, 2931, 2864, 2796, 1653, 1607, 1455 cm^{-1} .

(S)-1,3-Dimethyl-5-(1-((1-(piperidine-4-carbonyl)piperidin-3-yl)methyl)-1H-benzo[d]imidazol-2-yl)pyridin-2(1H)-one 70

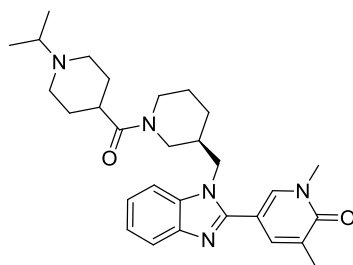


Chemical Formula: $\text{C}_{26}\text{H}_{33}\text{N}_5\text{O}_2$
Molecular Weight: 447.57 amu

DIPEA (130 μL , 0.743 mmol) was added to a solution of 1-(*tert*-butoxycarbonyl)piperidine-4-carboxylic acid (34 mg, 0.149 mmol) and HATU (71 mg, 0.186 mmol) in DMF (0.5 mL) at RT. The reaction mixture was stirred at RT under air for 10 minutes, after which a solution of (*R*)-1,3-dimethyl-5-(1-(piperidin-3-ylmethyl)-1H-benzo[d]imidazol-2-yl)pyridin-2(1H)-one **60** (50 mg, 0.149 mmol) in DMF (0.5 mL) was added. The reaction mixture was stirred at RT under air for 1 h. The reaction mixture was diluted with and partitioned between EtOAc (20 mL) and a 5% (by wt) aqueous solution of lithium chloride (20 mL), and the phases were separated. The aqueous phase was further extracted with EtOAc (20 mL). The combined organic phases were washed with a 5% (by wt) aqueous solution of lithium chloride (20 mL), dried by passing through a hydrophobic frit, and concentrated *in vacuo* to yield *tert*-butyl (*S*)-4-(3-((2-(1,5-dimethyl-6-oxo-1,6-dihydropyridin-3-yl)-1H-benzo[d]imidazol-1-yl)methyl)piperidine-1-carbonyl)piperidine-1-carboxylate (236 mg, 0.147 mmol) as a brown oil. This was taken forward crude. *tert*-Butyl (*S*)-4-(3-((2-(1,5-dimethyl-6-oxo-1,6-dihydropyridin-3-yl)-1H-benzo[d]imidazol-1-yl)methyl)piperidine-1-carbonyl)piperidine-1-carboxylate (236 mg, 0.147 mmol) was added to a solution of hydrochloric acid in 1,4-dioxane (4 M, 0.5 mL, 2 mmol). The reaction mixture was stirred at

RT under a nitrogen atmosphere for 3 h. The reaction mixture was concentrated *in vacuo*. The residue was dissolved in 1:1 MeOH:DMSO (1 mL) and purified MDAP using a solvent system of 10 mM ammonium bicarbonate adjusted to pH 10 with ammonia in water (solvent A) and acetonitrile (solvent B). Fractions containing the desired product were combined and extracted with DCM (3 x 50 mL). The combined organic phases were dried by passing through a hydrophobic frit, and concentrated *in vacuo* to yield (S)-1,3-dimethyl-5-(1-((1-(piperidine-4-carbonyl)piperidin-3-yl)methyl)-1H-benzo[d]imidazol-2-yl)pyridin-2(1H)-one **70** (17 mg, 36 μ mol, 25% yield) as a white solid. **LCMS (HPLC)**: rt = 0.80 min, [M+H]⁺ 448. **¹H NMR δ (400 MHz, DMSO-*d*₆, VT)**: 7.89 – 8.06 (1H, m), 7.61 – 7.68 (2H, m), 7.52 – 7.61 (1H, m), 7.17 – 7.31 (2H, m), 4.18 – 4.35 (2H, m), 3.83 – 3.99 (1H, m), 3.61 – 3.72 (1H, m), 3.59 (3H, s), 2.74 – 2.94* overlapping with H₂O peak (4H, integrates as 7H, m), 2.64 – 2.73 (1H, m), 2.30 – 2.47 (3H, m), 2.14 (3H, s), 1.87 – 1.99 (1H, m), 1.54 – 1.64 (2H, m), 1.14 – 1.48 (6H, m). **HRMS (ESI)** exact mass calculated for C₂₆H₃₄N₅O₂ [M+H]⁺ m/z 448.2713, found m/z 448.2710. **ν_{\max} (solid)**: 3398, 2921, 2853, 1654, 1604, 1452 cm⁻¹.

(S)-5-(1-((1-(1-Isopropylpiperidine-4-carbonyl)piperidin-3-yl)methyl)-1H-benzo[d]imidazol-2-yl)-1,3-dimethylpyridin-2(1H)-one **71**

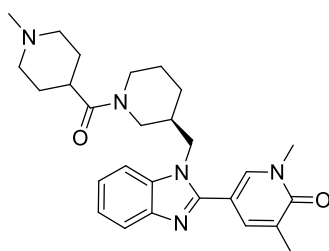


Chemical Formula: C₂₉H₃₉N₅O₂
Molecular Weight: 489.65 amu

DIPEA (39 μ L, 0.223 mmol) was added to a solution of 1-*isopropyl*piperidine-4-carboxylic acid (13 mg, 0.076 mmol) and HATU (35 mg, 0.093 mmol) in DMF (0.5 mL) at RT. The reaction mixture was stirred at RT under air for 10 minutes, after which a solution of (*R*)-1,3-dimethyl-5-(1-(piperidin-3-ylmethyl)-1*H*-benzo[*d*]imidazol-2-yl)pyridin-2(1*H*)-one **60** (25 mg, 0.074 mmol) in DMF (0.5 mL) was added. The reaction mixture was stirred at RT under air for 1 h. The reaction mixture was dissolved in and partitioned between DCM (20 mL) and a 10% (by wt) aqueous solution of lithium chloride (2 x 20 mL), and the phases were separated. The aqueous phase was further extracted with 4:1 CHCl₃:IPA (2 x 20 mL). The combined organic phases were washed with a 10% (by wt) aqueous solution of lithium chloride (3 x 20 mL), dried by passing through a hydrophobic frit, and concentrated *in vacuo*. The residue was dissolved in 1:1 MeOH:DMSO (1 mL) and purified by EZ preparative HPLC, eluting with 15 – 100% 10 mM ammonium bicarbonate (aq)/MeCN. Fractions containing the desired product were combined and extracted with 4:1 CHCl₃:IPA (2 x 20 mL), dried by passing through a hydrophobic frit, and concentrated *in vacuo* to yield (*S*)-5-(1-((1-(1-*isopropyl*piperidine-4-carbonyl)piperidin-3-yl)methyl)-1*H*-benzo[*d*]imidazol-2-yl)-1,3-dimethylpyridin-2(1*H*)-one **71** (21 mg, 0.041 mmol, 58% yield) as a pale yellow solid. **LCMS (HpH)**: rt = 0.88 min, [M+H]⁺ 490 **¹H NMR δ (400 MHz, DMSO-*d*₆, VT)**: *rotamer 1* 7.98 (1H, d, *J* = 2.4 Hz), 7.61 – 7.68 (2H, m), 7.55 – 7.60 (1H, m), 7.25 (2H, s), 4.20 – 4.32 (2H, m), 3.87 – 3.98 (1H, m), 3.60 – 3.71 (1H, m), 3.59 (3H, s), 2.58 – 2.88* overlapping H₂O peak (5H, integrates as 12H, m), 2.13 – 2.23 (4H, m), 1.87 – 2.07 (3H, m), 1.39 – 1.64 (5H, m), 1.14 – 1.37 (3H, m), 1.09 (6H, d, *J* = 5.9 Hz). *rotamer 2* 7.98 (1H, d, *J* = 2.4 Hz), 7.61 – 7.68 (2H, m), 7.55 – 7.60 (1H, m), 7.25 (2H, s), 4.20 – 4.32 (2H, m), 3.87 – 3.98 (1H, m), 3.60 – 3.71 (1H, m), 3.59 (3H, s), 2.58 – 2.88* overlapping H₂O peak (5H, integrates as 12H, m), 2.13 – 2.23 (4H, m), 1.87 – 2.07 (3H, m), 1.39 – 1.64 (5H, m), 1.14 – 1.37 (3H, m), 0.97 (6H, d, *J* = 6.4 Hz). **¹³C NMR δ (176 MHz, DMSO-*d*₆)**: *additional peaks due to rotamers present* 172.6, 172.1, 161.7, 150.5, 150.3, 142.4, 142.4, 138.3, 136.7, 136.6, 135.8, 127.9, 127.8, 122.2, 121.9, 118.8, 111.2, 111.0, 108.1, 108.0, 62.0, 53.7, 47.9, 47.6, 47.5, 47.3, 46.8, 46.7,

45.1, 44.3, 41.4, 40.4, 40.3, 40.2, 40.1, 40.1, 40.0, 38.1, 38.0, 37.8, 37.3, 35.8, 28.9, 28.8, 28.6, 28.0, 27.3, 25.4, 24.6, 24.2, 18.0, 17.9, 17.8, 16.8. **HRMS (ESI)** exact mass calculated for $C_{29}H_{40}N_5O_2$ $[M+H]^+$ m/z 490.3183, found m/z 490.3177. $\nu_{\max}(\text{solid})$: 3440, 2932, 2864, 1655, 1611, 1453 cm^{-1} .

(S)-1,3-Dimethyl-5-(1-((1-(1-methylpiperidine-4-carbonyl)piperidin-3-yl)methyl)-1H-benzo[d]imidazol-2-yl)pyridin-2(1H)-one 72

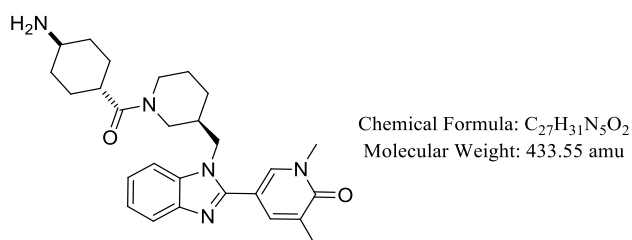


Chemical Formula: $C_{27}H_{35}N_5O_2$
Molecular Weight: 461.60 amu

DIPEA (78 μL , 0.446 mmol) was added to a stirring solution of 1-methylpiperidine-4-carboxylic acid (21 mg, 0.149 mmol) and HATU (71 mg, 0.186 mmol) in DMF (0.5 mL) at RT. The reaction was stirred at RT under air for 10 minutes, after which a solution of (*R*)-1,3-dimethyl-5-(1-(piperidin-3-ylmethyl)-1H-benzo[d]imidazol-2-yl)pyridin-2(1H)-one **60** (50 mg, 0.149 mmol) in DMF (0.5 mL) was added. The reaction mixture was stirred for at RT under air for 1 h. The reaction mixture was diluted with and partitioned between EtOAc (20 mL) and a 5% (by wt) aqueous solution of lithium chloride (20 mL), and the phases were separated. The aqueous phase was further extracted with 4:1 CHCl_3 :IPA (3 x 20 mL). The aqueous phase was salted by addition of solid sodium chloride (approximately 2 g), and the aqueous phase further extracted with 4:1 CHCl_3 :IPA (3 x 20 mL). The combined organic phases were washed with brine (2 x 20 mL), dried by passing through a hydrophobic frit, and concentrated *in vacuo*. The residue was dissolved in 1:1 MeOH:DMSO (1 mL) and purified by MDAP using a solvent system of 10 mM ammonium bicarbonate adjusted to pH 10 with ammonia in water (solvent A) and acetonitrile (solvent B). Fractions containing the desired

product were combined and extracted with DCM (2 x 40 mL). The combined organic phases were dried by passing through a hydrophobic frit, and concentrated *in vacuo* to yield (*S*)-1,3-dimethyl-5-(1-((1-(1-methylpiperidine-4-carbonyl)piperidin-3-yl)methyl)-1*H*-benzo[*d*]imidazol-2-yl)pyridin-2(1*H*)-one **72** (19 mg, 0.039 mmol, 28% yield) as a yellow solid. **LCMS (HPLC)**: rt = 0.80 min, [M+H]⁺ 462. **¹H NMR δ(400 MHz, DMSO-*d*₆, VT)**: 7.98 (1H, d, *J* = 2.2 Hz), 7.62 – 7.68 (2H, m), 7.56 – 7.60 (1H, m), 7.20 – 7.30 (2H, m), 4.21 – 4.33 (2H, m), 3.90 (1H, br. d, *J* = 12.7 Hz), 3.65 (1H, br. d, *J* = 12.0 Hz), 3.59 (3H, s), 2.74 – 2.85*overlapping with H₂O peak (1H, integrates as 6H, m), 2.61 – 2.73 (3H, m), 2.16 – 2.24 (1H, m), 2.14 (6H, s), 1.88 – 1.99 (1H, m), 1.72 – 1.87 (2H, m), 1.48 – 1.64 (4H, m), 1.38 – 1.48 (1H, m), 1.17 – 1.36 (3H, m). **¹³C NMR δ(176 MHz, DMSO-*d*₆)**: additional peaks due to rotamers present 172.5, 172.0, 161.7, 150.4, 150.3, 142.4, 138.3, 136.7, 136.6, 135.8, 127.9, 127.8, 122.2, 122.0, 121.9, 118.9, 118.8, 111.1, 111.0, 108.1, 108.0, 54.6, 54.6, 54.5, 54.5, 47.9, 46.8, 46.7, 46.1, 46.1, 45.1, 44.3, 41.5, 37.7, 37.4, 37.3, 37.1, 37.0, 35.8, 35.8, 28.4, 28.3, 28.3, 28.1, 27.9, 27.3, 24.6, 24.1, 16.8. **HRMS (ESI)** exact mass calculated for C₂₇H₃₆N₅O₂ [M+H]⁺ m/z 462.2870, found m/z 462.2863.

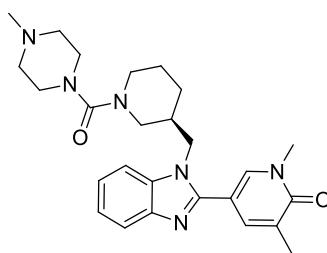
5-(1-(((*S*)-1-((1*r*,4*S*)-4-Aminocyclohexane-1-carbonyl)piperidin-3-yl)methyl)-1*H*-benzo[*d*]imidazol-2-yl)-1,3-dimethylpyridin-2(1*H*)-one **73**



DIPEA (76 μL, 0.357 mmol) was added to a stirring solution of (1*r*,4*r*)-4-((*tert*-butoxycarbonyl)amino)cyclohexane-1-carboxylic acid (36 mg, 0.149 mmol) and HATU (71 mg, 0.186 mmol) in DMF (0.5 mL) at RT. The reaction was stirred at RT under air for 10

minutes, after which a solution of (*R*)-1,3-dimethyl-5-(1-(piperidin-3-ylmethyl)-1*H*-benzo[*d*]imidazol-2-yl)pyridin-2(1*H*)-one **60** (50 mg, 0.149 mmol) in DMF (0.5 mL) was added. The reaction mixture was stirred at RT under air for 1 h. The reaction mixture was diluted with and partitioned between DCM (20 mL) and a 10% (by wt) aqueous solution of lithium chloride (20 mL), and the phases were separated. The aqueous phase was further extracted with DCM (20 mL). The combined organics were washed with a 10% (by wt) aqueous solution of lithium chloride (2 x 20 mL), dried by passing through a hydrophobic frit, and concentrated *in vacuo*. The crude mixture was dissolved in solution of hydrochloric acid in 1,4-dioxane (4 M, 1 mL, 4 mmol). The reaction mixture was stirred at RT under air for 16 h. The reaction mixture was concentrated *in vacuo*. The residue was dissolved in 1:1 MeOH:DMSO (1 mL), and purified by EZ preparative HPLC, eluting with 15 – 100% 10 mM ammonium bicarbonate (aq)/MeCN. Fractions containing the desired product were combined and extracted with DCM (2 x 20 mL). The combined organic phases were dried by passing through a hydrophobic frit, and concentrated *in vacuo* to yield 5-(1-(((*S*)-1-((1*r*,4*S*)-4-aminocyclohexane-1-carbonyl)piperidin-3-yl)methyl)-1*H*-benzo[*d*]imidazol-2-yl)-1,3-dimethylpyridin-2(1*H*)-one **73** (2 mg, 4.12 μmol, 3% yield) as a white solid. **LCMS (HpH)**: *rt* = 0.80 min [M+H]⁺ 462. **¹H NMR δ(400 MHz, DMSO-*d*₆)**: 8.09 – 8.18 (1H, m), 7.60 – 7.77 (3H, m), 7.18 – 7.32 (2H, m), 3.78 – 4.43 (3H, m), 3.50 – 3.65 (4H, m), 2.96 – 3.07 (1H, m), 2.57 – 2.72 (1H, m), 2.31 – 2.42 (1H, m), 2.10 (3H, br. s), 1.63 – 1.98 (3H, m), 0.95 – 1.61 (10H, m), 0.63 – 0.93 (1H, m).

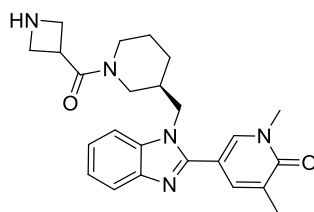
(*S*)-1,3-Dimethyl-5-(1-((1-(4-methylpiperazine-1-carbonyl)piperidin-3-yl)methyl)-1*H*-benzo[*d*]imidazol-2-yl)pyridin-2(1*H*)-one **74**



Chemical Formula: C₂₆H₃₄N₆O₂
Molecular Weight: 462.59 amu

4-Methylpiperazine-1-carbonyl chloride (24 μ L, 0.178 mmol) was added to a stirring solution of (*R*)-1,3-dimethyl-5-(1-(piperidin-3-ylmethyl)-1*H*-benzo[*d*]imidazol-2-yl)pyridin-2(1*H*)-one **60** (50 mg, 0.149 mmol) and DIPEA (76 μ L, 0.446 mmol) in DCM (1 mL) at RT. The reaction mixture was stirred at RT under air for 1 h. The residue was dissolved in 1:1 MeOH:DMSO (1 mL), and purified by EZ preparative HPLC, eluting with 0 – 100% 10 mM ammonium bicarbonate (aq)/MeCN. Fractions containing the desired product were combined and extracted with DCM (2 x 20 mL). The combined organic phases were dried by passing through a hydrophobic frit, and concentrated *in vacuo* to yield (*S*)-1,3-dimethyl-5-((1-(4-methylpiperazine-1-carbonyl)piperidin-3-yl)methyl)-1*H*-benzo[*d*]imidazol-2-yl)pyridin-2(1*H*)-one **74** (26 mg, 0.053 mmol, 36% yield) as a white solid. **LCMS (HpH)**: rt = 0.80 min [M+H]⁺ 463. **¹H NMR δ (400 MHz, DMSO-*d*₆, VT)**: 7.88 - 8.03 (1H, m), 7.59 – 7.70 (2H, m), 7.50 – 7.59 (1H, m), 7.17 – 7.30 (2H, m), 4.15 – 4.32 (2H, m), 3.59 (3H, s), 3.47 – 3.53 (1H, m), 3.35 – 3.43 (1H, m), 3.20 – 3.25 (3H, m), 3.14 – 3.20 (1H, m), 2.94 – 3.02 (3H, m), 2.67 – 2.75 (1H, m), 2.52 – 2.58 (1H, m), 2.10 – 2.17 (7H, m), 1.97 – 2.07 (1H, m), 1.50 – 1.68 (2H, m), 1.27 – 1.41 (1H, m), 1.09 – 1.22 (1H, m). **¹³C NMR δ (101 MHz, DMSO-*d*₆)**: 162.8, 161.7, 150.2, 142.4, 138.2, 136.6, 135.9, 127.8, 122.2, 121.9, 118.8, 111.0, 108.1, 54.0, 49.8, 48.5, 46.9, 46.7, 46.0, 45.6, 37.4, 36.1, 27.8, 23.8, 16.8. **HRMS (ESI)** exact mass calculated for C₂₆H₃₅N₆O₂ [M+H]⁺ m/z 463.2822, found m/z 463.2820. **ν_{\max} (solid)**: 3445, 2929, 2852, 2793, 1654, 1611, 1423 cm⁻¹.

(*S*)-5-((1-((1-(Azetidine-3-carbonyl)piperidin-3-yl)methyl)-1*H*-benzo[*d*]imidazol-2-yl)-1,3-dimethylpyridin-2(1*H*)-one **75**

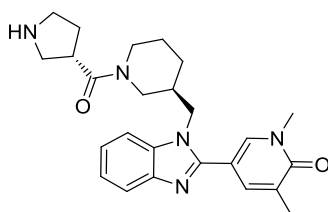


Chemical Formula: C₂₄H₂₉N₅O₂
Molecular Weight: 419.52 amu

DIPEA (78 μ L, 0.446 mmol) was added to a stirring solution of 1-(*tert*-butoxycarbonyl)azetidino-3-carboxylic acid (30 mg, 0.149 mmol) and HATU (71 mg, 0.186 mmol) in DMF (0.5 mL) at RT. The reaction was stirred at RT under air for 10 minutes, after which a solution of (*R*)-1,3-dimethyl-5-(1-(piperidin-3-ylmethyl)-1*H*-benzo[*d*]imidazol-2-yl)pyridin-2(1*H*)-one **60** (50 mg, 0.149 mmol) in DMF (0.5 mL) was added. The reaction mixture was stirred for at RT under air for 16 h. LCMS analysis indicated incomplete conversion to desired product. Additional 1-(*tert*-butoxycarbonyl)azetidino-3-carboxylic acid (30 mg, 0.149 mmol) and HATU (71 mg, 0.186 mmol) were added, and the reaction mixture stirred at RT under air for 4 h. The reaction mixture was diluted with and partitioned between DCM (20 mL) and a 10% (by wt) aqueous solution of lithium chloride (20 mL), and the phases were separated. The aqueous phase was further extracted with DCM (20 mL). The combined organic phases were washed with 10% (by wt) aqueous solution of lithium chloride (2 x 20 mL), dried by passing through a hydrophobic frit, and concentrated *in vacuo* to yield *tert*-butyl (S)-3-(3-((2-(1,5-dimethyl-6-oxo-1,6-dihydropyridin-3-yl)-1*H*-benzo[*d*]imidazol-1-yl)methyl)piperidine-1-carbonyl)azetidino-1-carboxylate (128 mg, 0.246 mmol) as a brown oil. This was used in the next reaction as a crude mixture. *tert*-Butyl (S)-3-(3-((2-(1,5-dimethyl-6-oxo-1,6-dihydropyridin-3-yl)-1*H*-benzo[*d*]imidazol-1-yl)methyl)piperidine-1-carbonyl)azetidino-1-carboxylate (128 mg, 0.246 mmol) was dissolved in a solution of hydrochloric acid 1,4-dioxane (4 M, 3 mL, 12 mmol). MeOH (1 mL) was added to aid solubility. The reaction mixture was stirred at RT under air for 4 h. The reaction mixture was concentrated *in vacuo*. The residue was dissolved in 1:1 MeOH:DMSO (1 mL) and purified by MDAP, using a solvent system of 10 mM ammonium bicarbonate adjusted to pH 10 with ammonia in water (solvent A) and acetonitrile (solvent B). Fractions

containing the desired product were combined and extracted with DCM (2 x 20 mL). The combined organic phases were dried by passing through a hydrophobic frit, and concentrated *in vacuo* to yield (*S*)-5-(1-((1-(azetidine-3-carbonyl)piperidin-3-yl)methyl)-1*H*-benzo[*d*]imidazol-2-yl)-1,3-dimethylpyridin-2(1*H*)-one **75** (20 mg, 0.044 mmol, 30% yield) as a yellow solid. **LCMS (HpH)**: rt = 0.67 min, [M+H]⁺ 420. **¹H NMR δ(400 MHz, DMSO-*d*₆, VT)**: 7.99 (1H, d, *J* = 2.4 Hz), 7.62 – 7.69 (2H, m), 7.55 – 7.60 (1H, m), 7.20 – 7.30 (2H, m), 4.19 – 4.32 (2H, m), 3.63 – 3.69 (5H, m), 3.32 – 3.52 (3H, m), 2.70 – 2.93* overlapping water peak (3H, integrates as 12H, m), 2.61 – 2.70 (1H, m), 2.15 (3H, s), 1.85 – 2.00 (1H, m), 1.53 – 1.62 (2H, m), 1.12 – 1.34 (3H, m). **¹³C NMR δ(101 MHz, DMSO-*d*₆)**: additional peaks due to rotamers present. 170.0, 169.7, 161.8, 161.7, 150.3, 150.2, 142.4, 142.3, 138.3, 138.3, 136.7, 136.6, 135.9, 127.9, 127.8, 122.2, 122.0, 121.9, 118.8, 118.8, 111.0, 111.0, 108.1, 108.1, 48.4, 48.3, 48.2, 48.0, 47.7, 46.8, 46.7, 44.7, 44.3, 41.4, 37.4, 37.2, 35.9, 35.9, 35.8, 27.7, 27.5, 24.4, 24.0, 16.8. **HRMS (ESI)** exact mass calculated for C₂₄H₃₀N₅O₂ [M+H]⁺ m/z 420.2400, found m/z 420.2395. **ν_{max}(solid)**: 3414, 2916, 2864, 1651, 1603, 1454, 1428 cm⁻¹.

1,3-Dimethyl-5-(1-(((*S*)-1-((*S*)-pyrrolidine-3-carbonyl)piperidin-3-yl)methyl)-1*H*-benzo[*d*]imidazol-2-yl)pyridin-2(1*H*)-one **76**

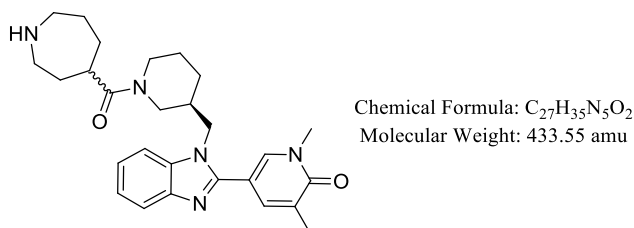


Chemical Formula: C₂₅H₃₁N₅O₂
Molecular Weight: 433.55 amu

DIPEA (94 μL, 0.357 mmol) was added to a stirring solution of (*S*)-1-(*tert*-butoxycarbonyl)pyrrolidine-3-carboxylic acid (40 mg, 0.184 mmol) and HATU (88 mg, 0.230 mmol) in DMF (0.5 mL) at RT. The reaction was stirred at RT under air for 10 minutes, after

which a solution of (*R*)-1,3-dimethyl-5-(1-(piperidin-3-ylmethyl)-1*H*-benzo[*d*]imidazol-2-yl)pyridin-2(1*H*)-one **60** (62 mg, 0.184 mmol) in DMF (0.5 mL) was added. The reaction mixture was stirred at RT under air for 66 h. The reaction mixture was diluted with and partitioned between DCM (20 mL) and a 10% (by wt) aqueous solution of lithium chloride (20 mL), and the phases were separated. The aqueous phase was further extracted with DCM (20 mL). The combined organics were washed with a 10% (by wt) aqueous solution of lithium chloride (3 x 20 mL), dried by passing through a hydrophobic frit, and concentrated *in vacuo*. The crude mixture was dissolved in solution of hydrochloric acid in 1,4-dioxane (4 M, 1 mL, 4 mmol). The reaction mixture was stirred at RT under air for 24 h. The reaction mixture was concentrated *in vacuo*. The residue was dissolved in 1:1 MeOH:DMSO (1 mL), and purified by EZ preparative HPLC, eluting with 0 – 100% 10 mM ammonium bicarbonate (aq)/MeCN. Fractions containing the desired product were combined and extracted with DCM (2 x 30 mL). The combined organic phases were dried by passing through a hydrophobic frit, and concentrated *in vacuo* to yield 1,3-dimethyl-5-(1-(((*S*)-1-((*S*)-pyrrolidine-3-carbonyl)piperidin-3-yl)methyl)-1*H*-benzo[*d*]imidazol-2-yl)pyridin-2(1*H*)-one (22 mg, 0.048 mmol, 26% yield) as a pale yellow solid. **LCMS (HpH):** *rt* = 0.77 min [M+H]⁺ 434. **¹H NMR δ(400 MHz, DMSO-*d*₆, VT) ppm:** 7.90 – 8.07 (1H, m), 7.61 – 7.69 (2H, m), 7.55 – 7.60 (1H, m), 7.19 – 7.29 (2H, m), 4.16 – 4.36 (2H, m), 3.83 – 3.98 (1H, m), 3.69 – 3.80 (1H, m), 3.59 (3H, s), 2.65 – 2.93* overlapping water peak (7H, integrates as 12H, m), 2.14 (3H, s), 1.86 – 2.00 (1H, m), 1.67 – 1.80 (2H, m), 1.52 – 1.64 (2H, m), 1.14 – 1.34 (3H, m). **¹³C NMR δ(101 MHz, DMSO-*d*₆):** *additional peaks due to rotamers present* 172.2, 171.9, 161.7, 150.4, 150.2, 142.4, 138.3, 138.2, 136.7, 136.6, 135.9, 135.8, 127.8, 122.2, 121.9, 121.9, 118.8, 111.0, 108.1, 50.6, 50.3, 48.5, 48.1, 47.0, 46.7, 45.2, 44.5, 41.7, 40.7, 40.5, 37.3, 37.3, 36.0, 30.1, 30.0, 27.8, 27.4, 24.5, 24.0, 16.8. **HRMS (ESI)** exact mass calculated for C₂₅H₃₂N₅O₂ [M+H]⁺ *m/z* 434.2557, found *m/z* 434.2560. ***v*_{max}(solid):** 3418, 2924, 2852, 1654, 1607, 1426 cm⁻¹.

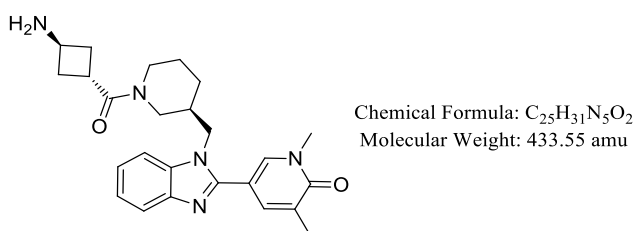
5-(1-(((3S)-1-(Azepane-4-carbonyl)piperidin-3-yl)methyl)-1H-benzo[d]imidazol-2-yl)-1,3-dimethylpyridin-2(1H)-one 77a and 77b



DIPEA (78 μ L, 0.446 mmol) was added to a stirring solution of 1-(*tert*-butoxycarbonyl)azepane-4-carboxylic acid (36 mg, 0.149 mmol) and HATU (71 mg, 0.230 mmol) in DMF (0.5 mL) at RT. The reaction was stirred at RT under air for 10 minutes, after which a solution of (*R*)-1,3-dimethyl-5-(1-(piperidin-3-ylmethyl)-1H-benzo[d]imidazol-2-yl)pyridin-2(1H)-one **60** (62 mg, 0.184 mmol) in DMF (0.5 mL) was added. The reaction mixture was stirred at RT under air for 1 h. The reaction mixture was diluted with and partitioned between DCM (20 mL) and a 10% (by wt) aqueous solution of lithium chloride (20 mL), and the phases were separated. The aqueous phase was further extracted with DCM (20 mL). The combined organics were washed with a 10% (by wt) aqueous solution of lithium chloride (2 x 20 mL), dried by passing through a hydrophobic frit, and concentrated *in vacuo* to give a brown oil. The crude mixture was dissolved in solution of hydrochloric acid in 1,4-dioxane (4 M, 3 mL, 12 mmol). MeOH (1 mL) was added to aid solubility. The reaction mixture was stirred at RT under air for 1 h. The reaction mixture was concentrated *in vacuo*. The residue was dissolved in 1:1 MeOH:DMSO (1 mL), and purified by MDAP using a solvent system of 10 mM ammonium bicarbonate adjusted to pH 10 with ammonia in water (solvent A) and acetonitrile (solvent B). Fractions containing the desired product were combined and extracted with DCM (2 x 20 mL). The combined organic phases were dried by passing through a hydrophobic frit, and concentrated *in vacuo* to yield 5-(1-(((3S)-1-(azepane-4-carbonyl)piperidin-3-yl)methyl)-1H-benzo[d]imidazol-2-yl)-1,3-dimethylpyridin-2(1H)-one (38 mg, 51% yield). This diastereomeric mixture was purified by chiral chromatography,

eluting with 3:1 heptane:ethanol with 0.2% isopropylamine modifier to yield 5-(1-(((3*S*)-1-(azepane-4-carbonyl)piperidin-3-yl)methyl)-1*H*-benzo[*d*]imidazol-2-yl)-1,3-dimethylpyridin-2(1*H*)-one **77a** (unknown diastereoisomer, 8 mg, 0.016 mmol, 11% yield) and 5-(1-(((3*S*)-1-(azepane-4-carbonyl)piperidin-3-yl)methyl)-1*H*-benzo[*d*]imidazol-2-yl)-1,3-dimethylpyridin-2(1*H*)-one **77b** (unknown diastereoisomer, 8 mg, 0.016 mmol, 11% yield). **LCMS (HpH)**: rt = 0.81 min [M+H]⁺ 462. **¹H NMR δ(400 MHz, DMSO-*d*₆, VT)**: 7.91 – 8.05 (1H, m), 7.61 – 7.68 (2H, m), 7.56 – 7.61 (1H, m), 7.20 – 7.31 (2H, m), 4.19 – 4.34 (2H, m), 3.82 – 3.98 (1H, m), 3.63 – 3.76 (1H, m), 3.59 (3H, s), 2.54 – 2.90* overlapping water peak (7H, integrates as 19H, m), 2.14 (3H, s), 1.87 – 2.04 (1H, m), 1.46 – 1.67 (7H, m), 1.15 – 1.37 (4H, m). **LCMS (HpH)**: rt = 0.81 min [M+H]⁺ 462. **¹H NMR δ(400 MHz, DMSO-*d*₆, VT)**: 7.87 – 8.07 (1H, m), 7.61 – 7.69 (2H, m), 7.52 – 7.61 (1H, m), 7.15 – 7.34 (2H, m), 4.16 – 4.35 (2H, m), 3.81 – 3.97 (1H, m), 3.63 – 3.72 (1H, m), 3.59 (3H, s), 2.53 – 2.91* overlapping water peak (7H, integrates as 19H, m), 2.14 (3H, s), 1.88 – 2.00 (1H, m), 1.48 – 1.70 (7H, m), 1.14 – 1.41 (4H, m).

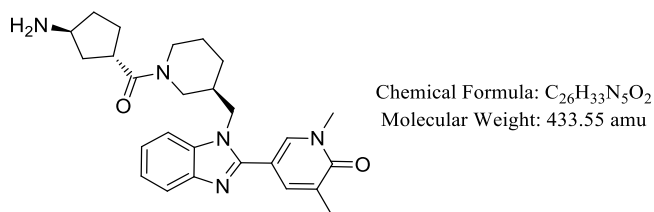
5-(1-(((*S*)-1-((1*r*,3*S*)-3-Aminocyclobutane-1-carbonyl)piperidin-3-yl)methyl)-1*H*-benzo[*d*]imidazol-2-yl)-1,3-dimethylpyridin-2(1*H*)-one **78**



DIPEA (76 μL, 0.357 mmol) was added to a stirring solution of (1*r*,3*r*)-3-((*tert*-butoxycarbonyl)amino)cyclobutane-1-carboxylic acid (32.0 mg, 0.149 mmol) and HATU (71 mg, 0.186 mmol) in DMF (0.5 mL) at RT. The reaction was stirred at RT under air for 5

minutes, after which a solution of (*R*)-1,3-dimethyl-5-(1-(piperidin-3-ylmethyl)-1*H*-benzo[*d*]imidazol-2-yl)pyridin-2(1*H*)-one **60** (50 mg, 0.149 mmol) in DMF (0.5 mL) was added. The reaction mixture was stirred at RT under air for 0.5 h. The reaction mixture was diluted with and partitioned between DCM (20 mL) and a 10% (by wt) aqueous solution of lithium chloride (20 mL), and the phases were separated. The aqueous phase was further extracted with DCM (20 mL). The combined organics were washed with a 10% (by wt) aqueous solution of lithium chloride (3 x 20 mL), dried by passing through a hydrophobic frit, and concentrated *in vacuo* to yield a brown oil. The crude mixture was dissolved in solution of hydrochloric acid in 1,4-dioxane (4 M, 1 mL, 4 mmol). The reaction mixture was stirred at RT under air for 16 h. The reaction mixture was concentrated *in vacuo*. The residue was dissolved in 1:1 MeOH:DMSO (2 mL), and purified by EZ preparative HPLC, eluting with 15 – 100% 10 mM ammonium bicarbonate (aq)/MeCN. Fractions containing the desired product were combined and extracted with DCM (2 x 20 mL). The combined organic phases were dried by passing through a hydrophobic frit, and concentrated *in vacuo* to yield 5-(1-(((*S*)-1-((1*r*,3*S*)-3-aminocyclobutane-1-carbonyl)piperidin-3-yl)methyl)-1*H*-benzo[*d*]imidazol-2-yl)-1,3-dimethylpyridin-2(1*H*)-one **78** (23 mg, 0.050 mmol, 34% yield) as a white solid. **LCMS (H_pH)**: rt = 0.75 min, [M+H]⁺ 434. **¹H NMR δ(400 MHz, DMSO-*d*₆, VT)**: 7.97 – 8.00 (1H, m), 7.63 – 7.68 (2H, m), 7.55 – 7.59 (1H, m), 7.20 – 7.29 (2H, m), 4.18 – 4.31 (2H, m), 3.66 – 3.85 (1H, m), 3.59 (3H, s), 3.27 – 3.36 (1H, m), 2.94 – 3.04 (1H, m), 2.70 – 2.91* overlapping water peak (3H, integrates as 5H, m), 2.62 – 2.69 (1H, m), 2.26 – 2.35 (1H, m), 2.17 – 2.25 (1H, m), 2.14 (3H, s), 1.85 – 1.97 (1H, m), 1.60 – 1.75 (2H, m), 1.51 – 1.60 (2H, m), 1.31 – 1.33 (1H, m), 1.12 – 1.31 (2H, m). **¹³C NMR δ(101 MHz, DMSO-*d*₆)**: additional peaks due to rotamers present 172.3, 171.9, 161.7, 150.2, 142.4, 142.3, 138.3, 136.7, 136.6, 136.0, 135.8, 127.9, 127.8, 122.2, 121.9, 118.8, 111.0, 108.1, 48.5, 47.8, 46.7, 45.1, 44.9, 44.8, 44.4, 41.5, 37.3, 37.3, 35.9, 35.4, 35.1, 35.1, 34.7, 30.2, 30.0, 27.9, 27.4, 24.2, 24.1, 16.8. **HRMS (ESI)** exact mass calculated for C₂₅H₃₂N₅O₂ [M+H]⁺ m/z 434.2557, found m/z 434.2559. **v_{max}(solid)**: 3355, 2928, 2852, 1652, 1607, 1455 cm⁻¹.

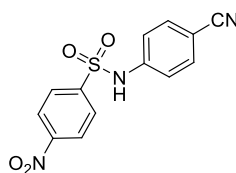
5-(1-(((S)-1-((1S,3S)-3-Aminocyclopentane-1-carbonyl)piperidin-3-yl)methyl)-1H-benzo[d]imidazol-2-yl)-1,3-dimethylpyridin-2(1H)-one 79



DIPEA (76 μ L, 0.357 mmol) was added to a stirring solution of (1S,3S)-3-((*tert*-butoxycarbonyl)amino)cyclopentane-1-carboxylic acid (34 mg, 0.149 mmol) and HATU (71 mg, 0.186 mmol) in DMF (0.5 mL) at RT. The reaction was stirred at RT under air for 5 minutes, after which a solution of (*R*)-1,3-dimethyl-5-(1-(piperidin-3-ylmethyl)-1H-benzo[d]imidazol-2-yl)pyridin-2(1H)-one **60** (50 mg, 0.149 mmol) in DMF (0.5 mL) was added. The reaction mixture was stirred at RT under air for 1 h. The reaction mixture was diluted with and partitioned between DCM (20 mL) and a 10% (by wt) aqueous solution of lithium chloride (20 mL), and the phases were separated. The aqueous phase was further extracted with DCM (20 mL). The combined organics were washed with a 10% (by wt) aqueous solution of lithium chloride (3 x 20 mL), dried by passing through a hydrophobic frit, and concentrated *in vacuo* to yield a brown oil. The crude mixture was dissolved in solution of hydrochloric acid in 1,4-dioxane (4 M, 1 mL, 4 mmol). The reaction mixture was stirred at RT under air for 16 h. The reaction mixture was concentrated *in vacuo*. The residue was dissolved in 1:1 MeOH:DMSO (2 mL), and purified by EZ preparative HPLC, eluting with 15 – 100% 10 mM ammonium bicarbonate (aq)/MeCN. Fractions containing the desired product were combined and extracted with DCM (2 x 20 mL). The combined organic phases were dried by passing through a hydrophobic frit, and concentrated *in vacuo* to yield 5-(1-(((S)-1-((1S,3S)-3-aminocyclopentane-1-carbonyl)piperidin-3-yl)methyl)-1H-benzo[d]imidazol-2-yl)-1,3-dimethylpyridin-2(1H)-one **79** (29 mg, 0.062 mmol, 41% yield) as a white solid. LCMS (HpH): rt = 0.78 min [M+H]⁺ 448. ¹H NMR δ (400 MHz, DMSO-*d*₆, VT): 7.95 –

8.02 (1H, m), 7.61 – 7.69 (2H, m), 7.53 – 7.60 (1H, m), 7.25 (2H, s), 4.18 – 4.34 (2H, m), 3.84 – 3.97 (1H, m), 3.69 – 3.77 (1H, m), 3.59 (3H, s), 3.25 – 3.33 (1H, m), 2.90 – 3.02 (1H, m), 2.64 – 2.88*overlapping water peak (3H, integrates as 5H, m), 2.52 – 2.55 (1H, m), 2.14 (3H, s), 1.86 – 1.99 (1H, m), 1.67 – 1.84 (3H, m), 1.53 – 1.66 (3H, m), 1.17 – 1.34 (4H, m). ¹³C NMR δ(101 MHz, DMSO-*d*6): additional peaks due to rotamers present 173.2, 172.9, 161.8, 150.4, 150.3, 142.4, 138.3, 136.7, 135.9, 135.8, 127.9, 127.8, 122.2, 122.2, 121.9, 121.9, 118.8, 111.1, 111.0, 108.1, 52.4, 48.5, 48.1, 46.8, 45.2, 44.5, 41.6, 40.4, 38.4, 38.3, 37.4, 37.3, 35.9, 35.2, 35.1, 27.9, 27.5, 27.4, 27.1, 24.6, 24.5, 24.1, 16.8. HRMS (ESI) exact mass calculated for C₂₆H₃₄N₅O₂ [M+H]⁺ m/z 448.2713, found m/z 448.2713. ν_{max}(solid): 3449, 2936, 2852, 1738, 1664, 1607, 1428 cm⁻¹.

N*-(4-Cyanophenyl)-4-nitrobenzenesulfonamide **82*

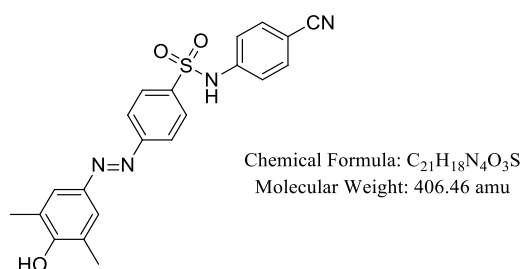


Chemical Formula: C₁₃H₉N₃O₄S
Molecular Weight: 303.29 amu

4-Aminobenzonitrile **80** (267 mg, 2.256 mmol) was added to a stirring solution of 4-nitrobenzenesulfonyl chloride **81** (500 mg, 2.256 mmol) and pyridine (0.182 mL, 2.256 mmol) in DCM (10 mL) at RT. The reaction mixture was stirred at RT under air for 72 h. The reaction mixture was diluted with and partitioned between DCM (20 mL) and brine (20 mL), and the phases were separated. The organics were dried by passing through a hydrophobic frit, and concentrated *in vacuo*. The crude material was then purified by normal phase chromatography, eluting with 0 – 50% EtOAc in cyclohexane over 17 CV. Fractions containing the desired

product were concentrated *in vacuo* to yield *N*-(4-cyanophenyl)-4-nitrobenzenesulfonamide **82** (464 mg, 1.453 mmol, 64% yield) as a pale yellow solid. LCMS (H_pH): rt = 0.69 min [M-H]⁺ 302. ¹H NMR δ(400 MHz, DMSO-*d*₆): 11.31 (1H, s), 8.39 (2H, d, *J* = 9.0 Hz), 8.05 – 8.10 (2H, m), 7.71 – 7.75 (2H, m), 7.25 – 7.30 (2H, m).

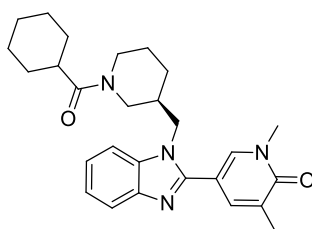
(*E*)-*N*-(4-Cyanophenyl)-4-((4-hydroxy-3,5-dimethylphenyl)diazenyl)benzenesulfonamide MS611 13



Ammonium chloride (368 mg, 6.88 mmol) and iron (231 mg, 4.13 mmol) were added to a solution of *N*-(4-cyanophenyl)-4-nitrobenzenesulfonamide **82** (464 mg, 1.377 mmol) in MeOH (4 mL) and water (4 mL) at RT. The reaction mixture was stirred at 70 °C under a nitrogen atmosphere for 18 h. After cooling, the reaction mixture was filtered through Celite®, washing through with acetone (100 mL). The filtrate was concentrated *in vacuo*. The residue was dissolved in acetone, causing a white precipitate. The filtrate was decanted and concentrated *in vacuo*. It was attempted to purify the crude product by reverse phase chromatography. The crude mixture was dissolved in 1:1 DMSO:MeOH, but was not fully soluble. To remove the DMSO, the crude mixture was dissolved with DCM (2 x 30 mL) and washed with brine (2 x 30 mL). The organic phase was dried by passing through a hydrophobic frit, and concentrated *in vacuo*. The residue was dissolved in DMF (1 mL) and purified by reverse phase chromatography, eluting with 5 – 30% 10mM ammonium bicarbonate (aq)/MeCN. Fractions containing the desired product were combined and extracted with DCM (2 x 20 mL) and 4:1 CHCl₃:IPA (3 x 50 mL). The combined organic phases were dried by

passing through a hydrophobic frit, and concentrated *in vacuo* to yield 4-amino-*N*-(4-cyanophenyl)benzenesulfonamide **83** (181 mg, 0.497 mmol) as yellow oil. This product was taken forward crude to the next step. 4-Amino-*N*-(4-cyanophenyl)benzenesulfonamide **83** (65 mg, 0.178 mmol) and hydrochloric acid (33 μ L, 1.070 mmol) and were dissolved in MeOH (0.8 mL) and water (0.8 mL). The reaction mixture was stirred at 0 $^{\circ}$ C under a nitrogen atmosphere for 15 min. Isoamyl nitrite (24 μ L, 0.178 mmol) was then added dropwise, and the reaction mixture was stirred at 0 $^{\circ}$ C under a nitrogen atmosphere for 50 minutes. In a separate flask, potassium carbonate (148 mg, 1.070 mmol) and 2,6-dimethylphenol (24 mg, 0.196 mmol) were dissolved in water (0.8 mL) and MeOH (0.1 mL). This reaction mixture was cooled to 0 $^{\circ}$ C and stirred under a nitrogen atmosphere for 15 min. After this time, the first yellow coloured diazonium solution was added dropwise to the solution of phenol over 15 min, resulting in a bright red solution. The reaction mixture was stirred at 0 $^{\circ}$ C under a nitrogen atmosphere for 15 min. The reaction mixture was acidified to pH 1 by addition of aqueous hydrochloric acid (2 M, 3 mL, 6 mmol), resulting in a red precipitate. This was filtered under vacuum and dried in a vacuum oven for 16 h to yield (*E*)-*N*-(4-cyanophenyl)-4-((4-hydroxy-3,5-dimethylphenyl)diazenyl)benzenesulfonamide MS611 **13** (35 mg, 0.077 mmol, 6% yield) as a red-orange solid. **LCMS (HpH)**: rt = 0.80 min, [M+H]⁺ 407. **¹H NMR δ (400 MHz, MeOD)**: 7.94 – 8.00 (2H, m), 7.87 – 7.92 (2H, m), 7.57 – 7.62 (4H, m), 7.28 – 7.32 (2H, m), 2.25 – 2.31 (6H, m).³⁴

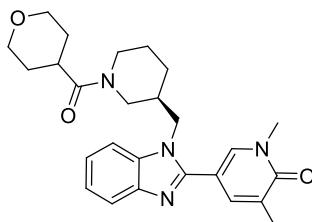
(*S*)-5-(1-((1-(Cyclohexanecarbonyl)piperidin-3-yl)methyl)-1*H*-benzo[d]imidazol-2-yl)-1,3-dimethylpyridin-2(1*H*)-one 84



Chemical Formula: C₂₇H₃₄N₄O₂
Molecular Weight: 446.58 amu

DIPEA (78 μ L, 0.446 mmol) was added to a stirring solution of cyclohexanecarboxylic acid (19 mg, 0.149 mmol) and HATU (71 mg, 0.186 mmol) in DMF (0.5 mL) at RT. The reaction mixture was stirred at RT under air for 10 minutes, after which a solution of (*R*)-1,3-dimethyl-5-(1-(piperidin-3-ylmethyl)-1*H*-benzo[*d*]imidazol-2-yl)pyridin-2(1*H*)-one **60** (50 mg, 0.149 mmol) in DMF (0.5 mL) was added. The reaction mixture was stirred at RT under air for 1 h. The reaction mixture was diluted with and partitioned between 4:1 CHCl₃:IPA (20 mL) and a 5% (by wt) aqueous solution of lithium chloride (20 mL), and the phases were separated. The aqueous phase was further extracted with 4:1 CHCl₃ (2 x 20 mL). The combined organic phases were washed with brine (2 x 20 mL), dried by passing through a hydrophobic frit, and concentrated *in vacuo*. The residue was dissolved in 1:1 MeOH:DMSO (1mL) and purified by MDAP using a solvent system of 10 mM ammonium bicarbonate adjusted to pH 10 with ammonia in water (solvent A) and acetonitrile (solvent B). Fractions containing the desired product were combined and extracted with DCM (2 x 40 mL). The combined organic phases were dried by passing through a hydrophobic frit, and concentrated *in vacuo* to yield (*S*)-5-(1-((1-(cyclohexanecarbonyl)piperidin-3-yl)methyl)-1*H*-benzo[*d*]imidazol-2-yl)-1,3-dimethylpyridin-2(1*H*)-one **84** (28 mg, 0.060 mmol, 40% yield) as a yellow gum. **LCMS (H₂O)**: rt = 1.00 min, [M+H]⁺ 447. **¹H NMR δ (400 MHz, DMSO-*d*₆, VT)**: 7.98 (1H, d, *J* = 2.4 Hz), 7.61 – 7.68 (2H, m), 7.55 – 7.60 (1H, m), 7.19 – 7.30 (2H, m), 4.20 – 4.32 (2H, m), 3.89 (1H, br. d, *J* = 13.0 Hz), 3.64 (1H, br. d, *J* = 12.7 Hz), 3.59 (3H, s), 3.47 – 3.54 (1H, m), 2.69 (1H, dd, *J* = 13.0, 10.0 Hz), 2.21 – 2.31 (1H, m), 2.14 (3H, s), 1.87 – 1.98 (1H, m), 1.37 – 1.71 (7H, m), 1.09 – 1.37 (7H, m) **¹³C NMR δ (176 MHz, DMSO-*d*₆)**: additional peaks due to rotamers present 173.2, 172.7, 161.7, 150.4, 150.3, 142.4, 138.3, 138.3, 136.7, 136.7, 136.6, 135.8, 127.9, 127.8, 122.2, 122.0, 121.9, 118.9, 118.8, 111.1, 111.0, 108.2, 108.1, 48.0, 46.8, 46.6, 45.1, 44.2, 41.4, 37.7, 37.4, 37.3, 35.7, 29.1, 29.0, 29.0, 28.9, 28.8, 27.9, 27.3, 25.5, 25.4, 25.1, 25.0, 25.0, 24.6, 24.1, 16.8. **HRMS (ESI)** exact mass calculated for C₂₇H₃₅N₄O₂ [M+H]⁺ m/z 447.2761, found m/z 447.2756. **ν_{\max} (solid)**: 3440, 2921, 2848, 1656, 1610, 1452, 1427 cm⁻¹.

(S)-1,3-Dimethyl-5-(1-((1-(tetrahydro-2H-pyran-4-carbonyl)piperidin-3-yl)methyl)-1H-benzo[d]imidazol-2-yl)pyridin-2(1H)-one 85

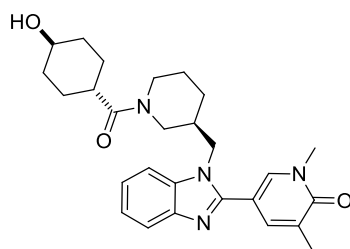


Chemical Formula: C₂₆H₃₂N₄O₃
Molecular Weight: 448.56 amu

DIPEA (78 μ L, 0.446 mmol) was added to a stirring solution of tetrahydro-2H-pyran-4-carboxylic acid (19 mg, 0.149 mmol) and HATU (71 mg, 0.186 mmol) in DMF (0.5 mL) at RT. The reaction was stirred at RT under air for 10 minutes, after which a solution of (R)-1,3-dimethyl-5-(1-(piperidin-3-ylmethyl)-1H-benzo[d]imidazol-2-yl)pyridin-2(1H)-one **60** (50 mg, 0.149 mmol) in DMF (0.5 mL) was added. The reaction mixture was stirred at RT under air for 1 h. The reaction mixture was diluted with and partitioned between 4:1 CHCl₃:IPA (20 mL) and a 5% (by wt) aqueous solution of lithium chloride (20 mL), and the phases were separated. The aqueous phase was further extracted with 4:1 CHCl₃ (2 x 20 mL). The combined organic phases were washed with brine (2 x 20 mL), dried by passing through a hydrophobic frit, and concentrated *in vacuo*. The residue was dissolved in 1:1 MeOH:DMSO (1ml) and purified by MDAP using a solvent system of 10 mM ammonium bicarbonate adjusted to pH 10 with ammonia in water (solvent A) and acetonitrile (solvent B). Fractions containing the desired product were combined and extracted with DCM (2 x 40 mL). The combined organic phases were dried by passing through a hydrophobic frit, and concentrated *in vacuo* to yield (S)-1,3-dimethyl-5-(1-((1-(tetrahydro-2H-pyran-4-carbonyl)piperidin-3-yl)methyl)-1H-benzo[d]imidazol-2-yl)pyridin-2(1H)-one **85** (29 mg, 0.061 mmol, 41% yield) as a yellow solid. **LCMS (H₂O)**: rt = 0.79 min, [M+H]⁺ 449. **¹H NMR δ (400 MHz, DMSO-*d*₆, VT)**: 7.99 (1H, d, *J* = 2.2 Hz), 7.62 – 7.68 (2H, m), 7.56 – 7.61 (1H, m), 7.20 – 7.29 (2H, m), 4.20 – 4.34 (2H, m), 3.92 (1H, br. d, *J* = 12.7 Hz), 3.71 – 3.83 (2H, m), 3.67

(1H, br. d, $J = 12.0$ Hz), 3.59 (3H, s), 3.17 – 3.32 (3H, m), 2.76 – 2.88* overlapping water peak (1H, integrates for 6H, m), 2.66 – 2.74 (1H, m), 2.14 (3H, s), 1.88 – 2.01 (1H, m), 1.45 – 1.64 (4H, m), 1.36 – 1.44 (1H, m), 1.14 – 1.32 (3H, m). ^{13}C NMR δ (176 MHz, DMSO- d_6): additional peaks due to rotamers present 172.0, 171.4, 161.7, 150.6, 150.3, 142.4, 138.4, 138.3, 136.7, 136.7, 135.8, 135.8, 127.9, 127.8, 122.2, 122.0, 121.9, 118.9, 118.8, 111.2, 111.0, 108.1, 108.0, 66.1, 66.0, 47.8, 46.8, 46.7, 45.0, 44.4, 41.5, 37.7, 37.3, 36.4, 36.3, 35.8, 28.9, 28.8, 28.8, 28.6, 27.8, 27.3, 24.7, 24.1, 16.8. HRMS (ESI) exact mass calculated for $\text{C}_{26}\text{H}_{33}\text{N}_4\text{O}_3$ [M+H] $^+$ m/z 449.2553, found m/z 449.2546. ν_{max} (solid): 2921, 2848, 1652, 1607, 1454 cm^{-1} .

5-(1-(((S)-1-((1*r*,4*S*)-4-Hydroxycyclohexane-1-carbonyl)piperidin-3-yl)methyl)-1*H*-benzo[*d*]imidazol-2-yl)-1,3-dimethylpyridin-2(1*H*)-one 86

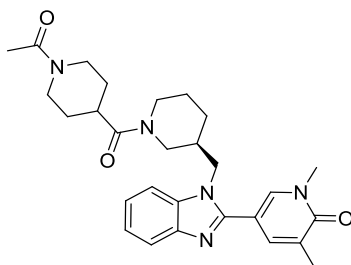


Chemical Formula: $\text{C}_{27}\text{H}_{34}\text{N}_4\text{O}_3$
Molecular Weight: 462.58 amu

DIPEA (61 μL , 0.357 mmol) was added to a stirring solution of *trans*-(1*r*,4*r*)-4-hydroxycyclohexanecarboxylic acid (17 mg, 0.119 mmol) and HATU (57 mg, 0.149 mmol) in DMF (0.5 mL) at RT. The reaction was stirred at RT under air for 10 minutes, after which a solution of (*R*)-1,3-dimethyl-5-(1-(piperidin-3-ylmethyl)-1*H*-benzo[*d*]imidazol-2-yl)pyridin-2(1*H*)-one **60** (40 mg, 0.119 mmol) in DMF (0.5 mL) was added. The reaction mixture was stirred at RT under air for 1 h. The reaction mixture was diluted with and partitioned between EtOAc (20 mL) and a 10% (by wt) aqueous solution of lithium chloride (20 mL), and the phases were separated. The aqueous phase was further extracted with EtOAc (2 x 20 mL), and DCM (30 mL). The combined organics were dried by passing through a

hydrophobic frit, and concentrated *in vacuo*. The residue was dissolved in 1:1 MeOH:DMSO (2 mL), and purified by EZ preparative HPLC, eluting with 15 – 100% 10 mM ammonium bicarbonate (aq)/MeCN. Fractions containing the desired product were combined and extracted with DCM (2 x 20 mL). The combined organic phases were dried by passing through a hydrophobic frit, and concentrated *in vacuo* to yield 5-(1-(((*S*)-1-((1*r*,4*S*)-4-hydroxycyclohexane-1-carbonyl)piperidin-3-yl)methyl)-1*H*-benzo[*d*]imidazol-2-yl)-1,3-dimethylpyridin-2(1*H*)-one **86** (26 mg, 0.053 mmol, 45% yield) as a white solid. **LCMS (H_pH)**: rt = 0.76 min [M+H]⁺ 463. **¹H NMR δ(400 MHz, DMSO-*d*₆, VT)**: 7.98 (1H, d, *J* = 2.4 Hz), 7.62 – 7.68 (2H, m), 7.55 – 7.60 (1H, m), 7.19 – 7.30 (2H, m), 4.20 – 4.32 (2H, m), 3.85 – 3.95 (1H, m), 3.61 – 3.70 (1H, m), 3.59 (3H, s), 3.29 – 3.38 (1H, m), 2.75 – 2.87* overlapping water peak (1H, integrates as 4H, m), 2.66 – 2.74 (1H, m), 2.15 – 2.26 (1H, m), 2.14 (3H, s), 1.88 – 1.99 (1H, m), 1.74 – 1.86 (2H, m), 1.00 – 1.63 (11H, m). **¹³C NMR δ(101 MHz, DMSO-*d*₆)**: *additional peaks due to rotamers present* 172.5, 161.7, 150.3, 142.4, 138.2, 136.7, 136.6, 135.8, 127.8, 122.2, 121.9, 121.9, 118.8, 118.8, 111.0, 108.1, 68.4, 68.3, 48.5, 47.9, 47.9, 46.8, 46.6, 45.1, 44.2, 41.4, 38.4, 37.6, 37.3, 35.7, 34.6, 34.5, 27.8, 27.4, 24.6, 24.1, 16.8. **HRMS (ESI)** exact mass calculated for C₂₇H₃₅N₄O₃ [M+H]⁺ m/z 463.2710, found m/z 463.2708. **v_{max}(solid)**: 3380, 2928, 2856, 1654, 1606, 1453 cm⁻¹.

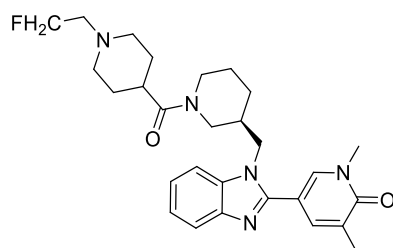
(*S*)-5-(1-((1-(1-Acetylpiperidine-4-carbonyl)piperidin-3-yl)methyl)-1*H*-benzo[*d*]imidazol-2-yl)-1,3-dimethylpyridin-2(1*H*)-one **87**



Chemical Formula: C₂₈H₃₅N₅O₃
Molecular Weight: 489.61 amu

DIPEA (39 μ L, 0.223 mmol) was added to a solution of 1-acetylpiperidine-4-carboxylic acid (13 mg, 0.074 mmol) and HATU (35 mg, 0.093 mmol) in DMF (0.5 mL) at RT. The reaction mixture was stirred at RT under air for 10 minutes, after which a solution of (*R*)-1,3-dimethyl-5-(1-(piperidin-3-ylmethyl)-1*H*-benzo[*d*]imidazol-2-yl)pyridin-2(1*H*)-one **60** (25 mg, 0.074 mmol) in DMF (0.5 mL) was added. The reaction mixture was stirred at RT under air for 66 h. The reaction mixture was dissolved in and partitioned between DCM (20 mL) and a 10% (by wt) aqueous solution of lithium chloride (20 mL), and the phases were separated. The aqueous phase was further extracted with DCM (20 mL). The combined organic phases were washed with a 10% (by wt) aqueous solution of lithium chloride (3 x 20 mL), dried by passing through a hydrophobic frit, and concentrated *in vacuo*. The residue was dissolved in 1:1 MeOH:DMSO (1 mL) and purified by EZ preparative HPLC, eluting with 15 – 100% 10 mM ammonium bicarbonate (aq)/MeCN. Fractions containing the desired product were combined and extracted with DCM (2 x 20 mL). The combine organic phases were dried by passing through a hydrophobic frit, and concentrated *in vacuo* to yield (*S*)-5-(1-((1-(1-acetylpiperidine-4-carbonyl)piperidin-3-yl)methyl)-1*H*-benzo[*d*]imidazol-2-yl)-1,3-dimethylpyridin-2(1*H*)-one **87** (19 mg, 0.036 mmol, 49% yield) as a white solid. **LCMS (HpH)**: rt = 0.76 min, [M+H]⁺ 490. **¹H NMR δ (400 MHz, DMSO-*d*₆, VT)**: ¹H NMR (400 MHz, DMSO-*d*₆) δ ppm 7.99 (1H, d, *J* = 2.2 Hz), 7.62 – 7.70 (2H, m), 7.55 – 7.62 (1H, m), 7.16 – 7.32 (2H, m), 4.20 – 4.35 (2H, m), 3.86 – 4.07 (3H, m), 3.64 – 3.75 (1H, m), 3.60 (3H, s), 2.67 – 2.91* overlapping H₂O peak (3H, integrates as 8H, m), 2.53 – 2.63 (1H, m), 2.15 (3H, s), 1.87 – 2.00 (4H, m), 1.14 – 1.65 (9H, m). **¹³C NMR δ (176 MHz, DMSO-*d*₆)**: *additional peaks due to rotamers present*. 172.0, 171.5, 167.8, 161.7, 150.4, 142.5, 142.4, 138.4, 138.3, 136.7, 136.7, 135.8, 135.8, 135.7, 127.9, 127.8, 127.8, 122.3, 122.2, 122.0, 122.0, 121.9, 118.9, 118.8, 111.2, 111.0, 111.0, 108.1, 108.0, 108.0, 48.5, 47.9, 46.8, 46.7, 46.7, 45.1, 45.1, 45.0, 44.9, 44.4, 44.3, 41.6, 41.5, 40.2, 40.1, 37.7, 37.5, 37.4, 37.3, 37.2, 37.2, 37.0, 35.9, 35.7, 28.7, 28.6, 28.5, 28.5, 28.1, 27.9, 27.8, 27.8, 27.4, 28.0, 24.7, 24.6, 24.1, 21.2, 21.2, 16.8. **ν_{max} (solid)**: 3398, 2916, 2853, 1654, 1606, 1428 cm⁻¹.

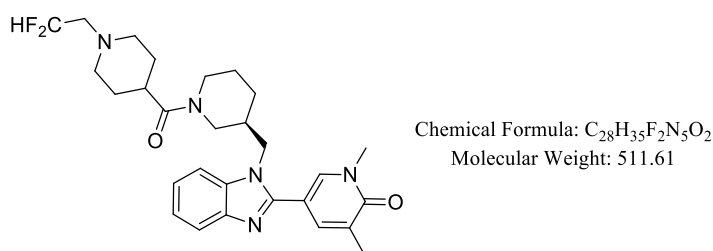
(S)-5-(1-((1-(1-(2-Fluoroethyl)piperidine-4-carbonyl)piperidin-3-yl)methyl)-1H-benzo[d]imidazol-2-yl)-1,3-dimethylpyridin-2(1H)-one 88



1-Bromo-2-fluoroethane (13 μ L, 0.181 mmol) was added to a stirring solution of sodium hydride (60% by wt dispersion in oil) (7 mg, 0.181 mmol) and (S)-1,3-dimethyl-5-(1-((1-(piperidine-4-carbonyl)piperidin-3-yl)methyl)-1H-benzo[d]imidazol-2-yl)pyridin-2(1H)-one **70** (54 mg, 0.121 mmol) in DMF (1 mL) at RT under a nitrogen atmosphere. The reaction mixture was stirred at RT under a nitrogen atmosphere for 0.5 h. LCMS analysis showed incomplete conversion to desired product. Additional sodium hydride (60% by wt dispersion in oil) (7 mg, 0.181 mmol) and 1-bromo-2-fluoroethane (13 μ L, 0.181 mmol) were added. The reaction mixture was stirred at 60 °C under a nitrogen atmosphere for 1 h. The reaction mixture was quenched by addition of MeOH (1 mL), and concentrated *in vacuo*. The residue was dissolved in 1:1 MeOH:DMSO (2 mL), and purified by EZ preparative HPLC, eluting with 0-100% 10mM ammonium bicarbonate (aq)/MeCN. Fractions containing the desired product were combined and extracted with DCM (2 x 20 mL). The combined organic phases were dried by passing through a hydrophobic frit, and concentrated *in vacuo* to yield (S)-5-(1-((1-(1-(2-fluoroethyl)piperidine-4-carbonyl)piperidin-3-yl)methyl)-1H-benzo[d]imidazol-2-yl)-1,3-dimethylpyridin-2(1H)-one **88** (22 mg, 0.042 mmol, 35% yield) as a white solid. **LCMS (H_pH)**: rt = 0.84 min [M+H]⁺ 494. **¹H NMR δ (400 MHz, DMSO-*d*₆, VT)**: 7.96 – 8.00 (1H, m), 7.62 – 7.68 (2H, m), 7.55 – 7.61 (1H, m), 7.19 – 7.30 (2H, m), 4.52 – 4.58 (1H, m), 4.40 – 4.45 (1H, m), 4.19 – 4.34 (2H, m), 3.84 – 3.98 (1H, m), 3.61 – 3.70 (1H, m), 3.59 (3H, s), 2.62 – 2.86* overlapping water peak (3H, integrates as

10H, m), 2.56 – 2.60 (1H, m), 2.18 – 2.29 (1H, m), 2.14 (3H, s), 1.89 – 2.08 (3H, m), 1.14 – 1.63 (10H, m). ¹³C NMR δ(101 MHz, DMSO-*d*6) ppm: additional peaks due to rotamers and fluorine coupling present 172.4, 161.7, 142.4, 138.3, 136.6, 135.8, 127.9, 122.2, 121.9, 121.9, 121.8, 118.9, 118.8, 111.1, 111.0, 108.1, 108.0, 82.6, 81.0, 57.8, 57.6, 52.7, 52.7, 52.6, 48.5, 47.9, 46.8, 46.7, 45.1, 44.7, 44.3, 37.7, 37.3, 35.9, 28.4, 28.3, 28.1, 27.9, 27.3, 24.6, 24.1, 16.8. HRMS (ESI) exact mass calculated for C₂₈H₃₇FN₄O₃ [M+H]⁺ m/z 494.2932, found m/z 494.2928.

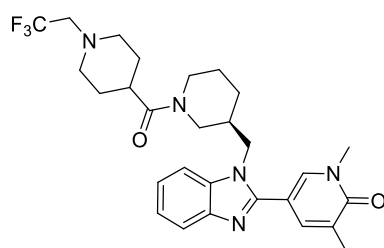
(S)-5-(1-((1-(1-(2,2-Difluoroethyl)piperidine-4-carbonyl)piperidin-3-yl)methyl)-1H-benzo[d]imidazol-2-yl)-1,3-dimethylpyridin-2(1H)-one 89



2-Bromo-1,1-difluoroethane (27 μL, 0.345 mmol) was added to a stirring solution of sodium hydride (60% by wt dispersion in oil) (14 mg, 0.345 mmol) and (S)-1,3-dimethyl-5-(1-((1-(piperidine-4-carbonyl)piperidin-3-yl)methyl)-1H-benzo[d]imidazol-2-yl)pyridin-2(1H)-one **70** (103 mg, 0.230 mmol) in DMF (2 mL) at RT under a nitrogen atmosphere. The reaction mixture was stirred at 60 °C under a nitrogen atmosphere for 16 h. LCMS analysis showed incomplete conversion to desired product. Additional sodium hydride (60% by wt dispersion in oil) (14 mg, 0.345 mmol) and 2-bromo-1,1-difluoroethane (27 μL, 0.345 mmol) were added. The reaction mixture was stirred at 70 °C under a nitrogen atmosphere for 1 h. LCMS analysis showed incomplete conversion to desired product. Additional 2-bromo-1,1-difluoroethane (54 μL, 0.690 mmol) was added and the reaction mixture stirred at 80 °C under

a nitrogen atmosphere for 2 h. LCMS analysis showed incomplete conversion to desired product. The reaction mixture was stirred at 90 °C under a nitrogen atmosphere for 2 h. LCMS analysis showed incomplete conversion to desired product. The reaction mixture was stirred at 90 °C under a nitrogen atmosphere for 16 h. The reaction mixture was quenched by addition of MeOH (2 mL), and concentrated *in vacuo*. The residue was dissolved in 1:1 MeOH:DMSO (2 mL), and purified by EZ preparative HPLC, eluting with 0-100% 10mM ammonium bicarbonate (aq)/MeCN. Fractions containing the desired product were combined and extracted with DCM (2 x 20 mL). The combined organic phases were dried by passing through a hydrophobic frit, and concentrated *in vacuo* to yield (*S*)-5-(1-((1-(1-(2,2-difluoroethyl)piperidine-4-carbonyl)piperidin-3-yl)methyl)-1*H*-benzo[*d*]imidazol-2-yl)-1,3-dimethylpyridin-2(1*H*)-one **89** (44 mg, 0.082 mmol, 36% yield) as a white solid. **LCMS (H_pH)**: rt = 0.88 min [M+H]⁺ 512. **¹H NMR δ(400 MHz, DMSO-*d*₆, VT)**: 7.95 – 8.00 (1H, m), 7.62 – 7.67 (2H, m), 7.55 – 7.60 (1H, m), 7.19 – 7.30 (2H, m), 5.82 – 6.14 (1H, m), 4.20 – 4.33 (2H, m), 3.85 – 3.96 (1H, m), 3.61 – 3.69 (1H, m), 3.59 (3H, s), 2.64 – 2.88* overlapping water peak (4H, integrates as 10H, m), 2.06 – 2.32 (6H, m), 1.88 – 1.99 (1H, m), 1.11 – 1.63 (10H, m). **¹⁹F NMR δ(376 MHz, DMSO-*d*₆)**: -118.64 – (-118.16) (m). **HRMS (ESI)** exact mass calculated for C₂₈H₃₆F₂N₄O₃ [M+H]²⁺/2 m/z 5256.6459, found [M+2H]²⁺/2 m/z 256.6457 **v_{max}(solid)**: 3460, 2929, 2858, 1656, 1615, 1454 cm⁻¹.

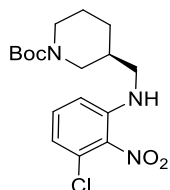
(*S*)-1,3-Dimethyl-5-(1-((1-(1-(2,2,2-trifluoroethyl)piperidine-4-carbonyl)piperidin-3-yl)methyl)-1*H*-benzo[*d*]imidazol-2-yl)pyridin-2(1*H*)-one **90**



Chemical Formula: C₂₈H₃₄F₃N₅O₂
Molecular Weight: 529.60 amu

Phenylsilane (13 μ l, 0.105 mmol) and TFA (7 μ l, 0.091 mmol) were added to a solution of (*S*)-1,3-dimethyl-5-(1-((1-(piperidine-4-carbonyl)piperidin-3-yl)methyl)-1*H*-benzo[*d*]imidazol-2-yl)pyridin-2(1*H*)-one **70** (23 mg, 0.051 mmol) in THF (0.2 mL) at RT. The vessel was sealed, and the reaction mixture was heated at 70 °C for 17 h. LCMS analysis indicated incomplete conversion to desired product. Additional phenylsilane (13 μ l, 0.105 mmol) and TFA (7 μ l, 0.091 mmol) were added, and the reaction mixture was heated at 70 °C for 2 h. After cooling to RT, the reaction mixture was concentrated *in vacuo*. The residue was dissolved in 1:1 MeOH:DMSO (1 mL), and purified by EZ preparative HPLC, eluting with 15–100% 10 mM ammonium bicarbonate (aq)/MeCN. Fractions containing the desired product were combined and extracted with DCM (2 x 20 mL), dried by passing through a hydrophobic frit, and concentrated *in vacuo* to yield (*S*)-1,3-dimethyl-5-(1-((1-(1-(2,2,2-trifluoroethyl)piperidine-4-carbonyl)piperidin-3-yl)methyl)-1*H*-benzo[*d*]imidazol-2-yl)pyridin-2(1*H*)-one **90** (12 mg, 0.022 mmol, 42% yield) as a white solid. **LCMS (HpH):** rt = 0.97 min, [M+H] 530. **¹H NMR δ (400 MHz, DMSO-*d*₆, VT):** 7.98 (1H, d, *J* = 2.4 Hz), 7.62 – 7.68 (2H, m), 7.56 – 7.60 (1H, m), 7.19 – 7.30 (2H, m), 4.20 – 4.34 (2H, m), 3.90 (1H, br d, *J* = 12.7 Hz), 3.61 – 3.70 (1H, m), 3.59 (3H, s), 3.07 (2H, d, *J* = 10.3 Hz), 2.77 – 2.91* overlapping water peak (3H, integrates as 11H, m), 2.65 – 2.74 (1H, m), 2.21 – 2.37 (3H, m), 2.14 (3H, s), 1.87 – 2.00 (1H, m), 1.39 – 1.65 (5H, m), 1.14 – 1.39 (3H, m). **¹³C NMR δ (176 MHz, DMSO-*d*₆):** additional peaks due to rotamers present. Fluorine coupling present. 172.3, 171.8, 161.7, 150.5, 150.3, 142.4, 142.4, 138.3, 136.7, 136.7, 135.8, 135.8, 127.9, 127.8, 126.9, 125.3, 122.2, 122.0, 121.9, 118.9, 118.8, 111.2, 111.0, 108.1, 108.0, 57.0, 56.9, 52.8, 52.7, 52.7, 52.6, 52.5, 47.8, 46.8, 46.7, 45.1, 44.4, 41.5, 37.6, 37.4, 37.3, 36.8, 36.7, 35.8, 28.3, 28.3, 28.2, 28.1, 27.9, 27.3, 27.3, 24.6, 24.1, 16.8. **¹⁹F NMR δ (376 MHz, DMSO-*d*₆):** -67.75 (dt, *J* = 75.9, 9.5 Hz). **HRMS (ESI)** exact mass calculated for C₂₈H₃₅F₃N₅O₂ [M+H]⁺ m/z 530.2744, found m/z 530.2742. **ν_{\max} (solid):** 3445, 2927, 2864, 1657, 1615, 1455, 1268 cm⁻¹.

tert*-Butyl (*S*)-3-(((3-chloro-2-nitrophenyl)amino)methyl)piperidine-1-carboxylate **45*

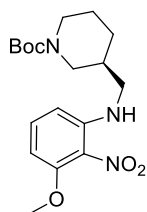


Chemical Formula: C₁₇H₂₄ClN₃O₄
Molecular Weight: 369.84 amu

1-Chloro-3-fluoro-2-nitrobenzene (400 mg, 2.28 mmol), *tert*-butyl (*S*)-3-(aminomethyl)piperidine-1-carboxylate **48** (488 mg, 2.28 mmol), potassium carbonate (472 mg, 3.42 mmol) and DMF (5 mL) were added to a round bottom flask. The reaction mixture was stirred at 100 °C under a nitrogen atmosphere for 2 h. After cooling to RT, the reaction mixture was diluted with and partitioned between EtOAc (20 mL) and a 5% (by wt) aqueous solution of lithium chloride (20 mL), and the phases were separated. The aqueous phase was further extracted with EtOAc (2 x 30 mL). The combined organic phases were washed with a 5% (by wt) aqueous solution of lithium chloride (3 x 20 mL), dried by passing through a hydrophobic frit, and concentrated *in vacuo* to yield *tert*-butyl (*S*)-3-(((3-chloro-2-nitrophenyl)amino)methyl)piperidine-1-carboxylate **45** (820 mg, 2.08 mmol, 91% yield) as an orange gum. LCMS (**HpH**): rt = 1.42 min, [M+H]⁺ 370 ¹H NMR δ(400 MHz, CDCl₃): 7.22 (1H, apparent t, *J* = 8.1 Hz), 6.76 (1H, d, *J* = 7.3 Hz), 6.69 (1H, d, *J* = 8.8 Hz), 5.85 (1H, br. s), 3.86 – 4.03 (1H, m), 3.77 – 3.86 (1H, m), 3.11 – 3.22 (1H, m), 3.01 – 3.11 (1H, m), 2.96 (1H, s), 2.68 – 2.82 (1H, m), 1.78 – 1.95 (2H, m), 1.64 – 1.74 (1H, m), 1.41 – 1.50 (10H, m), 1.22 – 1.33 (1H, m).

***tert*-Butyl (*S*)-3-(((3-methoxy-2-nitrophenyl)amino)methyl)piperidine-1-carboxylate**

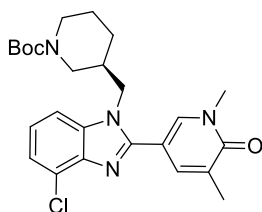
96



Chemical Formula: $C_{18}H_{27}N_3O_5$
Molecular Weight: 365.42 amu

Potassium carbonate (557 mg, 4.03 mmol), *tert*-butyl (*S*)-3-(aminomethyl)piperidine-1-carboxylate **48** (634 mg, 2.96 mmol), 1-fluoro-3-methoxy-2-nitrobenzene (460 mg, 2.69 mmol) and DMF (5 mL) were added to a round bottom flask. The reaction mixture was stirred at 100 °C under a nitrogen atmosphere for 3 h. LCMS analysis showed incomplete conversion to desired product. Additional *tert*-butyl (*S*)-3-(aminomethyl)piperidine-1-carboxylate **48** (122 mg, 0.57 mmol) was added. The reaction mixture was stirred at 100 °C under a nitrogen atmosphere for 1 h. After cooling to RT, the reaction mixture was diluted with and partitioned between EtOAc (30 mL) and a 5% (by wt) aqueous solution of lithium chloride (30 mL), and the phases were separated. The aqueous phase was further extracted with EtOAc (30 mL). The combined organic phases were washed with a 5% (by wt) aqueous solution of lithium chloride (2 x 30 mL), dried by passing through a hydrophobic frit, and concentrated *in vacuo*. The crude material was then purified by normal phase chromatography, eluting with 0 – 30% EtOAc in cyclohexane over 16 CV. Fractions containing the desired product were concentrated *in vacuo* to yield *tert*-butyl (*S*)-3-(((3-methoxy-2-nitrophenyl)amino)methyl)piperidine-1-carboxylate **96** (752 mg, 1.89 mmol, 70% yield, > 92% purity) as an orange gum. **LCMS (HpH)**: rt = 1.32 min, [M+H]⁺ 366 **¹H NMR δ(400 MHz, CDCl₃)**: 7.21 – 7.27 (1H, m), 6.33 – 6.38 (1H, m), 6.25 – 6.30 (1H, m), 6.13 – 6.23 (1H, m), 3.89 – 4.05 (1H, m), 3.87 (3H, s), 3.78 – 3.85 (1H, m), 3.10 – 3.20 (1H, m), 2.99 – 3.09 (1H, m), 2.86 – 2.99 (1H, m), 2.63 – 2.85 (1H, m), 1.78 – 1.96 (2H, m), 1.65 (1H, s), 1.44 – 1.51 (10H, m), 1.15 – 1.33 (1H, m).

tert*-Butyl (*S*)-3-((4-chloro-2-(1,5-dimethyl-6-oxo-1,6-dihydropyridin-3-yl)-1H-benzo[d]imidazol-1-yl)methyl)piperidine-1-carboxylate **46*

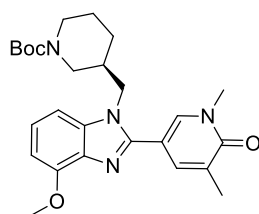


Chemical Formula: C₂₅H₃₁ClN₄O₃

Molecular Weight: 470.99 amu

1,5-Dimethyl-6-oxo-1,6-dihydropyridine-3-carbaldehyde **36** (335 mg, 2.22 mmol), *tert*-butyl (*S*)-3-(((3-chloro-2-nitrophenyl)amino)methyl)piperidine-1-carboxylate **45** (820 mg, 2.22 mmol), EtOH (10 mL) and water (5 mL) were added to a round bottom flask. The reaction mixture was heated to 80 °C, after which sodium dithionite (1.16 g, 6.65 mmol) was added. The reaction mixture was then stirred at 100 °C under a nitrogen atmosphere for 18 h. After cooling to RT, the reaction mixture was diluted with and partitioned between EtOAc (30 mL) and water (30 mL), and the phases were separated. The aqueous phase was further extracted with EtOAc (2 x 30 mL). The combined organic phases were washed with brine (50 mL), dried by passing through a hydrophobic frit, and concentrated *in vacuo*. The crude material was then purified by normal phase chromatography, eluting with 0 – 100% 3:1 EtOAc in cyclohexane over 18 CV. Fractions containing the desired product were concentrated *in vacuo* to yield *tert*-butyl (*S*)-3-((4-chloro-2-(1,5-dimethyl-6-oxo-1,6-dihydropyridin-3-yl)-1H-benzo[d]imidazol-1-yl)methyl)piperidine-1-carboxylate **46** (461 mg, 0.881 mmol, 40% yield, 90% purity) as a white solid. **LCMS (HpH)**: *rt* = 1.15 min, [M+H]⁺ 471 **¹H NMR δ(400 MHz, CDCl₃)**: 7.76 – 7.86 (1H, m), 7.43 – 7.52 (1H, m), 7.19 – 7.38 (3H, m), 4.05 – 4.23 (2H, m), 3.77 – 3.90 (1H, m), 3.66 (3H, s), 2.71 – 2.85 (1H, m), 2.53 (1H, dd, *J* = 12.7, 9.8 Hz), 2.25 (3H, s), 1.98 – 2.06 (1H, m), 1.71 – 1.80 (1H, m), 1.49 – 1.62 (2H, m), 1.27 – 1.47 (10H, m), 0.98 – 1.14 (1H, m).

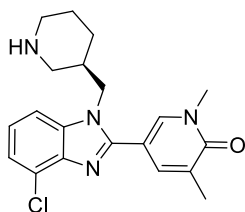
tert-Butyl (*S*)-3-((2-(1,5-dimethyl-6-oxo-1,6-dihydropyridin-3-yl)-4-methoxy-1H-benzo[d]imidazol-1-yl)methyl)piperidine-1-carboxylate **97**



Chemical Formula: C₂₆H₃₄N₄O₄
Molecular Weight: 466.57 amu

1,5-Dimethyl-6-oxo-1,6-dihydropyridine-3-carbaldehyde **36** (353 mg, 2.34 mmol), *tert*-butyl (*S*)-3-(((3-methoxy-2-nitrophenyl)amino)methyl)piperidine-1-carboxylate **96** (709 mg, 1.79 mmol), EtOH (5 mL) and water (2.5 mL) were added to a round bottom flask. The reaction mixture was heated to 80 °C, after which sodium dithionite (1.02 g, 5.84 mmol) was added. The reaction mixture was stirred at 100 °C under a nitrogen atmosphere for 16 h. After cooling to RT, the reaction mixture was diluted with and partitioned between EtOAc (30 mL) and brine (30 mL), and the phases were separated. The organic phases were further washed with brine (30 mL). The organic phase was dried by passing through a hydrophobic frit, and concentrated *in vacuo*. The crude material was then purified by normal phase chromatography, eluting with 0 – 60% 3:1 EtOAc:EtOH in cyclohexane over 20 CV. Fractions containing the desired product were concentrated *in vacuo* to yield *tert*-butyl (*S*)-3-((2-(1,5-dimethyl-6-oxo-1,6-dihydropyridin-3-yl)-4-methoxy-1H-benzo[d]imidazol-1-yl)methyl)piperidine-1-carboxylate **97** (516 mg, 1.05 mmol, 62% yield) as a white solid. **LCMS (HpH)**: rt = 1.06, min [M+H]⁺ 467. **¹H NMR δ(400 MHz, CDCl₃)**: 7.76 – 7.82 (1H, m), 7.47 – 7.53 (1H, m), 7.20 – 7.25 (1H, m), 6.98 (1H, d, *J* = 8.3 Hz), 6.72 (1H, d, *J* = 7.8 Hz), 3.99 – 4.20 (6H, m), 3.75 – 3.85 (1H, m), 3.64 (3H, s), 2.72 – 2.83 (1H, m), 2.48 – 2.60 (1H, m), 2.23 (3H, s), 1.98 – 2.10 (1H, m), 1.48 – 1.61 (2H, m), 1.29 – 1.44 (10H, m), 0.94 – 1.11 (1H, m). **¹³C NMR δ(101 MHz, CDCl₃)**: 162.7 (C), 154.6 (C), 151.7 (C), 149.1 (C), 137.8 (CH), 137.2 (C), 136.1 (CH), 133.2 (C), 129.6 (C), 123.7 (CH), 109.3 (2 x CH), 103.0 (C), 79.7 (C), 55.7 (CH₃), 47.8 (2 x CH₂), 44.3 (CH₂), 38.0 (CH₃), 36.4 (CH), 28.3 (br., CH₂ and CH₃), 24.1 (CH₂), 17.4 (CH₃).

(R)-5-(4-Chloro-1-(piperidin-3-ylmethyl)-1H-benzo[d]imidazol-2-yl)-1,3-dimethylpyridin-2(1H)-one 98

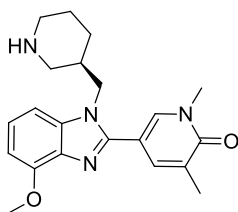


Chemical Formula: C₂₀H₂₃ClN₄O

Molecular Weight: 370.88 amu

tert-Butyl (*S*)-3-((4-chloro-2-(1,5-dimethyl-6-oxo-1,6-dihydropyridin-3-yl)-1H-benzo[d]imidazol-1-yl)methyl)piperidine-1-carboxylate **46** (461 mg, 0.979 mmol) was dissolved in a solution of hydrochloric acid in 1,4-dioxane (4 M, 4 mL, 16 mmol). MeOH (1mL) was added to aid solubility. The reaction mixture was stirred at RT under air for 1 h. The reaction mixture was diluted with methanol (20 mL) and then added to a SCX 20 g column (pre-wet with methanol) and allowed to settle by gravity. The column was then washed with methanol (50 mL) under vacuum. Into a separate flask, the column was washed with a solution of ammonia in MeOH (2 M, 50 mL). The filtrate was concentrated *in vacuo* to yield (*R*)-5-(4-chloro-1-(piperidin-3-ylmethyl)-1H-benzo[d]imidazol-2-yl)-1,3-dimethylpyridin-2(1H)-one **98** (332 mg, 0.806 mmol, 82% yield, 90% purity) as a yellow gum. **LCMS (H_{PLC})**: *rt* = 0.82 min, [M+H]⁺ 371. **¹H NMR δ(400 MHz, CDCl₃)**: 7.78 (1H, s), 7.42 – 7.48 (1H, m), 7.19 – 7.27 (2H, m), 7.08 – 7.16 (1H, m), 3.95 – 4.13 (2H, m), 3.56 (3H, s), 2.78 – 2.88 (1H, m), 2.62 – 2.71 (1H, m), 2.43 – 2.53 (1H, m), 2.17 – 2.26 (2H, m), 2.15 (3H, s), 1.90 – 2.03 (1H, m), 1.47 – 1.57 (2H, m), 1.23 – 1.36 (1H, m), 0.95 – 1.08 (1H, m).

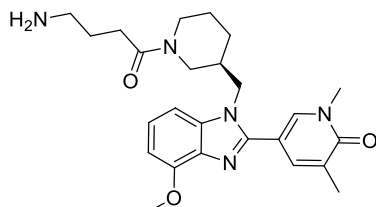
(R)-5-(4-Methoxy-1-(piperidin-3-ylmethyl)-1H-benzo[d]imidazol-2-yl)-1,3-dimethylpyridin-2(1H)-one 99



Chemical Formula: $C_{21}H_{26}N_4O_2$
Molecular Weight: 366.46 amu

tert-Butyl (S)-3-((2-(1,5-dimethyl-6-oxo-1,6-dihydropyridin-3-yl)-4-methoxy-1H-benzo[d]imidazol-1-yl)methyl)piperidine-1-carboxylate **97** (516 mg, 1.11 mmol) was dissolved in a solution of hydrochloric acid in 1,4-dioxane (4 M, 3 mL, 12 mmol). The reaction mixture was stirred at RT under air for 24 h. The reaction mixture was diluted with methanol (20 mL) and then added to a SCX 20 g column (pre-wet with methanol) and allowed to settle by gravity. The column was then washed with methanol (80 mL) under vacuum. Into a separate flask, the column was washed with a solution of ammonia in MeOH (2 M, 80 mL). The filtrate was concentrated *in vacuo* to yield (R)-5-(4-methoxy-1-(piperidin-3-ylmethyl)-1H-benzo[d]imidazol-2-yl)-1,3-dimethylpyridin-2(1H)-one **99** (329 mg, 0.853 mmol, 77% yield) as a yellow solid. **LCMS (H₂O)**: rt = 0.77 min, [M+H]⁺ 367. **¹H NMR δ (400 MHz, CDCl₃)**: 7.83 – 7.88 (1H, m), 7.52 – 7.58 (1H, m), 7.18 – 7.24 (1H, m), 7.00 (1H, d, *J* = 8.3 Hz), 6.72 (1H, d, *J* = 7.8 Hz), 4.06 – 4.20 (2H, m), 4.03 (3H, s), 3.64 (3H, s), 2.88 – 2.96 (1H, m), 2.72 – 2.80 (1H, m), 2.52 – 2.60 (1H, m), 2.27 – 2.35 (1H, m), 2.24 (3H, s), 2.01 – 2.13 (1H, m), 1.58 – 1.67 (3H, m), 1.33 – 1.44 (1H, m), 1.04 – 1.16 (1H, m).

(S)-5-(1-((1-(4-Aminobutanoyl)piperidin-3-yl)methyl)-4-methoxy-1H-benzo[d]imidazol-2-yl)-1,3-dimethylpyridin-2(1H)-one 100

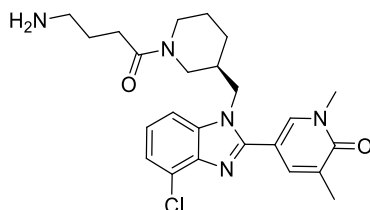


Chemical Formula: $C_{25}H_{33}N_5O_3$
Molecular Weight: 451.56 amu

DIPEA (119 μ L, 0.682 mmol) was added to a stirring solution of HATU (64 mg, 0.168 mmol) and 4-((*tert*-butoxycarbonyl)amino)butanoic acid (28 mg, 0.136 mmol) in DMF (0.5 mL). The reaction mixture was stirred at RT under air for 10 minutes, after which a solution of (*R*)-5-(4-methoxy-1-(piperidin-3-ylmethyl)-1*H*-benzo[*d*]imidazol-2-yl)-1,3-dimethylpyridin-2(1*H*)-one **99** (50 mg, 0.136 mmol) in DMF (0.5 mL) was added. The reaction mixture was stirred at RT under air for 30 minutes. The reaction mixture was diluted with and partitioned between EtOAc (10 mL) and a 5 % (by wt) aqueous solution of lithium chloride (20 mL), and the phases were separated. The aqueous phase was further extracted with EtOAc (20 mL). The combined organic phases were washed with a 5 % (by wt) aqueous solution of lithium chloride (3 x 20 mL), dried by passing through a hydrophobic frit, and concentrated *in vacuo* to yield *tert*-butyl (*S*)-(4-(3-((2-(1,5-dimethyl-6-oxo-1,6-dihydropyridin-3-yl)-4-methoxy-1*H*-benzo[*d*]imidazol-1-yl)methyl)piperidin-1-yl)-4-oxobutyl)carbamate (93 mg, 0.135 mmol) as a brown oil. This was taken forward crude. *tert*-butyl (*S*)-(4-(3-((2-(1,5-dimethyl-6-oxo-1,6-dihydropyridin-3-yl)-4-methoxy-1*H*-benzo[*d*]imidazol-1-yl)methyl)piperidin-1-yl)-4-oxobutyl)carbamate (93 mg, 0.135 mmol) was dissolved in a solution of hydrochloric acid in 1,4-dioxane (4 M, 1 mL, 4 mmol). MeOH (1 mL) was added to aid solubility. The reaction mixture was stirred at RT under air for 2 h. After this time, the reaction mixture was concentrated *in vacuo*. The residue was dissolved in 1:1 MeOH:DMSO and purified by MDAP using a solvent system of 10 mM ammonium bicarbonate adjusted to pH 10 with ammonia in water (solvent A) and acetonitrile (solvent B). Fractions containing the desired product were combined and extracted with DCM (2 x 20 mL). The combined organic phases were dried by passing through a hydrophobic frit, and concentrated *in vacuo* to yield (*S*)-5-(1-((1-(4-aminobutanoyl)piperidin-3-yl)methyl)-4-methoxy-1*H*-benzo[*d*]imidazol-2-yl)-1,3-dimethylpyridin-2(1*H*)-one **100** (20 mg, 0.042 mmol, 31% yield). **LCMS (HpH)**: rt = 0.76 min, [M+H]⁺ 452. **¹H NMR δ (400 MHz, CDCl₃)**: *rotamer 1* 7.82 – 7.87 (1H, m), 7.44 – 7.49 (1H, m), 7.21 (1H, s), 6.97 (1H, d, *J* = 8.3 Hz), 6.68 – 6.77 (1H, m), 4.34 – 4.47 (1H, m), 4.05 – 4.31 (2H, m), 4.03 (3H, s), 3.56 – 3.73 (4H, m), 3.25 –

3.38 (1H, m), 2.67 – 2.77 (2H, m), 2.47 – 2.65 (2H, m), 2.28 – 2.39 (2H, m), 2.23 (3H, s), 1.87 – 2.13 (2H, m), 0.93 – 1.78* overlapping H₂O peak (6H, integrates as 11H, m). *rotamer 2* 7.76 – 7.82 (1H, m), 7.49 – 7.53 (1H, m), 7.21 (1H, s), 6.97 (1H, d, *J* = 8.3 Hz), 6.68 – 6.77 (1H, m), 4.05 – 4.31 (3H, m), 4.03 (3H, s), 3.56 – 3.73 (4H, m), 2.95 – 3.08 (1H, m), 2.67 – 2.77 (2H, m), 2.47 – 2.65 (2H, m), 2.28 – 2.39 (2H, m), 2.23 (3H, s), 1.87 – 2.13 (2H, m), 0.93 – 1.78* overlapping H₂O peak (6H, integrates as 11H, m). ¹³C NMR δ(101 MHz, CDCl₃): 171.4 (C), 162.7 (C), 151.6 (C), 149.0 (C), 137.9 (CH), 137.1 (C), 136.2 (CH), 133.1 (C), 129.6 (C), 123.8 (CH), 109.3 (C), 103.1 (CH), 103.0 (CH), 55.7 (CH₃), 47.7 (CH₂), 46.0 (CH₂), 45.2 (CH₂), 41.7 (CH₂), 38.1 (CH₃), 36.1 (CH), 30.6 (CH₂), 28.9 (CH₂), 28.2 (CH₂), 24.8 (CH₂), 17.3 (CH₃). HRMS (ESI) exact mass calculated for C₂₅H₃₄N₅O₃ [M+H]⁺ m/z 452.2662, found m/z 452.2665.

(S)-5-(1-((1-(4-Aminobutanoyl)piperidin-3-yl)methyl)-4-chloro-1H-benzo[d]imidazol-2-yl)-1,3-dimethylpyridin-2(1H)-one 101

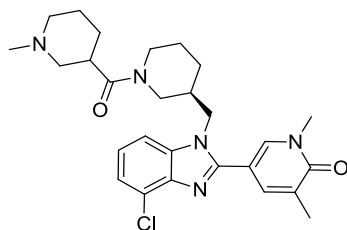


Chemical Formula: C₂₄H₃₀ClN₅O₂
Molecular Weight: 455.98 amu

DIPEA (111 μ L, 0.634 mmol) was added to a stirring solution of 4-((*tert*-butoxycarbonyl)amino)butanoic acid (26 mg, 0.127 mmol) and HATU (64 mg, 0.168 mmol) in DMF (0.5 mL) at RT. The reaction mixture was stirred at RT under air for 5 minutes, after which a solution of (*R*)-5-(4-chloro-1-(piperidin-3-ylmethyl)-1H-benzo[d]imidazol-2-yl)-1,3-dimethylpyridin-2(1H)-one **98** (47 mg, 0.127 mmol) in DMF (0.5 mL) was added. The reaction mixture was stirred at RT under air for 1 h. The reaction mixture was diluted with and partitioned between EtOAc (20 mL) and a 5% (by wt) aqueous solution of lithium chloride (20 mL), and the phases were separated. The aqueous phase was further extracted with EtOAc (2 x 20 mL). The combined organic phases were washed with a 5% (by wt) aqueous solution of lithium chloride (20 mL), dried by passing through a hydrophobic frit, and concentrated *in vacuo*. The residue was dissolved in 1:1 MeOH:DMSO (1 mL) and purified by MDAP using a solvent system of 10 mM ammonium bicarbonate adjusted to pH 10 with ammonia in water (solvent A) and acetonitrile (solvent B). Fractions containing the desired product were combined and extracted with DCM (3 x 20 mL). The combined organic phases were dried by passing through a hydrophobic frit, and concentrated *in vacuo* to yield *tert*-butyl (*S*)-(4-(3-((4-chloro-2-(1,5-dimethyl-6-oxo-1,6-dihydropyridin-3-yl)-1H-benzo[d]imidazol-1-yl)methyl)piperidin-1-yl)-4-oxobutyl)carbamate (40 mg) as a white solid. *tert*-Butyl (*S*)-(4-(3-((4-chloro-2-(1,5-dimethyl-6-oxo-1,6-dihydropyridin-3-yl)-1H-benzo[d]imidazol-1-yl)methyl)piperidin-1-yl)-4-oxobutyl)carbamate (35 mg, 0.063 mmol) was dissolved in a solution of hydrochloric acid in 1,4-dioxane (4 M, 2 mL, 4 mmol). MeOH (1 mL) was added

to aid solubility. The reaction mixture was stirred at RT under air for 16 h. The reaction mixture was diluted with methanol (10 mL) and then added to a SCX 10 g column (pre-wet with methanol) and allowed to settle by gravity. The column was then washed with methanol (50 mL) under vacuum. Into a separate flask, the column was washed with a solution of ammonia in MeOH (2 M, 50 mL). The filtrate was concentrated *in vacuo* and placed on high vacuum for 2 h. The compound was not sufficiently pure, therefore further purification was required. The residue was dissolved in 1:1 MeOH:DMSO (1 mL) and purified by MDAP using a solvent system of 10 mM ammonium bicarbonate adjusted to pH 10 with ammonia in water (solvent A) and acetonitrile (solvent B). Fractions containing the desired product were combined and extracted with DCM (2 x 10 mL). The combined organic phases were dried by passing through a hydrophobic frit, and concentrated *in vacuo* to yield (*S*)-5-(1-((1-(4-aminobutanoyl)piperidin-3-yl)methyl)-4-chloro-1*H*-benzo[*d*]imidazol-2-yl)-1,3-dimethylpyridin-2(1*H*)-one **101** (12 mg, 25 μ mol, 20% yield) as a colourless gum. **LCMS (HpH)**: rt = 0.82 min, [M+H]⁺ 456. **¹H NMR δ (400 MHz, CDCl₃)**: *rotamer 1* 7.79 – 7.85 (1H, m), 7.47 (1H, br s), 7.19 – 7.37* overlapping CDCl₃ (3H, integrates as 4H, m), 4.03 – 4.32 (3H, m), 3.66 (4H, s), 2.96 – 3.08 (1H, m), 2.67 – 2.78 (2H, m), 2.47 – 2.61 (2H, m), 2.29 – 2.39 (2H, m), 2.25 (3H, s), 2.00 (2H, s), 0.99 – 1.77* overlapping H₂O peak (6H, integrates as 10H, m). *rotamer 2* 7.85 – 7.93 (1H, m), 7.47 (1H, br s), 7.19 – 7.37* overlapping CDCl₃ (3H, integrates as 4H, m), 4.35 – 4.45 (1H, m), 4.03 – 4.32 (2H, m), 3.66 (4H, s), 3.29 – 3.40 (1H, m), 2.67 – 2.78 (2H, m), 2.47 – 2.61 (2H, m), 2.29 – 2.39 (2H, m), 2.25 (3H, s), 2.00 (2H, s), 0.99 – 1.77* overlapping H₂O peak (6H, integrates as 10H, m). **¹³C NMR δ (101 MHz, CDCl₃)**: *rotamers present* 171.4, 162.7, 151.0, 140.2, 138.4, 138.3, 136.6, 135.8, 135.4, 129.9, 124.8, 123.6, 123.5, 122.9, 122.7, 108.8, 108.6, 49.2, 49.1, 48.1, 47.9, 46.0, 45.1, 41.7, 41.5, 38.2, 37.5, 36.1, 30.6, 28.9, 28.8, 28.3, 24.8, 17.4. **HRMS (ESI)** exact mass calculated for C₂₄H₃₁ClN₅O₂ [M+H]⁺ m/z 456.2167, found m/z 456.2174.

5-(4-Chloro-1-(((3S)-1-(1-methylpiperidine-3-carbonyl)piperidin-3-yl)methyl)-1H-benzo[d]imidazol-2-yl)-1,3-dimethylpyridin-2(1H)-one 102

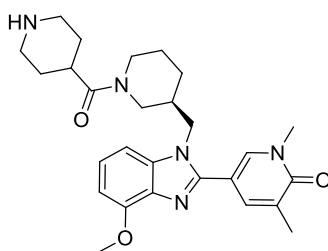


Chemical Formula: C₂₇H₃₄ClN₅O₂
Molecular Weight: 496.04 amu

DIPEA (118 μ L, 0.674 mmol) was added to a stirring solution of 1-methylpiperidine-3-carboxylic acid (20 mg, 0.140 mmol) and HATU (64 mg, 0.168 mmol) in DMF (1 mL) at RT. The reaction mixture was stirred at RT under air for 10 minutes, after which a solution of (*R*)-5-(4-chloro-1-(piperidin-3-ylmethyl)-1H-benzo[d]imidazol-2-yl)-1,3-dimethylpyridin-2(1H)-one **98** (50 mg, 0.135 mmol) in DMF (1 mL) was added. The reaction mixture was stirred at RT under air for 1 h. The reaction mixture was diluted with and partitioned between EtOAc (20 mL) and a 5% (by wt) aqueous solution of lithium chloride (20 mL), and the phases were separated. The aqueous phase was further extracted with EtOAc (2 x 20 mL). The combined organic phases were washed with a 5% (by wt) aqueous solution of lithium chloride (20 mL), dried by passing through a hydrophobic frit, and concentrated *in vacuo*. The aqueous phase was further extracted with DCM (2 x 20 mL). These combined organics were dried by passing through a hydrophobic frit, combined with the first batch, and concentrated *in vacuo*. The residue was dissolved in 1:1 MeOH:DMSO (1 mL) and purified by MDAP using a solvent system of 10 mM ammonium bicarbonate adjusted to pH 10 with ammonia in water (solvent A) and acetonitrile (solvent B). Fractions containing the desired product were combined and extracted with DCM (3 x 20 mL). The combined organic phases were dried by passing through a hydrophobic frit, and concentrated *in vacuo* to yield 5-(4-chloro-1-(((3S)-1-(1-methylpiperidine-3-carbonyl)piperidin-3-yl)methyl)-1H-benzo[d]imidazol-2-yl)-1,3-dimethylpyridin-2(1H)-one **102** (52 mg, 0.1 mmol, 74% yield) as a colourless gum. **LCMS (HpH)**: rt = 0.90 min, [M+H]⁺ 496. **¹H NMR δ (400 MHz, DMSO-*d*₆, VT)**: 7.97 – 8.06 (1H,

m), 7.63 – 7.69 (1H, m), 7.57 (1H, d, $J = 7.8$ Hz), 7.20 – 7.31 (2H, m), 4.19 – 4.36 (2H, m), 3.81 – 3.93 (1H, m), 3.63 – 3.75 (1H, m), 3.59 (3H, s), 2.76 – 2.90* overlapping H₂O peak (1H, integrates as 7H, m), 2.64 – 2.73 (2H, m), 2.52 – 2.61 (2H, m), 2.10 – 2.17 (6H, m), 1.76 – 1.97 (3H, m), 1.14 – 1.64 (8H, m) ¹³C NMR δ (101 MHz, CDCl₃): additional peaks due to rotamers present 172.7, 172.7, 162.7, 151.1, 140.2, 140.2, 138.4, 136.6, 135.8, 135.5, 129.9, 124.8, 123.5, 122.7, 108.8, 108.6, 58.1, 58.1, 55.6, 48.0, 47.7, 46.5, 45.9, 45.8, 45.2, 45.1, 39.6, 39.5, 38.2, 36.2, 36.0, 28.5, 28.1, 27.1, 27.1, 25.2, 25.0, 25.0, 24.8, 17.4. HRMS (ESI) exact mass calculated for C₂₇H₃₅ClN₅O₂ [M+H]⁺ m/z 496.2480, found m/z 496.2482. ν_{max} (solid): 2937, 2853, 2790, 1654, 1618, 1431 cm⁻¹.

(S)-5-(4-Methoxy-1-((1-(piperidine-4-carbonyl)piperidin-3-yl)methyl)-1H-benzo[d]imidazol-2-yl)-1,3-dimethylpyridin-2(1H)-one 103



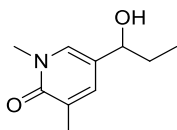
Chemical Formula: C₂₇H₃₅N₅O₃
Molecular Weight: 477.60 amu

DIPEA (119 μ L, 0.682 mmol) was added to a stirring solution of 1-(*tert*-butoxycarbonyl)piperidine-4-carboxylic acid (31 mg, 0.136 mmol) and HATU (64 mg, 0.168 mmol) in DMF (0.5 mL) at RT. The reaction mixture was stirred at RT under air for 10 minutes, after which a solution of (*R*)-5-(4-methoxy-1-(piperidin-3-ylmethyl)-1H-benzo[d]imidazol-2-yl)-1,3-dimethylpyridin-2(1H)-one **99** (50 mg, 0.136 mmol) in DMF (0.5 mL) was added. The reaction mixture was stirred at RT under air for 1 h. The reaction mixture was diluted with and partitioned between EtOAc (20 mL) and a 5% (by wt) aqueous solution of lithium chloride (20 mL), and the phases were separated. The organic phase washed with a 5% (by wt) aqueous solution of lithium chloride (2 x 20 mL), and brine (20 mL). The

organic phase was dried by passing through a hydrophobic frit, and concentrated *in vacuo* to yield *tert*-butyl (S)-4-(3-((2-(1,5-dimethyl-6-oxo-1,6-dihydropyridin-3-yl)-4-methoxy-1*H*-benzo[*d*]imidazol-1-yl)methyl)piperidine-1-carbonyl)piperidine-1-carboxylate (117 mg, 0.132 mmol) as a brown gum. This was used in the next reaction as a crude mixture. *tert*-Butyl (S)-4-(3-((2-(1,5-dimethyl-6-oxo-1,6-dihydropyridin-3-yl)-4-methoxy-1*H*-benzo[*d*]imidazol-1-yl)methyl)piperidine-1-carbonyl)piperidine-1-carboxylate (117 mg, 0.132 mmol) was dissolved in a solution of hydrochloric acid in 1,4-dioxane (4 M, 3 mL, 12.0 mmol). MeOH (1 mL) was added to aid solubility. The reaction mixture was stirred at RT under air for 16 h. The reaction mixture was concentrated *in vacuo*. The residue was dissolved in 1:1 MeOH:DMSO (1 mL) and purified by MDAP, using a solvent system of 10 mM ammonium bicarbonate adjusted to pH 10 with ammonia in water (solvent A) and acetonitrile (solvent B). Fractions containing the desired product were combined and extracted with DCM (2 x 20 mL). The combined organic phases were dried by passing through a hydrophobic frit, and concentrated *in vacuo* to yield (S)-5-(4-methoxy-1-((1-(piperidine-4-carbonyl)piperidin-3-yl)methyl)-1*H*-benzo[*d*]imidazol-2-yl)-1,3-dimethylpyridin-2(1*H*)-one **103** (36 mg, 0.072 mmol, 53% yield) as a white solid. **LCMS (HpH)**: rt = 0.79 min, [M+H]⁺ 478. **¹H NMR δ(400 MHz, DMSO-*d*₆, VT)**: 7.96 (1H, d, *J* = 2.2 Hz), 7.60 – 7.70 (1H, m), 7.15 (2H, s), 6.69 – 6.82 (1H, m), 4.14 – 4.30 (2H, m), 4.04 (3H, s), 3.84 – 3.95 (1H, m), 3.61 – 3.70 (1H, m), 3.59 (3H, s), 2.63 – 2.95* overlapping H₂O peak (5H, integrates to 16H, m), 2.31 – 2.46 (3H, m), 2.14 (3H, s), 1.84 – 1.97 (1H, m), 1.54 – 1.65 (2H, m), 1.13 – 1.48 (6H, m). **¹³C NMR δ(101 MHz, CDCl₃)**: CH₂ obscured. 173.6 (C), 162.7 (C), 151.6 (C), 137.9 (CH), 137.1 (C), 135.8 (CH), 133.2 (C), 129.6 (C), 124.0 (C), 123.8 (CH), 109.3 (C), 103.3 (CH), 103.1 (CH), 55.7 (CH), 47.5 (CH₂), 45.5 – 46.2 (m, CH₂), 45.3 (CH₂), 39.0 (CH), 38.1 (CH₃), 36.0 (CH₃), 29.7 (CH₂), 28.0 (CH₂), 24.9 (CH₂), 17.4 (CH₃). **HRMS (ESI)** exact mass calculated for C₂₇H₃₆N₅O₃

[M+H]⁺ m/z 478.2819, found m/z 478.2816. $\nu_{\text{max}}(\text{solid})$: 3424, 2931, 2859, 1652, 1602, 1265 cm⁻¹.

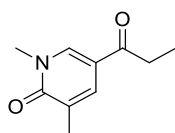
5-(1-Hydroxypropyl)-1,3-dimethylpyridin-2(1H)-one **105**



Chemical Formula: C₁₀H₁₅NO₂
Molecular Weight: 181.23 amu

Ethylmagnesium bromide in THF (1 M, 1.5 mL, 1.5 mmol) was added dropwise to a solution of 1,5-dimethyl-6-oxo-1,6-dihydropyridine-3-carbaldehyde **36** (150 mg, 0.992 mmol) in THF (6 mL) at 0 °C under a nitrogen atmosphere. The reaction mixture was stirred at 0 °C under a nitrogen atmosphere for 1 h. The reaction mixture was quenched by the addition of a saturated aqueous solution of ammonium chloride (20 mL). The reaction mixture was diluted with and partitioned between EtOAc (20 mL) and water (20 mL), and the phases were separated. The aqueous phase was further extracted with EtOAc (20 mL) and DCM (5 x 20 mL). The combined organics were concentrated *in vacuo* to yield 5-(1-hydroxypropyl)-1,3-dimethylpyridin-2(1H)-one **105** (164 mg, 0.860 mmol, 87% yield) as a white solid. **LCMS (For)**: rt = 0.53 min, [M+H]⁺ 182. **¹H NMR δ (400 MHz, CDCl₃) ppm** 7.20 – 7.24 (1H, m), 7.07 – 7.11 (1H, m), 4.31 (1H, t, *J* = 6.6 Hz), 3.51 (3H, s), 2.55 (1H, br. s), 2.11 – 2.15 (3H, m), 1.61 – 1.83 (2H, m), 0.90 (3H, t, *J* = 7.6 Hz). **¹³C NMR δ (101 MHz, CDCl₃) ppm**: 163.2 (C), 135.4 (CH), 132.7 (CH), 129.6 (C), 122.0 (C), 72.9 (CH), 37.8 (CH₃), 30.8 (CH₂), 17.3 (CH₃), 10.0 (CH₃) **HRMS (ESI)** exact mass calculated for C₁₀H₁₆NO₂ [M+H]⁺ m/z 182.1103, found m/z 182.1189.

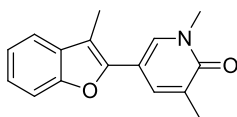
1,3-dimethyl-5-propionylpyridin-2(1H)-one **106**



Chemical Formula: C₁₀H₁₃NO₂
Molecular Weight: 179.22 amu

Manganese dioxide (729 mg, 8.39 mmol) was added to a stirring solution of 5-(1-hydroxypropyl)-1,3-dimethylpyridin-2(1H)-one **105** (152 mg, 0.839 mmol) in DCM (15 mL). The reaction mixture was stirred at RT under air for 70 h. LCMS analysis showed incomplete conversion to the desired product. Additional manganese dioxide (365 mg, 4.19 mmol) was added. The reaction mixture was stirred at RT under air for 30 min. The reaction mixture was filtered through Celite®, washing through with DCM (50 mL). The filtrate was concentrated *in vacuo* to yield 1,3-dimethyl-5-propionylpyridin-2(1H)-one **106** (129 mg, 0.684 mmol, 82% yield) as a yellow solid. **LCMS (HpH)**: rt = 0.67 min, [M+H]⁺ 180. **¹H NMR δ(400 MHz, CDCl₃) ppm**: 8.02 (1H, d, *J* = 2.9 Hz), 7.72 – 7.79 (1H, m), 3.62 (3H, s), 2.79 (2H, q, *J* = 7.0 Hz), 2.19 (3H, s), 1.20 (3H, t, *J* = 7.1 Hz). **¹³C NMR δ(101 MHz, CDCl₃) ppm**: 196.3 (C), 163.4 (C), 140.0 (CH), 134.5 (CH), 128.8 (C), 116.9 (C), 38.5 (CH₃), 30.9 (CH₂), 17.2 (CH₃), 8.3 (CH₃). **HRMS (ESI)** exact mass calculated for C₁₀H₁₄NO₂ [M+H]⁺ m/z 180.1025, found m/z 180.1030.

1,3-dimethyl-5-(3-methylbenzofuran-2-yl)pyridin-2(1H)-one **108**



Chemical Formula: C₁₆H₁₅NO₂
Molecular Weight: 253.30 amu

Methanesulfonic acid (36 μL, 0.558 mmol) was added to a stirring solution of 1,3-dimethyl-5-propionylpyridin-2(1H)-one **106** (50 mg, 0.279 mmol) and *O*-phenylhydroxylamine hydrochloride **107** (41 mg, 0.279 mmol) in THF (3 mL) at RT. The reaction mixture was stirred at 60 °C under a nitrogen atmosphere for 18 h. LCMS analysis showed incomplete

conversion to desired product. Additional O-phenylhydroxylamine hydrochloride **106** (10 mg, 0.068 mmol) was added. The reaction mixture was stirred at 60 °C under a nitrogen atmosphere for 2 h. LCMS analysis showed incomplete conversion to desired product. The reaction mixture was stirred at 65 °C under a nitrogen atmosphere for 3 h. After cooling to RT, the reaction mixture was concentrated *in vacuo*. The residue was dissolved in 1:1 MeOH:DMSO and purified by MDAP using a solvent system of 10 mM ammonium bicarbonate adjusted to pH 10 with ammonia in water (solvent A) and acetonitrile (solvent B). Fractions containing the desired product were blown down under a stream of nitrogen to yield 1,3-dimethyl-5-(3-methylbenzofuran-2-yl)pyridin-2(1H)-one **107** (34 mg, 0.128 mmol, 46% yield) as a brown gum. **LCMS (For):** rt = 1.11 min, [M+H]⁺ 254. **¹H NMR δ(400 MHz, CDCl₃) ppm:** 7.66 – 7.71 (1H, m), 7.63 – 7.66 (1H, m), 7.48 – 7.52 (1H, m), 7.41 – 7.45 (1H, m), 7.22 – 7.31 (2H, m), 3.66 (3H, s), 2.40 (3H, s), 2.24 – 2.27 (3H, m). **¹³C NMR δ(101 MHz, CDCl₃) ppm:** 162.4 (C), 153.5 (C), 147.4 (C), 134.9 (CH), 134.1 (CH), 130.9 (C), 129.7 (C), 124.2 (CH), 122.6 (CH), 119.0 (CH), 110.7 (C), 110.6 (CH), 109.9 (C), 38.2 (CH₃), 17.4 (CH₃), 9.2 (CH₃).

Biology Experimental

The human biological samples used within this thesis were sourced ethically and their research use was in accord with the terms of the informed consents.

ChromLogD_{7.4}. Chromatographic hydrophobicity index (Chi-LogD_{7.4}) was determined by fast-gradient HPLC, according to literature procedures,⁵¹⁻⁵² using a Waters Aquity UPLC System, Phenomenex Gemini NX 50 × 2 mm, 3 μm HPLC column, 0–100% pH 7.40 ammonium acetate buffer/acetonitrile gradient. Retention time was compared to standards of known pH to derive the Chromatographic Hydrophobicity Index (CHI). ChromLogD = 0.0857CHI – 2.

Artificial Membrane Permeability. Permeability across a lipid membrane was measured using the published protocol.⁵³

pKa Predictions. pKa predictions were calculated using Epik pKa predictor software, published by Schrödinger.⁵⁴

hWB MCP-1 Assay. Compounds to be tested were diluted in 100% DMSO to give a range of appropriate concentrations at 140x the required final assay concentration, of which 1 μL was added to a 96 well tissue culture plate. 130 μL of human whole blood, collected into sodium heparin anticoagulant, (1 unit/mL final) was added to each well and plates were incubated at 37 °C (5% CO_2) for 30 min before the addition of 10 μL of 2.8 $\mu\text{g}/\text{mL}$ LPS (Salmonella Typhosa), diluted in complete RPMI 1640 (final concentration 200 ng/mL), to give a total volume of 140 μL per well. After further incubation for 24 h at 37 °C, 140 μL of PBS was added to each well. The plates were sealed, shaken for 10 min and then centrifuged (2500 rpm \times 10 min). 100 μL of the supernatant was removed and MCP-1 levels assayed immediately by immunoassay (Meso Scale Discovery Technology).

TR-FRET Assays. BET proteins were produced using published protocols.⁵ Compounds were screened against either 6H-Thr BRD4 (1–477) (Y390A) (BRD4 BD2 mutation to monitor compound binding to BD1) or 6H-Thr BRD4 (1–477) (Y97A) (BRD4 BD1 mutation to monitor compound binding to BD2) in a dose–response format in a TR-FRET assay measuring competition between test compound and an AlexaFluor647 derivative of 2. Compounds were titrated from 10 mM in 100% DMSO and 50 nL transferred to a low volume black 384-well microtiter plate using a Labcyte Echo 555. A Thermo Scientific Multidrop Combi was used to dispense 5 μL of 20 nM protein in an assay buffer of 50 mM HEPES, 150 mM NaCl, 5% glycerol, 1 mM DTT, and 1 mM CHAPS, pH 7.4, and in the presence of 100 nM fluorescent ligand ($\sim\text{Kd}$ concentration for the interaction between BRD4 BD1 and ligand). After equilibrating for 30 min in the dark at rt, the bromodomain protein:fluorescent ligand interaction was detected using TR-FRET following a 5 μL addition of 3 nM europium chelate-

labelled anti-6His antibody (PerkinElmer, W1024, AD0111) in assay buffer. Time-resolved fluorescence (TRF) was then detected on a TRF laser equipped PerkinElmer Envision multimode plate reader (excitation = 337 nm; emission 1 = 615 nm; emission 2 = 665 nm; dual wavelength bias dichroic = 400 nm, 630 nm). TR-FRET ratio was calculated using the following equation: ratio = ((acceptor fluorescence at 665 nm)/(donor fluorescence at 615 nm)) × 1000. TR-FRET ratio data was normalized to high (DMSO) and low (compound control derivative of 2) controls and IC50 values determined for each of the compounds tested by fitting the fluorescence ratio data to a four-parameter model: $y = a + \frac{(b - a)}{1 + (10x/10c)^d}$, where a is the minimum, b is the Hill slope, c is the IC50, and d is the maximum.

7.0 References

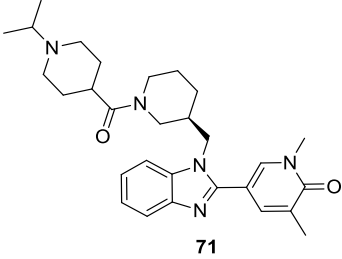
1. International Human Genome Sequencing Consortium, *Nature* **2004**, *431*, 931-945.
2. Arrowsmith, C. H.; Bountra, C.; Fish, P. V.; Lee, K.; Schapira, M., *Nat. Rev. Drug. Discov.* **2012**, *11*, 384-400.
3. Theodoulou, N. H.; Tomkinson, N. C. O.; Prinjha, R. K.; Humphreys, P. G., *Curr. Opin. Chem. Biol.* **2016**, *33*, 58-66.
4. Annunziato, A., *Nature Education* **2008**, *1*.
5. Chung, C.-W.; Coste, H.; White, J. H.; Mirguet, O.; Wilde, J.; Gosmini, R. L.; Delves, C.; Magny, S. M.; Woodward, R.; Hughes, S. A.; Boursier, E. V.; Flynn, H.; Bouillot, A. M.; Bamborough, P.; Brusq, J.-M. G.; Gellibert, F. J.; Jones, E. J.; Riou, A. M.; Homes, P.; Martin, S. L.; Uings, I. J.; Toum, J.; Clément, C. A.; Boullay, A.-B.; Grimley, R. L.; Blandel, F. M.; Prinjha, R. K.; Lee, K.; Kirilovsky, J.; Nicodème, E., *J. Med. Chem.* **2011**, *54*, 3827-3838.
6. Muller, S.; Filippakopoulos, P.; Knapp, S., *Expert Rev. Mol. Med.* **2011**, *13*, e29.
7. Falkenberg, K. J.; Johnstone, R. W., *Nat. Rev. Drug. Discov.* **2014**, *13*, 673-691.
8. Filippakopoulos, P.; Qi, J.; Picaud, S.; Shen, Y.; Smith, W. B.; Fedorov, O.; Morse, E. M.; Keates, T.; Hickman, T. T.; Felletar, I.; Philpott, M.; Munro, S.; McKeown, M. R.; Wang, Y.; Christie, A. L.; West, N.; Cameron, M. J.; Schwartz, B.; Heightman, T. D.; La Thangue, N.; French, C. A.; Wiest, O.; Kung, A. L.; Knapp, S.; Bradner, J. E., *Nature* **2010**, *468*, 1067-1073.
9. Bamborough, P., *GSK Unpubslihed Work* **2014**.
10. Furdas, S. D.; Carlino, L.; Sippl, W.; Jung, M., *Med. Chem. Commun.* **2012**, *3*, 123-134.
11. Dawson, M. A.; Prinjha, R. K.; Dittmann, A.; Giotopoulos, G.; Bantscheff, M.; Chan, W. I.; Robson, S. C.; Chung, C.-W.; Hopf, C.; Savitski, M. M.; Huthmacher, C.; Gudgin, E.; Lugo, D.; Beinke, S.; Chapman, T. D.; Roberts, E. J.; Soden, P. E.; Auger, K. R.; Mirguet, O.; Doehner, K.; Delwel, R.; Burnett, A. K.; Jeffrey, P.; Drewes, G.; Lee, K.; Huntly, B. J.; Kouzarides, T., *Nature* **2011**, *478*, 529-533.
12. Nicodeme, E.; Jeffrey, K. L.; Schaefer, U.; Beinke, S.; Dewell, S.; Chung, C.-W.; Chandwani, R.; Marazzi, I.; Wilson, P.; Coste, H.; White, J.; Kirilovsky, J.; Rice, C. M.; Lora, J. M.; Prinjha, R. K.; Lee, K.; Tarakhovsky, A., *Nature* **2010**, *468*, 1119-1123.
13. Mirguet, O.; Gosmini, R.; Toum, J.; Clément, C. A.; Barnathan, M.; Brusq, J.-M.; Mordaunt, J. E.; Grimes, R. M.; Crowe, M.; Pineau, O.; Ajakane, M.; Daugan, A.; Jeffrey, P.; Cutler, L.; Haynes, A. C.; Smithers, N. N.; Chung, C.-W.; Bamborough, P.; Uings, I. J.; Lewis, A.; Witherington, J.; Parr, N.; Prinjha, R. K.; Nicodème, E., *J. Med. Chem.* **2013**, *56*, 7501-7515.
14. Gallenkamp, D.; Gelato, K. A.; Haendler, B.; Weinmann, H., *Chem. Med. Chem.* **2014**, *9*, 438-464.
15. Zhang, G.; Smith, S. G.; Zhou, M.-M., *Chem. Rev.* **2015**, *115*, 11625-11668.
16. Miyoshi, S.; Ooike, S.; Iwata, K.; Hikawa, H.; Sugahara, K. PCT/JP2008/073864 (WO/2009/084693), 2009.
17. Bradner, J. E.; Brown, J.; Plutzky, J. PCT/US2011/036647 (WO/2011/143651), 2011.
18. Bradner, J. E.; Zuber, J.; Shi, J.; Vakoc, C. R. PCT/US2011/036672 (WO/2011/143660), 2011.
19. Hewings, D. S.; Rooney, T. P. C.; Jennings, L. E.; Hay, D. A.; Schofield, C. J.; Brennan, P. E.; Knapp, S.; Conway, S. J., *J. Med. Chem.* **2012**, *55*, 9393-9413.
20. Zhang, G.; Liu, R.; Zhong, Y.; Plotnikov, A. N.; Zhang, W.; Zeng, L.; Rusinova, E.; Gerona-Navarro, G.; Moshkina, N.; Joshua, J.; Chuang, P. Y.; Ohlmeyer, M.; Cijiang He, J.; Zhou, M.-M., *J. Biol. Chem.* **2012**, *287*, 28840-28851.

21. Albrecht, B. K.; Audia, J. E.; Cote, A.; Gehling, V. S.; Harmange, J.; Hewitt, M. C.; Leblanc, C. G.; Taylor, A. M.; Vaswani, R. G. PCT/US2011/063046 (WO/2012/075383), 2011.
22. Seal, J.; Lamotte, Y.; Donche, F.; Bouillot, A.; Mirguet, O.; Gellibert, F.; Nicodeme, E.; Krysa, G.; Kirilovsky, J.; Beinke, S.; McCleary, S.; Rioja, I.; Bamborough, P.; Chung, C.-W.; Gordon, L.; Lewis, T.; Walker, A. L.; Cutler, L.; Lugo, D.; Wilson, D. M.; Witherington, J.; Lee, K.; Prinjha, R. K., *Bioorg. Med. Chem. Lett.* **2012**, *22*, 2968-2972.
23. Zhao, L.; Cao, D.; Chen, T.; Wang, Y.; Miao, Z.; Xu, Y.; Chen, W.; Wang, X.; Li, Y.; Du, Z.; Xiong, B.; Li, J.; Xu, C.; Zhang, N.; He, J.; Shen, J., *J. Med. Chem.* **2013**, *56*, 3833-3851.
24. Wang, L.; Pratt, J. K.; Mcdaniel, K. F. (WO2013097601), 2013.
25. Wang, L.; Pratt, K. K.; Mcdaniel, K. F.; Dai, Y.; Fidanze, S. D.; Hasvold, J. H.; Holms, J. H.; Kati, W. M.; Liu, D.; Mantei, R. A.; McClellan, W. J.; Sheppard, G. S.; Wada, C. K. (WO2013097601), 2013.
26. Amorim, S.; Stathis, A.; Gleeson, M.; Iyengar, S.; Magarotto, V.; Leleu, X.; Morschhauser, F.; Karlin, L.; Broussais, F.; Rezai, K.; Herait, P.; Kahatt, C.; Lokiec, F.; Salles, G.; Facon, T.; Palumbo, A.; Cunningham, D.; Zucca, E.; Thieblemont, C., *The Lancet Haematology* **2016**, *3*, e196-e204.
27. Zengerle, M.; Chan, K.-H.; Ciulli, A., *ACS Chem. Biol.* **2015**, *10*, 1770-1777.
28. Zhang, G.; Plotnikov, A. N.; Rusinova, E.; Shen, T.; Morohashi, K.; Joshua, J.; Zeng, L.; Mujtaba, S.; Ohlmeyer, M.; Zhou, M.-M., *J. Med. Chem.* **2013**, *56*, 9251-9264.
29. Picaud, S.; Wells, C.; Felletar, I.; Brotherton, D.; Martin, M.; Savitsky, P.; Diez-Dacal, B.; Philpott, M.; Bountra, C.; Lingard, H.; Fedorov, O.; Müller, S.; Brennan, P. E.; Knapp, S.; Filippakopoulos, P., *PNAS* **2013**, *110*, 19754-19759.
30. McLure, K. G.; Gesner, E. M.; Tsujikawa, L.; Kharenko, O. A.; Attwell, S.; Campeau, E.; Wasiak, S.; Stein, A.; White, A.; Fontano, E.; Suto, R. K.; Wong, N. C. W.; Wagner, G. S.; Hansen, H. C.; Young, P. R., *PLoS One* **2013**, *8*, e83190.
31. Kharenko, O. A.; Gesner, E. M.; Patel, R. G.; Norek, K.; White, A.; Fontano, E.; Suto, R. K.; Young, P. R.; McLure, K. G.; Hansen, H. C., *Biochem. Biophys. Research Commun.* **2016**, *477*, 62-67.
32. Shadrack, W. R.; Slavish, P. J.; Chai, S. C.; Waddell, B.; Connelly, M.; Low, J. A.; Tallant, C.; Young, B. M.; Bharatham, N.; Knapp, S.; Boyd, V. A.; Morfouace, M.; Roussel, M. F.; Chen, T.; Lee, R. E.; Kiplin Guy, R.; Shelat, A. A.; Potter, P. M., *Bioorg. Med. Chem.* **2018**, *26*, 25-36.
33. Law, R. P.; Atkinson, S. J.; Bamborough, P.; Chung, C.-W.; Demont, E. H.; Gordon, L. J.; Lindon, M.; Prinjha, R. K.; Watson, A. J. B.; Hirst, D. J., *J. Med. Chem.* **2018**, *61*, 4317-4334.
34. Gacias, M.; Gerona-Navarro, G.; Plotnikov, A. N.; Zhang, G.; Zeng, L.; Kaur, J.; Moy, G.; Rusinova, E.; Rodriguez, Y.; Matikainen, B.; Vincek, A.; Joshua, J.; Casaccia, P.; Zhou, M.-M., *Chemistry and Biology* **2014**, *21*, 841-854.
35. Hugle, M.; Lucas, X.; Weitzel, G.; Ostrovskiy, D.; Breit, B.; Gerhardt, S.; Einsle, O.; Günther, S.; Wohlwend, D., *J. Med. Chem.* **2016**, *59*, 1518-1530.
36. Raux, B.; Voitovich, Y.; Derviaux, C.; Lugari, A.; Rebuffet, E.; Milhas, S.; Priet, S.; Roux, T.; Trinquet, E.; Guillemot, J.-C.; Knapp, S.; Brunel, J.-M.; Fedorov, A. Y.; Collette, Y.; Roche, P.; Betzi, S.; Combes, S.; Morelli, X., *J. Med. Chem.* **2016**, *59*, 1634-1641.
37. Liu, Z.; Tian, B.; Chen, H.; Wang, P.; Brasier, A. R.; Zhou, J., *Eur. J. Med. Chem.* **2018**, *151*, 450-461.
38. Baud, M. G. J.; Lin-Shiao, E.; Cardote, T.; Tallant, C.; Pschibul, A.; Chan, K.; Zengerle, M.; Garcia, J. R.; Kwan, T. T.-L.; Ferguson, F. M.; Ciulli, A., *Science* **2014**, *346*, 638-641.
39. Baud, M. G. J.; Lin-Shiao, E.; Zengerle, M.; Tallant, C.; Ciulli, A., *J. Med. Chem.* **2016**, *59*, 1492-1500.

40. Runcie, A. C.; Zengerle, M.; Chan, K.-H.; Testa, A.; van Beurden, L.; Baud, M. G. J.; Epemolu, O.; Ellis, L. C. J.; Read, K. D.; Coulthard, V.; Brien, A.; Ciulli, A., *Chem. Sci.* **2018**, *9*, 2452-2468.
41. Bunnage, M. E.; Piatnitski Chekler, E. L.; Jones, L. H., *Nat. Chem. Biol.* **2013**, *9*, 195-199.
42. Epigenetics, D. P. U., *GSK Unpublished Results* **2017**.
43. Wellaway, C. R.; Alder, C.; Bamborough, P.; Barnett, H.; Bit, R. A.; Brown, J. A.; Craggs, P. D.; Chung, C.; Cooper, A. W. J.; Cutler, L.; Davis, R. P.; Dean T. W.; Demont E. H.; Ferrie A. R.; Gordon, L.; Hirst, D. J.; Humphreys, P. G.; Jones, K. L.; Lewis, T.; Lindon, M. J.; Lugo, D.; Medeiros, P.; Mitchell, D. J.; Patel, V. K.; Patten, C.; Poole, D. L.; Prinjha, R. K.; Reid, I.; Shah, R.; Smith, J.; Stafford, K.; O'Sullivan, M.; McCleary, S.; Taylor, S.; Vimal, M.; Wall, I. D.; Watson, R. J.; Wellaway, N.; Yao, G., *GSK Unpublished Results*.
44. WO2015/022322 A1, 2015.
45. Epigenetics, D. P. U., *GSK Unpublished Results* **2016**.
46. Andrews, K. G.; Faizova, R.; Denton, R. M., *Nat. Commun.* **2017**, *8*, 15913.
47. Fusani, L., *GSK Unpublished Results* **2018**.
48. Tucker, J., *GSK Unpublished Results* **2017**.
49. Tomkinson, N. C. O.; Contiero, F.; Jones, K. M.; Matts, E. A.; Porzelle, A., *Synlett* **2009**, *2009*, 3003-3006.
50. Freeman-Cook, K. D.; Hoffman, R. L.; Johnson, T. W., *Future Med. Chem.* **2013**, *5*, 113-115.
51. Valko, K. N., S.; Bevan, C.; Abraham, M. H.; Reynolds, P., D., *J. Pharm. Sci.* **2003**, *92*, 2236-2248.
52. Camurri, G.; Zaramella, A., *Anal. Chem.* **2001**, *73*, 3716-3722.
53. Ballell, L.; Bates, R. H.; Young, R. J.; Alvarez-Gomez, D.; Alvarez-Ruiz, E.; Barroso, V.; Blanco, D.; Crespo, B.; Escribano, J.; Gonzalez, R.; Lozano, S.; Huss, S.; Santos-Villarejo, A.; Martin-Plaza, J.; Mendoza, A.; Rebollo-Lopez, M. J.; Remuinan-Blanco, M.; Lavandera, J. L.; Perez-Herran, E.; Gamo-Benito, F. J.; Garcia-Bustos, J. F.; Barros, D.; Castro, J. P.; Cammack, N., *Chem. Med. Chem.* **2013**, *8*, 313-321.
54. Shelley, J. C.; Cholleti, A.; Frye, L. L.; Greenwood, J. R.; Timlin, M. R.; Uchimaya, M., *J. Comput. Aided. Mol. Des.* **2007**, *21*, 681-691.

8.0 Appendix

Complete Data for Bromoscan assays of isopropyl piperidine **71** (Table 21).



The chemical structure of compound **71** is shown above the table. It consists of a benzimidazole core substituted with a 4-isopropylpiperidin-1-yl group at the 2-position, a 2,6-dimethyl-4-(1-(4-isopropylpiperidin-1-yl)butan-1-yl)pyridin-5(1H)-one group at the 4-position, and a benzene ring at the 5-position.

BRD4 BD1/BD2 pIC₅₀	8.1/5.6 (2.5)
BRD2 BD1/BD2 pIC₅₀	8.5/5.5 (3.0)
BRD3 BD1/BD2 pIC₅₀	8.4/5.8 (2.6)
BRDT BD1/BD2 pIC₅₀	8.1/5.5 (2.6)
ATAD2A pIC₅₀	< 4.50
ATAD2B pIC₅₀	< 4.50
CECR2 pIC₅₀	< 4.50
EP300 pIC₅₀	5.00
PCAF pIC₅₀	< 4.50
BAZ2A pIC₅₀	< 4.50
BAZ2B pIC₅₀	< 4.50
BRD1 pIC₅₀	< 4.50
BRD7 pIC₅₀	< 4.50
BRD8 BD1 pIC₅₀	< 4.50
BRD8 BD2 pIC₅₀	< 4.50
BRD9 pIC₅₀	4.60
BRPF1 pIC₅₀	4.80
BRPF3 pIC₅₀	< 4.50
CREBBP pIC₅₀	4.80
FALZ pIC₅₀	< 4.50
GCN5L2 pIC₅₀	< 4.50
PBRM1 BD2 pIC₅₀	< 4.50
PBRM1 BD5 pIC₅₀	< 4.50
SMARCA2 pIC₅₀	< 4.50

Table 22: Extended data table of Bromoscan assays for benzimidazole **71**. The potency data disclosed is the mean of at least 2 test occasions.